Frost Resistance of Building Materials : Proceedings of the 3rd Nordic Research Seminar in Lund, 1999

Fridh, Katja

1999

FROST RESISTANCE OF BUILDING MATERIALS

K Fridh, Editor

Proceedings of the 3rd Nordic Research Seminar in Lund, 1999

Report TVBM-3087

Division of Building Materials
Lund Institute of Technology

FROST RESISTANCE OF BUILDING MATERIALS

K Fridh, Editor

Proceedings of the 3rd Nordic Research Seminar in Lund, August 31 – September 1

Report TVBM-3087

ISRN LUTVDG/TVBM--99/3087--SE(1-159)
ISSN 0348-7911 TVBM

Lund Institute of Technology
Division of Building Materials
Box 118
SE-221 00 Lund, Sweden

Telephone: 46-46-2227415
Telefax: 46-46-2224427
www.byggnadsmaterial.lth.se

Preface

This report contains papers presented at a Research Seminar, or rather "workshop", organised by our Department. It is the third in a series. The previous seminars were held in 1993 and 1996[1]. The seminar is "Nordic", by which is meant that the speakers came from the Scandinavian countries -Denmark, Norway, Sweden- and Finland. Certainly there are other Nordic countries in which frost is a real problem, but this time there were no participants from these countries. Most participants were invited personally and asked to give presentations. The seminar language was English making it possible also for participants from outside Scandinavia to take part. This time some German guest research students took part as "observers" and as contributors to the discussions.

The papers cover many aspects of frost damage. Some papers discuss the very important problem of moisture uptake before and during a freeze/thaw test. Other papers treat the destruction mechanisms behind salt-frost scaling and internal frost attack. There are also papers dealing with the assessment of the service life of concrete exposed to frost action. Some papers present data from field exposure of specimens and from real structures. Altogether, the seminar gives a good picture of what is going on in frost research in the Nordic countries. Almost all papers, however, treat concrete. There are many more building materials for which frost damage is a problem, but no papers were presented. This does not necessarily mean that work is not done on materials such as clay brick, natural stone, etc, but evidently the activities are much smaller than for concrete. One reason might be that it is much more difficult to find research funding for studies of these types of materials.

A fourth research seminar will possibly be arranged within a few years time. Maybe, the invitations will then be sent to a wider circle of potential participants.

Lund, September 1999

Göran Fagerlund

1. S. Lindmark (Editor). *Frost Resistance of Building Materials*. Proceedings of a Nordic Research Seminar in Lund, April 16-17, 1996. Div. of Building Materials, Lund Institute of Technology, Report TVBM-3072, 1996.

Contents

A CONCEPTUAL MODEL FOR THE FREEZE-THAW DAMAGE OF CONCRETE

Dirch H. Bager, Chief Concrete Technologist, Ph.D.
Aalborg Portland A/S, Cement and Concrete Laboratory
Rørdalsvej 44, P.O. Box 165, DK-9100 Aalborg, Denmark

Stefan Jacobsen, Research Engineer, Ph.D.
Norwegian Building Research Institute
Forskningsveien 3b, P.O. Box 123 Blindern, N-0314 Oslo, Norway

1 INTRODUCTION

This paper outlines the model for freeze/thaw damage in concrete presented by Bager and Jacobsen at the Minneapolis Workshop on Freeze/thaw damage in Concrete in June 1999 [1].

The model gives a qualitative description on the mechanisms which cause damage to concrete during freeze/thaw, and the influence different climatic or test conditions have on the damage.

Some ideas for further experimental justification of the model are presented. To the author's opinion, the model can be made quantitative to such an extent, that fairly simple measurements can be used to predict freeze/thaw durability.

2 TEST PROCEDURES AND MATERIALS

2.1 Test methods

The main test method used for the experiments is the Swedish standard test SS137244 for scaling. This test method is almost identical with the coming European reference test for scaling, the Slab test [2]. The main difference between these two methods is the lowest temperature in the freezing cycle, respectively -18°C and –20°C for the Swedish and the European slab test.

The experiments have been carried out within the framework of NORDTEST by five laboratories: The Norwegian Building Research Institute (NBI), The Swedish Research and Testing Institute (SP), Technical Research Centre of Finland (VTT), Lund Institute of Technology/Division of Building Materials (LTH) and the Cement and Concrete Laboratory / Aalborg Portland (CBL). Most of the results presented in this paper have been obtained at the latter. The NORDTEST projects, which concern simultaneous measurement

of scaling, internal damage and water-uptake on the same samples and during the same test, have been reported in [3,4].

A part of the test is the preconditioning of the specimen. During the preconditioning the specimens are dried for seven days at a relative humidity of 65 %. After this drying, the upper surface of the specimen is allowed to absorb water by capillary suction for three days.

Besides measurement of scaling also transmission time of ultrasonic pulses (UPTT), dilation and water-uptake have been measured.

For the UPTT, 54 Hz conical transducers have been used. Contact between the transducers and the concrete has been obtained through the rubbersleeve. No other contact media has been used. A special measuring equipment was built, which presses the transducers correct aligned on the opposite sides of the specimen by pneumatic pressure cylinders. The UPTT are calculated as changes relative to the 0-cycle value.

Length change was measured with an electrical digital gauge. Steel studs were glued into holes in the specimen. A special measuring stand for these measurements, which secure the same position of the sample for each measurement, has been constructed.

Water-uptake was determined by weighing the surface dry specimen after each scaling measurement. Weight of scaled material, corrected for evaporable water content, was included. The water-uptake was calculated as kg/m^2.

Three different types of freeze/thaw environments have been used in the tests:

1. Freezing in wet state, but without access to free water or de-icing salt solutions on surface. In this paper called the "classical" test. In order to avoid evaporation from the specimen to the cold spots in the freezing cabinet during the freeze/thaw cycles, a thin plastic foil was placed directly on the saturated surface dry specimen.
2. Freezing in saturated state, with access to free water on the surface; the "wet" test.
3. Freezing in saturated state, with access to de-icing solution on the surface; the "salt" test.

It is well known that high porosity and fast cooling rate can give rise to such fast ice-formation, that hydraulic pressure can introduce cracks. This mechanism is not dealt with in this paper, since the authors feel, that this mechanism is only effective in laboratory testing, and not relevant in practice, in particular for those concrete qualities used in aggressive environments in the Nordic countries today.

2.2 Materials

In the tests the concrete types in table 1 have been used

Table 1: Concrete types. The differences in water/cement-ratios between the Norwegian and the Swedish produced concrete are caused by different ways of calculating the water/cement-ratio. In Norway the amount of free water is used, while Sweden uses total amount of water.

Type	w/c	air	Cube strength MPa	testtype	Cement
I/97/salt	0.32	0	105.1	Salt	Swedish SRPC
I/98/salt	0.31	0	94.4	Salt	Norwegian OPC
I/99/salt	0.32	0	107.1	Salt	Swedish SRPC
II/98/wet	0.48	0	62,6	Wet	Norwegian OPC
II/99/air/wet	0.50	3.8	52.7	Wet	Swedish SRPC
II/99/air/salt	0,50	3.8	52.7	Salt	Swedish SRPC
III/97/classical	0,70	0	33.5	Classical	Swedish SRPC
III/97/wet	0.70	0	33,6	Wet	Swedish SRPC
III/98/wet	0.67	0	36,0	Wet	Norwegian OPC

3 DESCRIPTION OF THE MODEL FOR NON AIR-ENTRAINED CONCRETE

3.1 Freezing of pore water

During cooling freezing of water will take place. However, three different situations have to be evaluated:

- "Classical": Without free water on the surface, ice formation will take place as nucleation of ice crystals randomly in the pore system. The ice will spread in the concrete through the continuous system of larger capillary pores.
- "Wet": Ice formation will generally start in the water layer on top of the specimen, since during cooling this will be the coldest spot on the sample. The ice will spread into the specimen via the continuous system of larger capillary pores as an icefront. During thawing there can be ice in the specimen and water on the surface.
- "Salt": Since the freezing point of the salt solution has been lowered due to the salt, then the first ice formation will be initiated as nucleation of ice crystals randomly in the pore system saturated with pure water. The ice will spread in the concrete through the continuous system of larger capillary pores as for the classical test. During thawing there can be ice in the specimen and liquid salt solution on the surface.

3.2 Micro ice body formation

The ice forms as micro ice bodies in the pores. Micro ice body formation has been thoroughly described by Setzer [5]. Such micro ice bodies in porous materials acts in two opposite ways:

i) They have a lower chemical potential than the "free" pore water. Therefore water will move towards the micro ice bodies which therefore will grow and exert pressure on the surrounding pore walls leading to an increase in volume of the paste.

ii) On the other hand, the driving forces for water to move towards these micro ice bodies are so strong, that water can be drawn from the gel pores, resulting in shrinkage of the paste.

We think that for highly saturated concrete with high water/cement ratio this mechanism will lead to a volume increase, while for low water/cement ratio concrete a shrinkage can be expected as long as the liquid uptake from the exterior is not sufficient.

3.3 Formation of empty cracks around the aggregate particles

When the paste expands due to formation of micro ice bodies, the cracks will appear around the individual aggregate particles. When these cracks open, they will be empty; i.e. they contain neither ice nor water.

In the freeze/thaw test, formation of such cracks will be monitored by an increase in length or volume of the specimen. Furthermore, since the passage time for the ultrasonic pulse is larger in air filled cracks than in water filled cracks. Therefore, for the same crack width, the UPTT will be larger when the cracks are empty than when they are water filled.

3.4 Water-uptake and increasing damage in concrete

After the cracks surrounding the individual aggregate particles has appeared, then further damage in the concrete is controlled by water-uptake in these cracks. Until they are saturated to a critical degree, no further damage will happen. When the critical degree of saturation in the cracks is reached, then the "particle" of aggregate and ice in the surrounding crack will expand. Expansion of particles leads to cracks in the paste, connecting the individual particles. Thus a continuous crack system will occur, leading to internal breakdown of the concrete.

The experimental set-up is a major controlling parameter for the water-uptake and the further breakdown of the concrete during the succeeding freeze/thaw cycles, as described in the following.

- **Classical**

In this set-up, water-uptake during the test can only take place when the specimen is at +20°C. The only driving force is capillary suction. However, before start of the frost test, the specimen had been exposed for capillary suction for three days. The remaining capacity for capillary suction is therefore very limited, and only a very small water-uptake takes place during each freeze/thaw cycle.

In a "semi-sealed" test like ASTM C671 freezing takes place in kerosene and the frozen specimens are returned to water for melting and further absorption. There is then good

possibility of further water uptake both due to migration/suction towards ice, and suction due to melting ice.

- **Wet**

In this set-up, water-uptake can take place during melting. We assume that the pure ice on the upper surface will melt before most of the ice inside the specimen. Therefore water-uptake can take place due to two mechanisms:

i) suction towards the micro ice bodies and
ii) suction due to the 9 vol% decrease when ice melts.

Assuming that melting in the specimen starts in the upper layer and gradually goes down towards the bottom, these mechanism results in a continuous water-uptake right down to the bottom layer. The moisture distribution will therefore be very even within the specimen.

- **Salt**

When a salt solution is applied as the freezing media, the water-uptake during the test differs from the previous. During freezing micro ice bodies forms randomly within the specimen before the salt solution freeze. Therefore water-uptake can take place during the cooling period of the freeze/thaw cycle. It must be expected that the major part of these micro ice bodies forms first in the upper part of the specimen, thus leading to water movement from the lower part. Furthermore, due to the salt ions present in the freezing media, water moves from the lower part of the specimen towards the upper part caused by osmotic forces. This result in a high saturation in the upper layer of the specimen, and expansion due to increase in volume of the micro ice bodies, while shrinkage prevails in the lower part caused by the removal of water towards the upper layer. Thus the specimen will be in an unstable internal stress situation which can be released by formation of vertical cracks. Therefore scaling is the major destructive mechanism when salt is used as freezing media, while internal damage prevails when water is used as freezing media.

- **Influence of water/cement ratio**

The higher the water/cement ratio, the faster the water-uptake and, consequently, the faster the critical degree of saturation in the cracks surrounding the aggregate particles will be reached.

Concrete with a high water/cement ratio will therefore be destroyed by internal cracking far earlier than concrete having a lower water/cement ratio.

4 INFLUENCE OF AIR-ENTRAINMENT

It is a well-known and accepted fact, that introducing a proper artificial air pore structure minimises freeze/thaw damage in concrete. The reason for this is, that these artificial air bubbles act as sinks for the ice formation. Ice formed in these pores has a lower chemical potential than ice formed directly in the pore system as micro ice bodies because no restraint for growing from the outer pore walls will influence the internal stress in the ice. Thus nearly no micro ice bodies are formed in the capillary pores in concrete with a proper artificial air entraining. No pressure will therefore be acting on the pore walls as long as the air voids are not filled critically.

One way of characterising a proper air pore structure, is the distance between the pores, the spacing factor. Practical experience during many years have demonstrated, that if the spacing factor is less than 0.2 mm, then the concrete generally will be durable in freeze/thaw environment.

However, in modern concrete, having water/cement ratios below 0.4, and with extensive use of mineral puzzolanic by-products such as flyash and microsilica, and water-reducing or superplasticizing agents, the spacing-factor concept is no longer general valid. It is believed that for low water/cement-ratios and also for some binders with pozzolans resulting in very refined and/or low porosity, the permeability or diffusivity is so low that transport towards the air voids is not sufficient to hinder pressure due to ice lenses. Freezing behaviour, and consequently damage, will therefore to a large extent be identical to the behaviour in non-air entrained concrete having the same water/cement-ratio. This can be the reason for the large scaling for dense concrete with w/c ratio = 0,30 – 0,40

5 EXPERIMENTS AND DISCUSSION.

In [1] more detailed information on the results are given. In this paper only a few typical results are shown in order to illustrate the model.

In figure 1 the accumulated dilation for I/98/SALT, II/98/WET & III/98/WET are shown. The dilation plotted has been measured when the specimens were at +20°C. The contraction caused by removal of water from the gel pores can easily be seen for the specimen I/98/SALT, having a water/cement ratio of 0.31, whereas no contraction has been measured for III/98/WET, having a high water/cement ratio of 0.67. However, if the specimen is left for 24 hours at 20°C before dilation is measured, no contraction is seen [6]. This observation can be caused by a slower re-entering of water into the gel in the dense low water/cement ratio concrete. Redistribution of water is further facilitated by access to free water on the surface, as will be discussed later in the discussion of variation of compressive strengths.

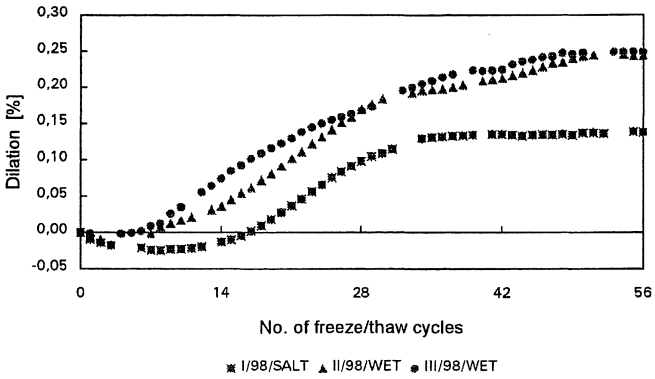

Figure 1: Accumulated dilation [%] as function of no. of freeze/thaw cycles [4].

Continuous measurement during the freeze/thaw cycle normally shows expansion during the heating part of the cycle. Figure 2 [4] illustrate this phenomenon.

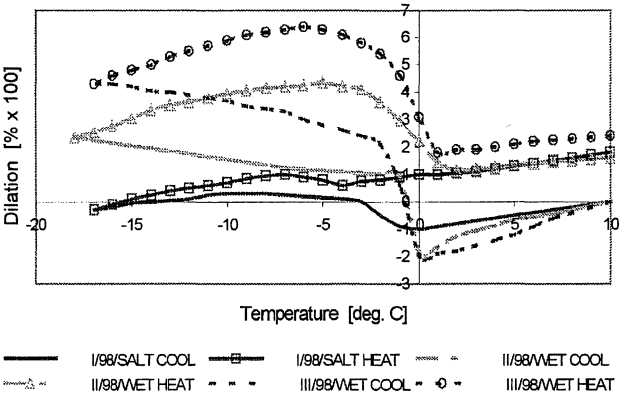

Figure 2: Continuous dilation during the 42'd freeze/thaw cycle, measured at LTH [4]

This can be explained by two mechanisms:

i) The thermal expansion of ice is larger than the thermal expansion of concrete. Since ice have been formed at lower temperatures than it melts, then the thermal expansion of the ice will exert pressure on the inner walls of the pores during heating, thus giving rise to expansion.

ii) When the water or salt solution on the outer surface is melted, suction of water takes place leading to an increase of volume of the micro-ice-bodies.

When the internal ice melts, the volume decrease by 9 vol.%, and the water can be redistributed in the specimen. The specimen will then shrink. Most of the ice melts close to 0°C, even if it freezes far lower. Bager and Sellevold [7] explains this with "ink-bottle" pores into which water first freezes when the "bottle-neck" freezes. (Spontaneous nucleation of ice in some of these pores might of cause happen)

The results presented in figure 2 clearly shows the influence of water/cement ratio. The higher the ratio, the larger the expansion during both the cooling and the heating.

Figure 3 shows the cracks around the individual aggregate particles obtained in I/98/SALT after 112 cycles. The concrete has been impregnated with fluorescent epoxy in order to see the cracks.

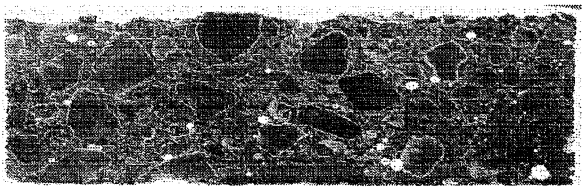

Figure 3: Crackpattern in #I/98/SALT after 112 cycles. Specimen width: 105 mm [4]

According to the model, empty cracks appear around the individual aggregate particles when the paste has reached a critical degree of saturation. In figure 4, this formation of cracks can be seen by the increase in UPTT. For concrete I/98/SALT, it is furthermore very clear, that the UPTT after approximately 14 additional cycles decrease to a lower value. This is, to the author's opinion, caused by water filling of these cracks. The same phenomenon can be seen for II/98/WET, but not for the concrete with water/cement ratio of 0.67, III/98/WET. Fast water-uptake caused by the high water/cement ratio explains why the phenomenon is not recognised when measurements have only been made for every 14 cycles.

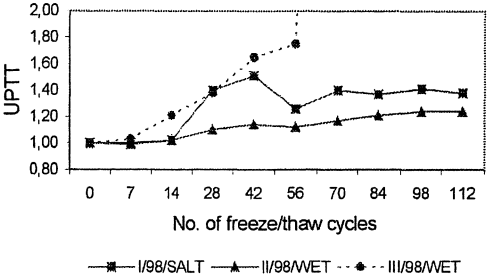

Figure 4: UPTT for concretes #I/98/SALT, #II/98/WET & #III/98/WET. [4]

It can be seen that for III/98/WET the UPTT increases to infinity between 56 and 70 cycles, as an indication of that the specimen totally disintegrated. The test had to be stopped after 98 cycles caused by this internal disintegration. It shall be noted that in spite of this disintegration, then the surface scaling was fairly low, only 0.235 kg/m^2 after 98 cycles.

Figure 5 shows the water-uptake in specimens I/98/SALT, II/98/WET & III/98/WET. The measured water-uptake in I/98/SALT is lowest during the first cycles as expected due to low permeability and the moisture distribution. According to the model, the water content in the upper part of the specimen is higher than in the lower part due to osmosis. This will of course reduce the overall water-uptake. The increasing water-uptake in III/98/WET at high number of cycles is due to a complete disintegration and very high porosity increase, see figure 6.

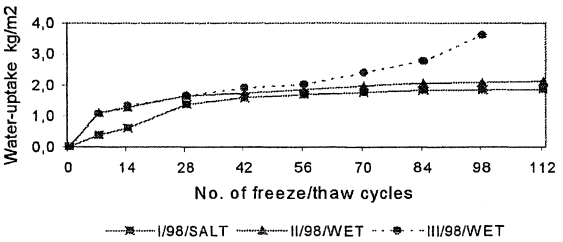

Figure 5: Water-uptake as function of freeze/thaw cycles [4]

Figure 6 shows the crack formation in concrete III/98/WET. As for I/98/SALT, the specimen has been impregnated with fluorescent epoxy in order to see the cracks. In this specimen, cracks can clearly be seen in the paste, connecting the individual aggregate particles.

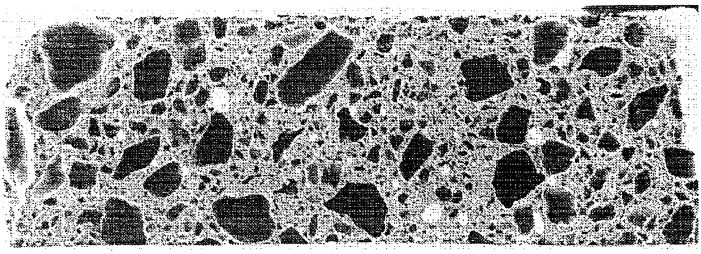

Figure 6: Crackformation in #III/98/WET after 98 cycles. Specimen width 150 mm [4]

Formation of cracks can be detected in several ways. Andersen [8] measured cracking in concrete during freezing using acoustic emission. Figure 7 shows the crack formation, measured as number of counts, as a function of the freeze/thaw cycles. Two types of concrete have been used, one with a water/cement ratio of 0.5, and one with a water/cement-ratio of 0.9. [The curves have been redrawn by the authors of this paper]

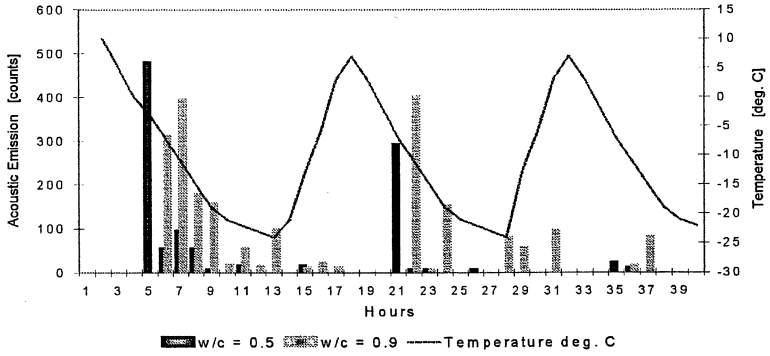

Figure 7: Acoustic emission as function of no. of cycles for two non-air entrained concretes [8]

From figure 7 it can clearly be seen, that the crack formation in the concrete with water/cement-ratio of 0.5 mainly takes place during the first cycle, while in the concrete with water/cement-ratio of 0.9, a larger portion of cracks forms in the succeeding cycles. This agrees well with the model. In the concrete with the high water/cement-ratio, the first formed cracks around the aggregate particles quickly get critically saturated, thus giving rise to further crack formation in the cement paste.

Andersen [8] also measured dilation of the specimens. In figure 8 the correlation between crack formation, measured by acoustic emission, and dilation of the specimen is shown. It is clearly seen, that for the water/cement-ratio of 0.5, there is an indication of a small contraction during the first cycle and only a very limited expansion during the next few cycles, while for the concrete with water/cement-ratio of 0.9, a linear relationship between crack formation and dilation is seen. It is noteworthy that this is the case, since the number of acoustic emission counts in the first cycle is almost identical for the two concretes. However, according to the model, this result could be foreseen.

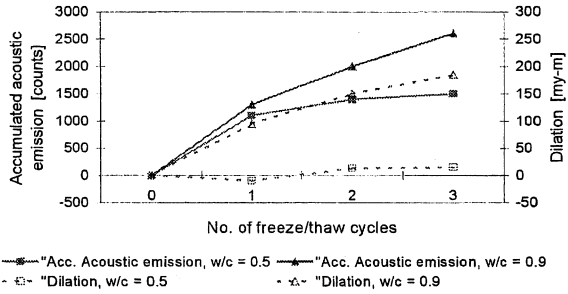

Figure 8: Relation between accumulated acoustic emission and dilation for two concrete types [8]

Internal damage caused by freeze/thaw action leads to decrease in elastic modulus and strength of the concrete. In the 1997 NORDTEST project [3], strength variations was measured as function of the number of freeze/thaw cycles. Figure 9 shows the relative compression strength variation. The figure displays three remarkable features:

i) An increase in compressive strength between 0 and 7 freeze/thaw cycles. It is believed that this is due to the redistribution of water from the gel-pores to the larger pores into which micro ice bodies have formed.

ii) Decrease in compressive strength between 14 and 28 freeze/thaw cycles for I/98/SALT and III/97/WET, presumably caused by the internal cracking. The

decrease in compressive strength appears during the same freeze/thaw cycles, as the increase in UPTT has been measured.

iii) For III/97/CLASSICAL, the strength increase during the first 7 freeze/thaw cycles is larger than for II/97/WET. It is believed that this is caused by the lower amount of water-uptake in the "classical" test than in the "wet" test, thereby giving rise to a more pronounced redistribution of water. At a higher number of freeze/thaw cycles, the water-uptake has lead to a situation, where the gel pores have regained their water-content. Due to the low water-uptake, no damage has taken place during the first 112 freeze/thaw cycles in this "classical" test.

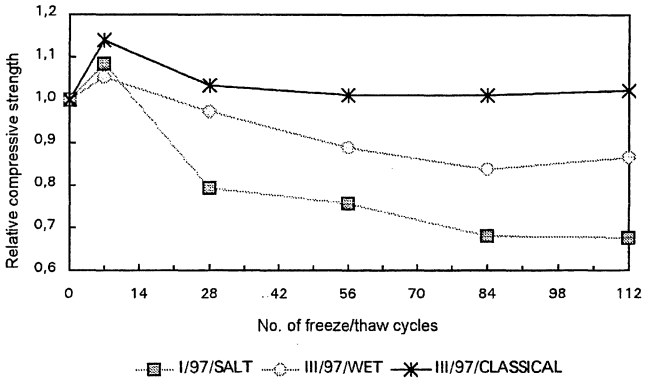

Figure 9: Relative compressive strength measured at SP in the 1997 NORDTEST project [3].

The influence of air entraining has been discussed previously. It is well known that both scaling and internal damage in most cases is reduced significantly if the concrete has a proper artificial air pore structure.

In some ongoing preliminary experiments [6], water-uptake has been monitored. The number of specimens is very limited, and there is no statistical documentation for the validity of the results.

In these tests concrete types II/99/AIR/WET & II/99/AIR/SALT are being used. The water-uptake has been measured as in the former tests. In addition to these measurements, some of the specimens have been removed from the freeze/thaw test at 2, 12 and 43 cycles. These specimens was split vertically by a splitting test in the compression testing machine, the halves specimens weighed, dried and the total water content calculated in weight

percent. Measurement of the relative water vapour pressure exerted by the upper surface and the lower surface confirmed the measurements. The results are presented in table 2.

Table 2: Water-uptake in II/99/AIR/WET and II/99/AIR/SALT in the ongoing measurements

			WET	***SALT***
Water-uptake, kg/m^2	2 cycles		0,270	0,146
		Water content, upper part, weight %	-	4,66%
		Water content, lower part, weight %	-	4,01%
		Mean		*4,34%*
Water-uptake, kg/m^2	6 cycles		0,503	0,331
Water-uptake, kg/m^2	12 cycles		0,637	0,424
		Water content, upper part, weight %	4,18%	4,72%
		Water content, lower part, weight %	5,13%	4,7%
		Mean	*4.66%*	*4.71%*
Water-uptake, kg/m^2	18 cycles		0,813	0,488
Water-uptake, kg/m^2	24 cycles		0,882	0,536
Water-uptake, kg/m^2	30 cycles		0,918	0,576
Water-uptake, kg/m^2	43 cycles		1,004	0,590
		Water content, upper part, weight %	-	5,05%
		Water content, lower part, weight %	-	4,86%
		Mean		*4,96%*

The model predicts an almost uniform moisture distribution in the WET specimen. The reason for the higher degree of saturation in the bottom of the WET specimen can be that the air entraining interrupt the expected almost continuously water filled capillary pore system.

A lower water-uptake (kg/m^2) in the SALT specimen than in the WET specimen is expected according to the model if the moisture transport from the bottom of the rather thick slab to the SALT surface is sufficient. The average water-uptake confirms this, however, the reason for almost identical total water-contents in the WET and the SALT specimen after 12 cycles is not clear.

The measured water-uptake in the SALT specimen is in contradiction to the results presented in [9] and further discussed in [10]. In these papers, the water-uptake in SALT specimens is always larger than in the WET specimens. These measurements have been made on non-air-entrained concretes. As discussed for the moisture distribution in the WET specimen, interrupted capillary system might be the reason for the observed discrepancy.

Parallel measurement of moisture distribution in the non air entrained I/99/SALT shows after 12 cycles a water content in the upper part of 4.1 weight %, and in the lower part of 3.5 weight %. This agrees well with the model.

In figure 10 water-uptake measured in the two NORDTEST projects are shown. The figure clearly illustrate that

i) Air entraining reduces the water-uptake for the same water/cement ratio {II/98/WET & II/99/AIR/SALT}
ii) Water-uptake in II/99/AIR/SALT {w/c = 0.50} is smaller than in I/98/SALT & I/99/SALT {w/c = 0.31}

The above mentioned data implies, that air entraining breaks the water-filled continuous capillary pore system, thus influencing the water-uptake.

This phenomenon has to be studied further in order to establish a general valid qualitative as well as quantitative description of the moisture migration inside the specimen, the water-uptake and the freeze/thaw damage.

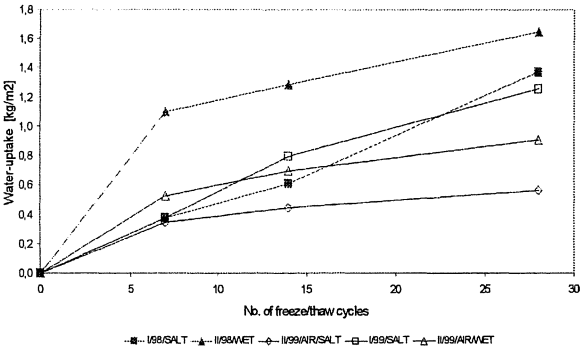

Figure 10: Water-uptake during the first 28 freeze/thaw cycles [4,6]

6 FURTHER WORK

For modern high-performance concrete it is obvious, that the traditional empirical acceptance criteria are not satisfactory. Particularly when using secondary cementing materials that affect transport properties, research is needed to understand their frost behaviour before extensive use under severe winter conditions. Further research regarding the relationship between actual moisture conditions for structural elements; their field performance and laboratory tests are strongly needed.

Essential further research to be carried out in order to make the model useable for quantitatively description of the freeze/thaw damage is, to the author's opinion:

- Measurement of water-uptake and dilation to assess whether there is contraction or expansion in the specimen. This also gives information about what kind of forces that are acting; pressure due to ice lenses acting on the pore walls (or hydraulic in very porous materials), or tension due to freezing of a non-critically saturated system.

- Measurements of moisture distribution within the sample as a function of freeze/thaw cycles and testing conditions for both air entrained and non-air entrained concretes. In order to measure internal transport during the freeze/thaw test, measurements shall be carried out continuously, for example by measurement of changes in electrical resistivity in different depths.

- Influence of water quality. It has several times been demonstrated, that increasing degree of hardness of the water also increase the freeze/thaw damage. [11]. (To the author's opinion, this is hard to explain by a physical mechanism, since the opposite seems to be much more reasonable. The softer the water, the more $Ca(OH)_2$ and C-S-H will dissolute, thus coarsening the pore structure.)

  However, the opposite has also been observed [12]. In this test, the same concrete has been freeze/thaw tested using two types of tap water from Aalborg (Carbonate hardness 8.8 dH, total hardness 13.4 dH, pH 7.6) and Borås (Carbonate hardness 9.8 dH, total hardness 5.7 dH, pH 8.0). The observed scaling was 0.15 kg/m^2 using the Aalborg water and 0.28 kg/m^2 for the Borås water.

  Ongoing tests in Aalborg [13] are studying the relationship between ice formation, physical- and thermodynamic properties of the adsorbed water and the freeze/thaw damage in concrete.

- Thermodynamic studies of the adsorbed water.

- Modelling of crack opening around the individual aggregate particles, for example by using microstructural modelling as developed by Prof. Dale Bentz from NIST [14].

- Calculation of the stresses arising from formation of microscopic ice bodies according to Setzer. This could be calibrated against the dilation measurements. This calculation can use the kind of moisture measurements described above, and also be calibrated against the dilation measurements

Finally it must be remembered, that the existing acceptance criteria for durable/non-durable concrete in a laboratory test basically is purely empirical and the acceptance criteria is related to a "worst situation". In practise: How often will concrete be exposed to water or salt solution of a pessimum concentration? A quantitative model can be used for

adjusting acceptance criteria for concrete which are going to be exposed in different climates and for concretes utilising secondary cementing materials and –fillers.

7 CONCLUSION

The model predicts, that frost damage in non-air entrained concrete is caused by the following events.

- During freezing microscopic ice bodies are formed in the capillary pores in the paste.
- Formation and primarily melting of these microscopic ice bodies leads to extensive water uptake from the surroundings, if free water is accessible.
- When the paste becomes critically saturated, formation of the microscopic ice bodies causes a volumetric expansion of the paste.
- This volumetric expansion of the paste results in formation of cracks surrounding the individual aggregate particles. These cracks are empty (air-filled) at the moment they appear.
- Further water uptake, and maybe also redistribution of water from paste towards these empty cracks due to ice formation as in artificial air-bubbles, lead to increased water content in these cracks.
- At a certain time these cracks become critically saturated. Thus the "particle" of aggregate + surrounding crack will expand during freezing.
- Such expanding particles will lead to cracks in the paste, connecting the individual particles. Gradually this crack formation will lead to total breakdown of the internal structure.

Entrained air decreases the degree of damage caused by freeze/thaw, both with regard to scaling and internal damage. The influence on water- or saltsolution-uptake is, however, not clear. This item has to be studied further.

Saltsolution as the freezing media results in much more severe scaling, than pure water. On the other hand, pure water results in higher degree of internal damage, than salt solutions. For non-air entrained concretes this is explained by the model.

The damage mechanism described implies, that it is not possible to produce absolute freeze/thaw resistant non air-entrained concrete unless that the pore structure is so fine and homogeneous that no micro ice bodies can form in the pores in the actual temperature regime. For air-entrained concrete with a fairly dense paste, i.e. water/cement ratios between app. 0.3 and 0.4, the mechanism also clarifies the often-recognised low freeze/thaw durability.

8 REFERENCES

1 Bager, D.H., Jacobsen, S.: "A Model for the Freeze/thaw Damage Mechanism in Concrete". Proceedings from Minneapolis Workshop on Freeze/thaw Damage in Concrete. Minneapolis, Minnesota, USA, June 1999. (To be published as a RILEM publication)

2 "Draft recommendations for test methods for the freeze/thaw resistance of concrete. Slab Test and Cube Test"., Materials and Structures 1995, vol. 28, p 366 – 371

3 Luping, T., Bager, D.H., Jacobsen, S. & Kukko, H.: "Evaluation of the Ultrasonic Method for Detecting the Freeze/thaw Cracking in Concrete" NORDTEST-project No. 1321-97. Swedish National testing and research Institute - Building Technology, SP Report 1997:37, 63 p (40p./8app.) ISBN 917848-693-3

4 Jacobsen, S., Bager, D.H., Kukko, H., Luping, T. & Nordström, K.: "Measurement of internal cracking as dilation in the SS137244 frost test", NORDTEST project 1389 - 98. Norwegian Building Research Institute Report No. 250 : 1999

5 Setzer, M.J.: "Micro Ice Lens Formation and Frost Damage", Proceedings from Minneapolis Workshop on Freeze/thaw Damage in Concrete. Minneapolis, Minnesota, USA, June 1999. (To be published as a RILEM publication)

6 Bager, D.H.: Unpublished results from ongoing tests, 1999

7 Bager, D.H., Sellevold, E.J.: "Ice formation in Hardened Cement Paste, Part I", Cement and Concrete Research, vol. 16, pp. 709 – 720, 1986.

8 Andersen, E.Y.: "Anvendelse af akustisk emission til frostbestandighedsvurdering af beton og konstruktionsovervågning", (In Danish), Ph.D. Thesis, Technical University of Denmark, Department of Structural Engineering, 1983

9 Siebel, E., Reschke, T.: "Three different methods for testing the freeze-thaw resistance of concrete with and without de-icing salt" . RILEM Proceeding No. 30 – "Freeze-Thaw Durability of Concrete", pp 231 - 246. Proceedings from the International Workshop on the Resistance of Concrete to Scaling due to Freezing in the Presence of De-icing Salts. Quebéc, Canada 1993.

10 Jacobsen, S., Sellevold, E.J: "Frost/Salt Scaling Testing of Concrete – Importance of Absorption during Test". Nordic Concrete Research, Publication No. 14/1994, pp 26 – 44.

11 Stark, J., Ludwig, H.-M.: "Influence of Water Quality on the Frost Resistance of Concrete". RILEM Proceeding No. 30 – "Freeze-Thaw Durability of Concrete", pp 157 – 164. Proceedings from the International Workshop on the Resistance of Concrete to Scaling due to Freezing in the Presence of De-icing Salts. Quebec, Canada 1993.

12 Bager, D.H. Unpublished data (1997)

13 Bager, D.H., Hansen, T.B.: "Influence of Water-binding on the ice formation and freeze/thaw damage in cement paste and concrete". To be published in the

proceedings for "Nordic Miniseminar on "Water in cement paste and concrete – hydration and pore structure", 7.-8. October 1999, Skagen, Denmark.

14 Bentz, D.P.: "Three-Dimensional Computer Simulation of Portland Cement Hydration and Microstructure Development.". J. Am. Ceram. Soc. Vol. 80, pp3 – 21, 1997.

FROST RESISTANCE OF FIBRE REINFORCED CONCRETE STRUCTURES

Ernst Jan de Place Hansen
Assistant Research Professor, Ph.D.
Dep. of Structural Eng. and Materials, Technical University of Denmark, Lyngby, Denmark

SUMMARY

Frost resistance of fibre reinforced concrete with 2.5-4.2% air and 6-9% air (% by volume in fresh concrete) casted in the laboratory and in-situ is compared. Steel fibres with hooked ends (ZP, length 30 mm) and polypropylene fibres (PP, CS, length 12 mm) are applied. It is shown that

- addition of 0.4-1% by volume of fibres cannot replace air entrainment in order to secure a frost resistant concrete; the minimum amount of air needed to make the concrete frost resistant is not changed when adding fibres
- the amount of air entrainment must be increased when fibres are added to establish the same amount of air pores as in the corresponding concrete without fibres

1 INTRODUCTION

In this paper results from frost resistance tests on fibre reinforced concrete (FRC) casted in the laboratory and in-situ at a full-scale test area are reported. The tests are performed as part of the Danish research project Design Methods of FRC, which took place from 1996 to 1999 [1], [2]. Overall conclusions from the durability part of the project is presented in [3]. A more detailed report is in writing [4].

The purpose of the durability tests performed in the research project is to indicate whether fibre reinforced concrete exposed to a combination of mechanical and environmental load (chloride, frost, water) is less or more durable than concrete without fibres. Secondly, it is the aim to identify important mechanisms for the effect of the fibres on the durability.

Originally the in-situ concretes were casted for a full-scale study of crack development versus fibre content and type of support. These concretes, opposed to the laboratory casted concretes, contained the expected amount of air, based on the mix design. Therefore, freeze-thaw tests were performed as well.

2 MATERIALS

2.1 Concrete mixes

Six different concretes are mixed in the laboratory (Table 1) and six different concretes in-situ (Table 2) at a full-scale test area near Ølstykke north west of Copenhagen. M, A and SA in Table 1 refer to different environmental classes (moderate, aggressive and more severe than aggressive). 0 refers to concrete without fibres, ZP and PP refers to Table 3.

When casting concrete with PP-fibres, the fibres are mixed with fine aggregate and water before they are mixed with the other ingredients.

At the full-scale test area 6 lanes, 3 m wide, 50 m long and about 120 mm thick are casted. An overview is given in Table 2. In the area where cores were taken, the concrete has been covered with plastic the first week after casting. The concrete in lane 1 is very similar to SA-0 in Table 1.

Table 1. Laboratory concrete mixes.

Material [kg/m^3]	M-0	M-ZP	A-ZP	SA-0	SA-PP	SA-ZP
Cement ASTM Type III	240	240				
ASTM Type V			298	285	313.5	285
Fly Ash	65	65	65	60	66	60
Silica Fume Slurry	15.5	15.5	15.5	24	26.4	24
Water	142.5	142.5	140.5	115	126.5	115
Air entrainment	0.313	0.313	0.427	0.357	0.393	0.357
Plasticizer	0.413	0.413	1.484	1.428	1.571	1.428
Superplasticizer	0.826	0.826	2.968	2.856	7.85	2.856
Aggregate 0-4 mm	774	774	702	758	758	758
Aggregate 2-8 mm			340			
Aggregate 4-8 mm	319	319				
Aggregate 8-16 mm	649	639	669	535	535	535
Aggregate 16-25 mm				565	473	554
Fibre ZP		31.2	31.2			31.2
PP					10.1	

Table 2. In-situ concrete mixes.

Material [kg/m^3]	Lane 1	Lane 2	Lane 3	Lane 4	Lane 5	Lane 6
Support	Gravel, more than 150 mm	Gravel, more than 150 mm	2x0.15 mm PE on PS	2x0.15 mm PE on PS	50 mm PS	50 mm PS
Cement ASTM Type V	285	320	300	320	300	320
Fly Ash	60	60	60	60	60	60
Silica Fume	12	12	12	12	12	12
Water	134	140	138	142	138	144
Air entrainment	0.339	0.823	0.372	0.823	0.372	0.823
Plasticizer	1.428	2.352	1.488	2.352	1.488	2.352
Superplasticizer	3.213	3.920	3.348	3.920	3.348	3.920
Aggr. 0-4 mm	708	715	656	706	654	697
Aggr. 4-8 mm		200		200		200
Aggr. 8-16 mm	535	775	535	775	535	775
Aggr.16-25 mm	565		565		565	
Fibre ZP		78		78		78
CS			0.6	0.6	1.2	1.2

The fibres are listed in Table 3. In the laboratory mixes PP- and ZP-fibres are used, in the full-scale mixes ZP- and CS-fibres are used, according to Table 1 and 2. The amounts of fibres in Table 1 corresponds to 0.4 % (ZP) and 1.0 % by volume (PP), in Table 2 to 1.0 % (ZP) and 0.066-0.132 % by volume (CS). CS-fibres are designed for control of cracking due to plastic shrinkage.

Table 3. Fibres. Material and size.

Fibre	CS	PP	ZP
Material	Polypropylene	Polypropylene	Steel, hooked ends
Length	12 mm	12 mm	30 mm
Cross-section	d = 18 μm	35 x 250-600 μm	d = 500 μm

3 TEST SETUP

3.1 Laboratory concrete

Reinforced beams with dimensions 100x200x1150 mm are used as specimens in the overall project on durability presented in [2]. A test set-up has been developed to permit beams to be subjected to combined mechanical and environmental load [5]. Mechanical load is obtained by exposing the beams to 4-point bending, resulting in transverse cracks on the centre part of the beam. The surface crack pattern is characterized using video-scanning and digital image analysis.

The beams were 5 months old at the time of exposure to mechanical load. They were kept under water until they were loaded and crack widths were measured. The loading of the beams was carried out within 15 minutes. After unloading the crack widths were measured again and specimens for the freeze-thaw test were sawn from the tensile side of the beams.

Each test series consisted of four specimens from two different beams cast in separate batches. Three of the specimens were tested with one mechanically induced crack in the longitudinal direction of the specimen. One specimen was tested without visible cracks as a reference. The dimensions of the test specimens were 50x125x200 mm.

3.2 In-situ concrete

Cores with diameter 150 mm were drilled from the concrete lanes, 7.5 months after casting, which took place in October 1997. One specimen with a thickness of 50 mm was sawn from each core. Each test series consisted of three specimens.

3.3 Freeze-thaw test

Testing was performed according to Swedish Standard SS 13 27 44 Procedure A [6] at the Technological Institute in Taastrup. Before testing the specimens are covered according to [6] and exposed to a 3 mm thick layer of 3% NaCl-solution, protected from evaporation with a plastic foil. The specimens are then exposed to freeze-thaw according to a specified temperature cycle. After 7, 14, 28, 42 and 56 cycles the amount of scaled material [kg/m^2] is determined and the concrete is characterized according to Table 4. Exposed surfaces are casted surfaces (laboratory concrete) and sawn surfaces (in-situ concrete), respectively.

Table 4. Characterization of the frost resistance according to [6].

Frost resistance	Requirement
Very good	For each specimen: $m < 0.1$ kg/m^2 after 56 cycles
Good	$m_{56} < 0.2$ kg/m^2 or { $m_{56} < 0.5$ kg/m^2 and $m_{56} / m_{28} < 2$ } or $m_{112} < 0.5$ kg/m^2
Acceptable	$m_{56} < 1.0$ kg/m^2 and $m_{56} / m_{28} < 2$ or $m_{112} < 1.0$ kg/m^2
Unacceptable	If the requirements for acceptable frost resistance are not met

M_{56}, m_{112}: the mean value for the material scaled after 56 or 112 cycles

3.4 Thin section analysis

Thin section analysis was performed on laboratory and full-scale specimens with ZP-fibres (A-ZP and lane 2 respectively) to study the pore structure, the mixing of fibres and the air content[1].

4 RESULTS

In Table 5 and 6 test results from the freeze-thaw test are shown as amount of scaled material [kg/m^2] after 28 and 56 cycles for all the specimens. In Table 5 the results are grouped according to the fact that specimens for each concrete mix originates from two different batches. Also the average crack width of visible cracks measured in loaded state is given in Table 5. After unloading the crack widths are reduced about 66%.

Measurements of air content in the fresh state (% by volume of concrete) showed that the laboratory concrete contained 2.5-4.2 % (SA), 4.5-6 % (A) and 6-7 % (M) respectively, while the designed air content was 5.5-6.5 %. The in-situ concrete contained 6-9% by volume as designed. Notice that the amount of air entrainment is increased 100% when fibres are added in the in-situ concrete (Table 2). In the laboratory the amount of air entrainment is not increased when fibres are added. Also notice that the maximum size of aggregates is reduced in the in-situ mixes when fibres are added.

Table 5. Freeze-thaw test, laboratory concrete. Casted surfaces. Amount of scaled material [kg/m^2] and crack width in loaded state [mm].

Concrete	M-0		M-ZP		A-ZP		SA-0		SA-PP		SA-ZP	
Beam ID	04	05	09	08	04	05	04	05	04	05	04	05
28 cycles	0.94	0.89	1.06	0.21	0.32	1.03	0.02	0.04	0.25	0.37	0.30	0.10
[kg/m^2]	0.97	0.92	0.64	0.15	0.66	1.12	0.04	0.03	0.53	0.32	0.54	0.09
56 cycles	1.21	1.11	1.54	0.32	0.89	1.94	0.05	0.11	0.97	1.09	0.91	0.31
[kg/m^2]	1.33	1.10	1.02	0.26	1.66	2.22	0.10	0.09	1.41	0.53	1.29	0.29
Crack width	0.09	0.17	0.24	0.17	0.19	0.11	0.19	0.12	0.15	0.07	0.08	0.16
[mm]	0 *	0.23	0 *	0.09	0 *	0.33	0 *	0.23	0 *	0.27	0 *	0.20

*: Specimens from areas without visible cracks (mechanically loaded beams).

Table 6. Freeze-thaw test, in-situ concrete. Sawn surfaces. Amount of scaled material [kg/m^2].

Lane	1	2	3	4	5	6
28 cycles	0.08	0.02	0.02	0.01	0.01	0.03
	0.04	0.01	0.01	0.01	0.01	0.04
[kg/m^2]	0.02	0.01	0.01	0.02	0.02	0.09
56 cycles	0.10	0.03	0.02	0.02	0.02	0.03
	0.04	0.03	0.01	0.01	0.01	0.06
[kg/m^2]	0.03	0.02	0.02	0.03	0.04	0.12

Figure 3 and 4 show examples of the pore structure of laboratory concrete (A-ZP, 0.4% by volume of steel fibre) and in-situ concrete (SA-ZP, 1% by volume of steel fibre). Each picture covers about 4 x 6 mm. Figure 1 and 2 show the results of the freeze-thaw test for the corresponding specimens.

[1] Thin section analysis was also performed on laboratory specimens with PP-fibres in connection with other exposure tests (chloride exposure) (not shown here)

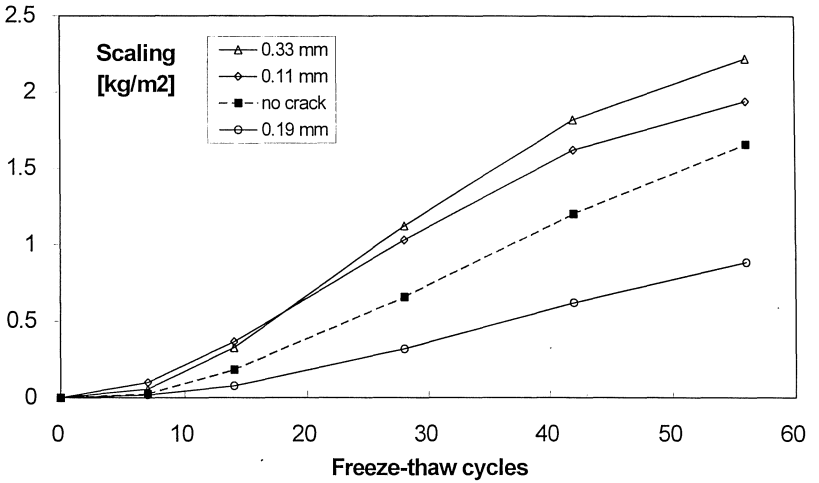

Figure 1. Scaling [kg/m^2] at freeze-thaw exposure. Laboratory concrete A-ZP. Air content in fresh state: 4.5-6 %. The specimens are identified by the crack width [mm] in loaded state.

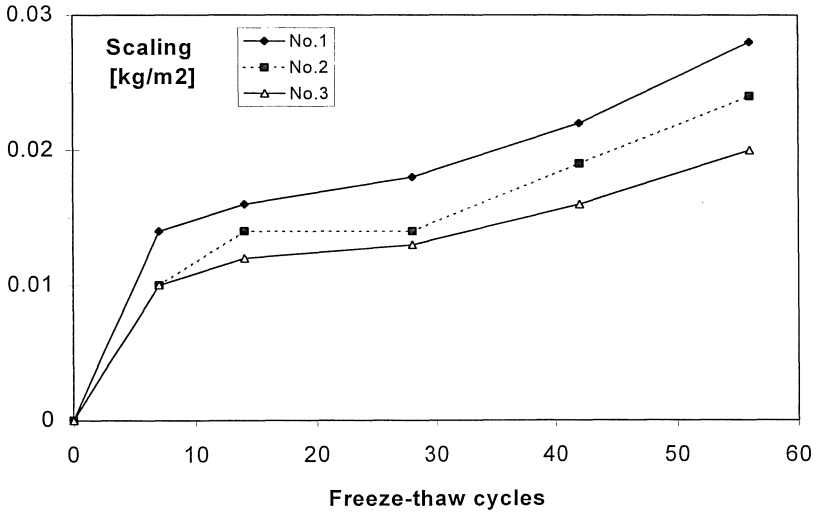

Figure 2. Scaling [kg/m^2] at freeze-thaw exposure. In-situ concrete SA-ZP (lane 2, Table 2). Air content in fresh state: 7.5%.

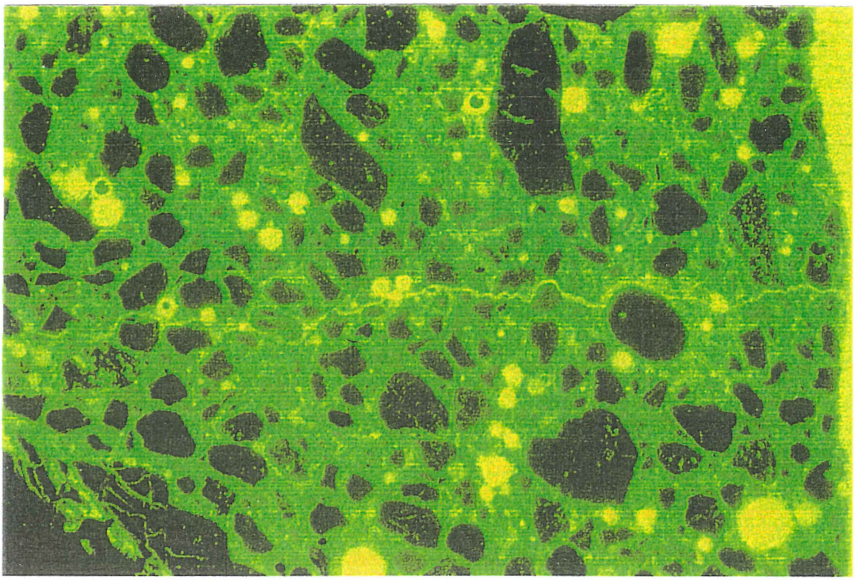

Figure 3. Thin section. Laboratory concrete, A with 0.4% by volume of steel fibre. Fluorescence microscopy. A mechanically induced crack (0.04 mm wide) is seen in the centre part of the figure. Freeze-thaw exposed surface is seen at the right.

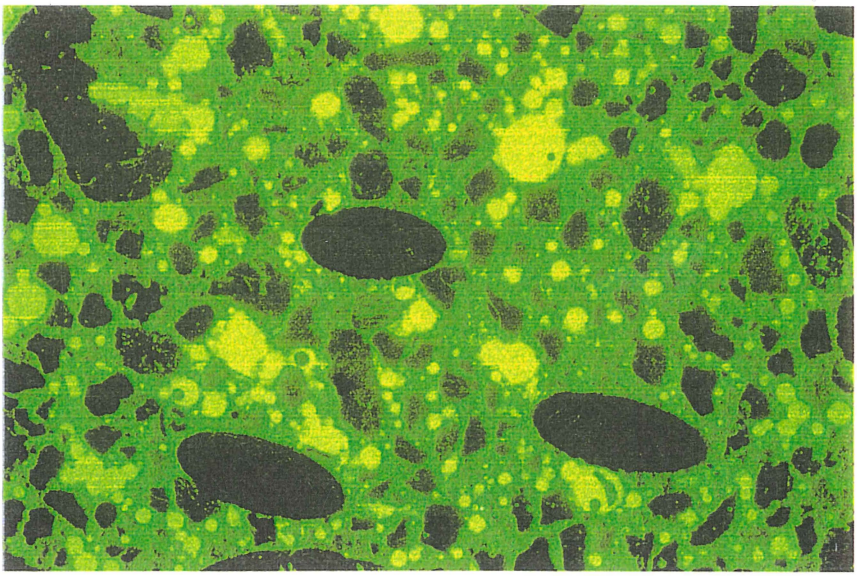

Figure 4. Thin section. In-situ concrete, SA with 1% by volume of steel fibre (lane 2, Table 2). Fluorescence microscopy.

5 DISCUSSION

A literature study shows that the addition of fibres in general do not have decisive importance on the frost resistance of concrete. On the other hand it shows that also FRC needs air entrainment to become frost resistant, regardless of the ability of fibres to arrest cracks and to minimize the extent of cracking. It also shows that addition of fibre can have a negative effect on the air pore structure, especially when adding PP-fibres, [7].

5.1 Laboratory concrete

Results for some of the laboratory mixes have previously been presented in [5].

According to Table 5 and [6] SA-0 has a very good frost resistance since no specimen has more than 0.1 kg/m^2 material scaled after 56 cycles. SA-PP shows a frost resistance on the border between acceptable and unacceptable and SA-ZP is characterized as acceptable (average value less than 1.0 kg/m^2 after 56 cycles). However, the results indicate that the scaling decreases when the crack width increases, especially for SA-ZP.

The fact that the specimens originate from different batches does not seem to explain the results. Neither the properties of the concrete in the fresh state nor the compressive strength after 28 days water curing indicates any differences between the batches.

While the concrete without fibres (SA-0) was designed for an air content of 5.5 % by volume, the actual air contents measured in the fresh state by the pressure method were much lower: SA-0 4.2 %, SA-ZP 3 % and SA-PP 2.5 %. The results therefore emphasize the need for a critical evaluation of the mix design and the mixing methods when designing FRC-structures. To be effective in relation to frost resistance not only the amount of air entrainment but also the stability of the air pore system is decisive. The tests show that the amount of air entrainment needs to be increased when fibres are added to maintain a certain air content.

Even when a satisfying air content is achieved (about 6 % by volume for a concrete with water-cement-ratio 0.4) the PP-FRC normally behaves worse than plain concrete when tested according to [6] although it is having an acceptable frost resistance according to the test method, [8]. On the other hand, in more than one case it seems that the laboratory test has been to tough compared with experiences from natural weathering, [9].

A-ZP and M-0 are characterized as "not acceptable" while the spread on the result for M-ZP is very large depending on which batch is studied. It is not surprising that the M-concretes fails in the freeze-thaw test in spite of 6-7% air (fresh concrete) since they are not designed for this type of exposure. The fact that A-ZP behaves very badly in the freeze-thaw test shows 1) the effect of a unsatisfactory air content, 2) the effect of a less dense concrete (higher water-cement ratio) compared with the SA-mix.

Compared to steel fibres PP-fibres have lower bond strength to the cement matrix [10], which could explain the higher scaling. During the freezing phase the pressure from the water could eventually loosen the PP-fibres from the matrix thereby open the material for more water and thereby accelerating the degradation. Thin section analysis (Figure 3 and 4) shows that the fibres (both PP and ZP) in general are well mixed into the concrete.

The existence of mechanically induced cracks (crack with 0.2-0.3 mm in loaded state) seem quite surprisingly to reduce the amount of scaling at freezing. A satisfactory explanation on this observation is not found. Of course the crack can contain some water and the specimen probably contains more cracks inside, thereby removing water from the surface of the specimen. On the other hand, both specimens with and without mechanically induced cracks and both specimens with a high and a low amount of scaled materials needed to be "refilled" with water during the test. It should also be noticed that the amount of scaled material in general is much higher than accepted to characterize the concrete as frost resistant no matter the induced cracks.

5.2 In-situ concrete

The amount of scaled material is lower than 0.1 kg/m^2 after 56 freeze-thaw-cycles for all the in-situ mixes (Table 6) i.e. the mixes are characterized as very good in relation to frost resistance cf. [6]. Therefore it is not relevant to distinguish further between the in-situ mixes.

The amount of scaled material of concrete without fibres (lane 1) is comparable with the corresponding laboratory concrete (SA-0).

The higher frost resistance of the in-situ mixes corresponds with the fact that they contain a higher amount of air in fresh state (6-9 % by volume) as a result of the higher amount of air entrainment compared with the laboratory mixes. This is supported by thin section analysis. Notice that the in-situ mixes do not include SA-PP. This combination of concrete and fibres gave the lowest workability and the most unsatisfactory air pore structure in the laboratory.

5.3 Thin section analysis

Figure 3 and 4 and corresponding figures of concrete with PP-fibres show that the fibres are well mixed into the concrete. When comparing Figure 3 and 4 one clearly sees the difference concerning the air pore system. In Figure 3 the amount of air pores is low compared with Figure 4 and the distribution of air pores is not satisfactory. Figure 4 shows that it is possible to achieve a high air content and still have a satisfactory distribution of the air pores when steel fibres are mixed into the concrete. The paste seems homogeneous and the concentration of air pores is neither lower nor higher around the fibres compared to the concrete in general. The effect of the different air pore systems on the frost resistance is clearly seen in Figure 1 and 2.

6 CONCLUSIONS

The tests show that concrete with an air content of 6-9 % by volume and a water/cement ratio 0.4 is frost resistant according to [6] and that the frost resistance is not affected by the addition of 1% by volume of steel fibres and/or 0.13 % by volume of CrackStop-fibres. If the air content and/or the concrete quality (expressed by the water/cement ratio) are lower, the concrete is not frost resistant no matter the type of fibre (steel or polypropylene). Thin section analysis show that the fibres in general are well mixed into the laboratory and in-situ concrete.

The addition of the specific PP-fibres tested in this project makes it harder to obtain a satisfying air content in relation to frost resistance. Also the PP-fibres seem to have a negative effect on the workability of the concrete. The tests show that a higher amount of air entrainment is needed to maintain a satisfactory amount of air when fibres are added. The results emphasize the need for a critical evaluation of the mix design and the mixing methods when designing FRC-structures, especially in relation to mixes with PP-fibres.

Addition of fibres does not change the importance of a good concrete quality, including a certain amount of air entrainment to secure the frost resistance.

7 ACKNOWLEDGEMENTS

The present work is part of the research project *Design Methods for Fibre Reinforced Concrete* funded by the Materials Technology Development Programme, MUP2, under the supervision of the Danish Council of Technology, the Danish Technical Research Council and the Danish Natural Science Research Council. Freeze-thaw tests were performed at The Concrete Centre at the Technological Institute in Taastrup.

8 REFERENCES

1. Stang H. (1996) Design methods for fibre reinforced concrete. Proc. Nordic Concrete Research Meeting, Espoo, Finland 1996. Pp.93-94.
2. Hansen, E.J. de Place and Hansen, K.K. (1996) Durability of fibre reinforced concrete structures. Proc. Nordic Concrete Research Meeting, Espoo, Finland 1996. Pp.277-278.
3. Hansen, E.J. de Place and Hansen, K.K. (1999) Durability of fibre reinforced concrete structures exposed to combined mechanical and environmental load. Submitted to XVII Symp. on Nordic Concrete Research, Reykjavik, Iceland, Aug 1999. 3p.
4. Hansen, E.J. de Place (1999): *Durability of fibre reinforced concrete structures. Final report. Experimental investigations.* (in Danish). Dep. of Structural Engineering and Materials, Technical University of Denmark. (in writing)
5. Hansen, E.J. de Place and Nielsen, L. (1997) Durability of cracked fibre reinforced concrete structures. Pp.145-152 in: *Advanced Design for Concrete Structures.* (Gylltoft et al, Eds.). A publication of Int. Center for Numerical Methods in Engineering. (CIMNE), Barcelona.
6. SS 13 72 44 (1995) *Concrete testing - Hardened concrete - Scaling at freezing* (in Swedish). SS 13 72 44, 3.udgave. Standardiseringen i Sverige, mar 1995.
7. Hansen, E.J. de Place (1998) *Durability of fibre reinforced concrete and cracked concrete structures. State-of-the-art* (in Danish with summary in English). Series R No 48. Dep. of Structural Engineering and Materials, Technical University of Denmark, Lyngby.
8. Larsen, E.S. (1992): *Service life prediction and fibre reinforced cementitious composites.* Ph.D.thesis. SBI Report 222, Danish Building Research Institute, Hørsholm.
9. Glavind M. (1993) *Fibre reinforced concrete* (in Danish). Materials Technology Development Programme (MUP1) 1989-92. Danish Technological Institute, Taastrup.
10. Rasmussen, T.V. (1997) *Time dependent interfacial parameters in cementitious composite materials.* Ph.D.thesis. Series R No. 33, Dep. of Structural Engineering and Materials, Technical University of Denmark, Lyngby.

MODIFIED PROCEDURE FOR DETERMINATION OF INTERNAL FROST RESISTANCE BY THE CRITICAL DEGREE OF SATURATION METHOD

Göran Fagerlund
Division of Building Materials, Lund Institute of Technology
Box 112, SE-221 00 Lund, Sweden

1 INTRODUCTION

More than 25 years ago the Critical Degree of Saturation Method, the S_{CR}-method, was suggested as a general method for determination of the internal frost resistance of porous materials, also giving a possibility to predict a sort of potential service life and making quantitative comparisons between quite different types of material possible [1]. The test procedure as applied to concrete was described in a RILEM Tentative Recommendation published in 1977 [2]. At the same time, its potential for testing concrete was investigated in an international cooperative test [3]. The deviation in the test results between different laboratories were remarkably small. Despite the big potential of the S_{CR}-method, it is only used at a few laboratories and then mostly as a research tool. Possibly the main obstacle for a more wide use is that the method is supposed to be laborious and time-consuming.

In this paper the test principles and test procedures are described. The main results of the cooperative test are presented indicating the potential of the method. Problems of more principal nature are discussed and solutions to solving these problems and refining the method are described. Many of the problems can be considerably reduced or avoided by using thin plates for determination of the critical degree of saturation. Examples from a study perfomed 20 years ago where such thin specimens were used are presented.

2 THE S_{CR}-METHOD. BASIC PRINCIPLES

The Critical Degree of Saturation Method (S_{CR}-method) is based on the following principles:

1: For each concrete there is a certain maximum water content that can accepted if the concrete shall remain undamaged by frost, [1, 4]. This maximum water content can be expressed in terms of a degree of saturation S_{CR} that can be defined

$$S_{CR} = W_{CR}/V_p \quad 0 \leq S_{CR} \leq 1 \qquad (1)$$

where W_{CR} is the maximum allowable (critical) water content [m^3/m^3]
V_p is the total pore volume in concrete including all pores (pores in cement paste, air-pores, pores in aggregate, porous interfaces, crack volume, etc) [m^3/m^3]

S_{CR} is an individual value for each concrete. Normally its value is reduced with increased air content, a fact that can be shown theoretically [4]. S_{CR} seems to be very little influenced by the freezing rate and the number of repeated freeze-thaw cycles. Probably, S_{CR} is decreased somewhat with decreased temperature. Since most ice is formed before -10°C, this effect is marginal when normal freeze-thaw cycles are used. Possibly, the problem can be avoided more or less completely when the degree of saturation is defined as an *effective* degree of saturation S_f:

$$S_{f,CR}=W_{f,CR}/(W_{f,CR}+V_a) \quad (2)$$

Where W_f is the freezable water [m^3/m^3]
V_a is the air-filled pore volume [m^3/m^3]

There is a simple relation between S_{CR} and $S_{f,CR}$. The relation depends on the amount of freezable water. Thus, it is a function of temperature. In the following, definition (1) is used. S_{CR} can be determined by a freeze-thaw experiment using moisture sealed specimens conditioned to different levels of S before the test, [2].

2: In a real structure, the same concrete will reach a moisture state that is highly variable and which depends on the moisture characteristics of the environment. This moisture content can be expressed:

$$S_{ACT}=W_{ACT}/V_p \quad (3)$$

Where W_{ACT} is the actually occurring degree of saturation [m^3/m^3].

S_{ACT} will be a function of time, $S_{ACT}(t)$. In theory, this function might be predicted by a theoretical calculation of the future moisture state provided one has access to precise quantitative information of the future outer environment and proper calculation tools as regards material data and equations for moisture transport in the "overcapillary" range. In reality, accurate calculations (predictions) of S_{ACT} are very difficult or even impossible since we have no good theories or calculation tools for this type of moisture transport.

3: Frost resistance F can now be quantified through the expression:

$$F= S_{CR}-S_{ACT} \quad (4)$$

Or, since S_{ACT} (and to a certain extent also S_{CR}) is a function of time:

$$F(t) = S_{CR}(t) -S_{ACT}(t)\approx S_{CR}-S_{ACT}(t) \quad (4')$$

Therefore, also frost resistance is a function of time. In a very moist environment with no possibility for the material to dry F will normally diminish with time. Possibly, it might even become negative. In environments with varying moisture contents F will fluctuate with time. Sometimes frost resistance is high (like in the summer or during dry winters), sometimes is is low, or even negative (like during a very moist autumn directly followed by a period of hard freezing). *Thus, frost resistance is not an absolute property but a function of the environment.*

S_{ACT} is a highly stochastic property (as is to a certain extent also S_{CR}). Therefore, F defined by eq (4') will also be a stochastic property. A probabalistic approach for determination of the risk of frost damage can therefore be used. An attempt is made in [5].

Frost resistance defined by eq (4') is, at a certain point of time, only a function of the amount of water in the concrete at that time. Therefore, frost resistance as defined by eq (4') goes up and down with the fluctuating moisture content. It can very well be lower when the concrete is young than when it is old provided the situation is such that the average water content diminishes with the concrete age, and/or when the critical degree of saturation increases with age. Some studies actually indicate that S_{CR} increases with time. An example of this is shown in Fig 1 [5].

Frost resistance as defined by eq (4´) is illustrated in Fig 2.

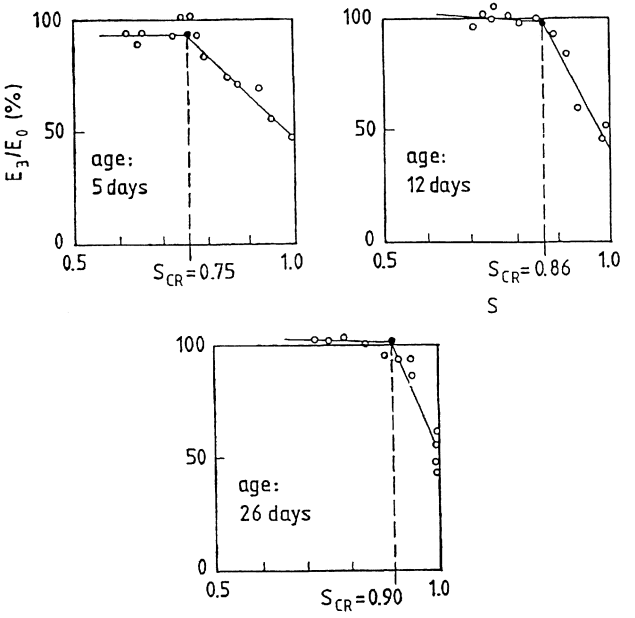

Figure 1. Example of the effect of concrete age on its critical degree of saturation [5].

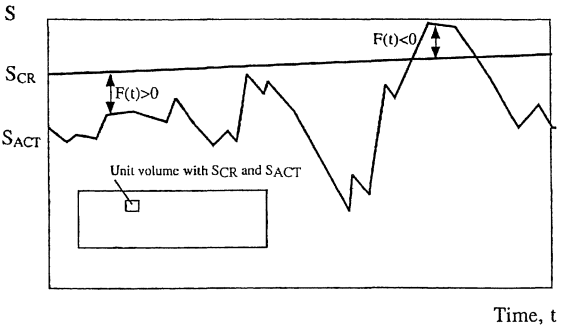

Figure 2. Illustration of "frost resistance" as defined by eq (4´).

4: Since it is impossible to predict the real moisture condition in all parts of the structure, S_{ACT} can be replaced by a simple water uptake test such as the moisture uptake during uninterrupted capillary suction in a thin concrete slice. This degree of saturation is called *the capillary degree of saturation*, $S_{CAP}(t)$, and is a function of the water uptake time.

Then, frost resistance is defined

$$F(t)=S_{CR}-S_{CAP}(t) \qquad (4'')$$

In capillary water uptake, the water content increases steadily with time. Therefore, frost resistance defined by eq (4´´) will gradually diminish with increasing time, provided S_{CR} is constant, or decreasing with time, or increasing with time by a slower rate than S_{CAP}.

F(t) can be called a *"potential frost resistance"* which is the frost resistance under very moist conditions with no possibility for the concrete to dry

Frost resistance as defined by eq (4´´) is illustrated in Fig 3.

3 SERVICE LIFE WITH REGARD TO FROST ATTACK

The definition of frost resistance according to eq (4) can be used for defining the service life with regard to frost. The assumption is that one single freezing of a given representative unit volume with a degree of saturation above the critical is sufficient for destroying the unit volume in question. Thus service life, t_{life}, is defined by the condition:

$$S_{ACT}(t_{life}) = S_{CR} \qquad (5)$$

Since it is impossible to predict exactly the future moisture content it is appropiate to use the concept *"potential service life"*, $t_{p,life}$. This is defined as the time it takes for the unit volume to become critically saturated when it is exposed to uninterrupted water absorption from an unlimited outer source of free water. Then S_{ACT} is replaced by the capillary degree of saturation, $S_{CAP}(t)$, and service life is defined

$$S_{CAP}(t_{p,life})=S_{CR} \qquad (5')$$

It can be shown by simple analytical modelling that the water uptake process in the air-pore system of a concrete during long-term water storage can be approximately expressed [6]:

$$S_{CAP}\approx A+B\cdot t^{C} \qquad (6)$$

Where the term A corresponds to the so-called "nick-point" in a capillary absorption experiment and the term $B\cdot t^{C}$ describes the long-term water absorption in the air-pores. B is a function of the diffusivity of dissolved air and C is a function of the shape of the air-pore system ($C\leq 0.5$), [6].

By combination of eq (5´) and (6) an analytical expression for the potential service life is obtained

$$t_{p,life}= \{(S_{CR}-A)/B\}^{1/C} \qquad (7)$$

Where the value S_{CR} is determined by a freeze/thaw experiment and the coefficients A, B and C are determined by a capillary absorption experiment.

The concept potential service life is illustrated in Fig 3.

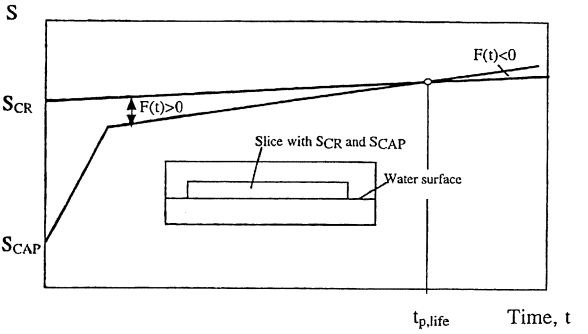

Figure 3. Illustration of "frost resistance" as defined by eq (4´´) and of "potential service life" as defined by eq (5´).

4 EXPERIMENTAL DETERMINATION OF FROST RESISTANCE BY THE S_{CR}-METHOD

4.1 General

In the experimental method for determination of frost resistance by the S_{CR}-method the definition (4´´) is used. The test principles are described in [2].

The test is composed of two parts:

Part 1: Determination of S_{CR} by a freeze-thaw experiment
Part 2: Determination of $S_{CAP}(t)$ by a capillary water uptake experiment.

The values S_{CR} and $S_{CAP}(t)$ are used for calculating the potential frost resistance by eq (4´´) and the potential service life by the general eq (5´) or the special eq (7).

4.2 Determination of S_{CR}

Specimen dimensions and origin
S_{CR} is determined on cylinders (or prisms) that are representative for the concrete, i.e their diameter shall be at least 3 times the biggest aggregate. Preferably, damage is determined by changes in the fundamental frequency of transverse vibration (a measure of the so-called dynamic E-modulus). Therefore, the diameter of the cylinder shall preferably be at least 2 to 3 times the diameter. For an aggregate size of 25 mm, a cylinder with the diameter 10 cm and length 20 to 30 cm is suitable.

The specimens can be cast and pre-cured as desired, or drilled from the structure.

Number of specimens
Normally, at least 10 specimens are required. If there are fewer specimens these can be used repeated times with gradually increased water content until damage occurs. Between each new freeze-thaw test, the water content in the specimen is increased by a new drying-resaturation cycle as described below.

Pre-treatment
The specimens are adjusted to different degrees of saturation between about 0.70 to 1.00. A lower spectrum of degrees of saturation are used when the air-content is high (≈0.70 to ≈0.90) and a higher spectrum when the air content is low (≈0.80 to ≈1.00).

The adjustment is made by pre-drying the specimen at about 50°C (involves a certain but not unnatural ageing effect, see paragraph 5 below), and the vacuum-treatment is made at about 2 torr residual air-pressure. Water is sucked into the specimen while the vacuum-pump is running. The specimens are stored in water until they can be regarded completely saturated. The dry weight and the weight in water and air are determined. From these weighings the weight corresponding to a certain degree of saturation can be calculated. Then, the specimen is dried in an oven at about 50°C until it reaches its desired weight. Then, drying is immediately interrupted and the specimen is sealed in heavy plastic foil.

Freeze-thaw test
After some time (a few days), moisture is more or less completely evenly distributed in the cylinder and the dynamic E-modulus is determined. The specimen is again sealed by plastic foil.

The sealed specimen is placed in a freeze-thaw cabinet and exposed to 5 to 10 freeze-thaw cycles down to about -20°C (or any other suitable temperature). Between each new cycle the specimen shall be completely thawed.

After terminated freeze-thaw, the residual E-modulus is determined and the specimen weighed.

After the test, the specimen is dried completely at +105°C and weighed. It is resaturated by vacuum and weighed in air and water. From these measurements the following can be determined:

1: The exact value of the degree of saturation that prevailed during the freeze-thaw test. Normally, since a certain permanent volume increse can be suspected to occur for some specimens, S shall be calculated on basis of the volume *before* the freeze-thaw test.
2: The residual, permanent, volume expansion.

The residual dynamic E-modulus is plotted versus the degree of saturation. Normally, a rather clear borderline between undamaged (or only slightly damaged) specimens and severely damaged specimens can be discerned at a certain degree of saturation. This borderline defines the value of S_{CR}. The least square method can be used for identifying the value of S_{CR}.

An example of a determination of S_{CR} of a concrete is shown in Fig 4. The S_{CR}-value is:

$$S_{CR}=0.845.$$

Fig 4 clearly shows that the number of freeze-thaw cycles has almost no influence on the S_{CR}-value. This is because the specimens are sealed so that each new cycle occurs with exactly the same internal water content. In "open" freeze-thaw, where the specimen has access to moisture, a gradual water uptake will normally occur during each cycle. Therefore, frost damage often increases with increasing number of freeze-thaw cycles. This is often referred to as a "fatigue effect" which in fact it is not. There is no true fatigue involved in freeze-thaw damage; only a few cycles are enough to severely damage the concrete if the water content is above the critical. There is a certian "low-cycle fatigue", but only for $S>S_{CR}$ a region which is of little interest for defining S_{CR}. This low-cycle fatigue and the effect of number of freeze-thaw cycles on damage is further treated in [7].

(NOTE: The volume change ΔV can be used as additional information. Then, ΔV is plotted versus the degree of saturation. Normally, a distinct borderline between no volume change and a marked volume change can be observed at about the same value of S as for the E-modulus [3].)

(NOTE: Instead of determining the critical degree of saturation one can determine the critical *moisture ratio* [kg/kg]. In this case, it is not necessary to determine the specimen volume, neither before adjusting the specimen before freeze-thaw, nor after terminated freeze-thaw. An example of the use of the moisture ratio is seen in Fig 16.)

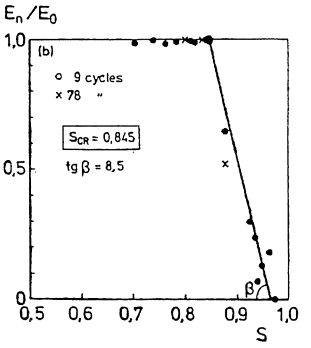

Figure 4. Example of a determination of the critical degree of saturation of a concrete (w/c=0.45, air content 6 %).

4.3 Determination of S_{CAP}

Specimen dimensions and origin
S_{ACT} is determined on thin slices sawn from cast cylinders or drilled-out cylinders. The slice has to be thin enough to enable the identification of an evident "nick-point" in a water uptake-time diagram separating the initial phase with a rising water front from a later phase where the coarse pore system (the air-pore system) is gradually water-filled. For normal concrete (w/c<0.45) a thickness of about 15 to 25 mm can be used. For high performance concrete with very low w/c-ratio the slice must sometimes be thinner.

It is also important that the long-term absorption in the air-pore system occurs simultaneously over the entire cross-section. If not, the calculated S_{CAP}-value, being an average value for the entire slice, under-estimates the degree of saturation in that part of the slice that is closest to the water source. Also for this reason it is important to use slices that are as thin as possible.

The specimens should be of the same origin as the specimens for S_{CR} in order to make a fair comparison beteween S_{CR} and S_{CAP} possible. The S_{CR}-cylinder is rather long, however, while the slice is thin. Therefore, in order to be representative, the slices should not be taken from one location only, but from different depths; see Fig 5. The pre-treatment of the cylinder from which the S_{CAP}-specimens are sawn should be exactly the same as for the S_{CR}-specimens.

Number of specimens
Normally, at least 5 specimens are required. More specimens can be used if the variation in the concrete is big.

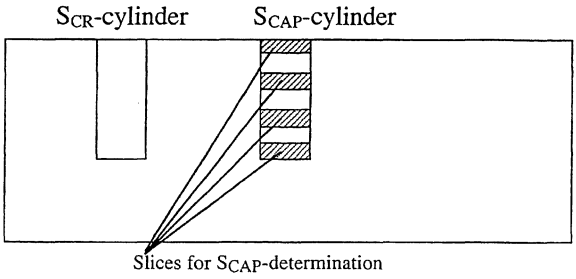

Figure 5. Principles for the selection of specimens for S_{CAP}-determination.

Pre-treatment
Before water uptake the slices are pre-dried. Theoretically, this drying should be made at about 50°C in order that the S_{CAP}-specimens shall have the same pre-treatment as the S_{CR}-specimens. Drying in room-atmosphere can be made, but then the eventual ageing effect caused by increased temperature will not be considered. Carbonation of the surface of the cylinder should preferably be avoided by storing and drying the slices under CO_2-free atmosphere.

Water uptake test
After cooling to room temperature the specimens are placed in a tray with water so that about 1 to 2 mm of the bottom surface is immersed. The weight increase is followed by rapidly taking the slice from the bath, drying its sorption surface with a moist sponge, and weighing it. Then, the slice is immediately put back into the bath. The weighings are made with short intervals during the first hours (5-15 minute interval) and with longer intervals thereafter (1 hour to 3 days, or more). The absorption experiment is run for at least 14 days but preferably it is prolonged.

After the test, the specimen is dried completely at +105°C and weighed. It is resaturated by vacuum in the same manner as the S_{CR}-specimens and weighed in air and water. From these measurements the pore volume can be determined for each specimen. Then, S_{CAP} as function of the water absorption time can be calculated. The mean value for the specimens defines the S_{CAP}-curve.

An example of a determination of S_{CAP} of the same concrete as in Fig 4 is shown in Fig 6. In this case the absorption curve can be expressed

$$S_{CAP}=0.66+3.81\cdot10^{-3}\cdot t^{0.42} \qquad \text{(t in hours)}$$

(NOTE: Instead of determining the capillary degree of saturation one might determine the capillary *moisture ratio* [kg/kg]. In this case it is not necessary to determine the specimen volume but only to dry the specimen completely after the test.)

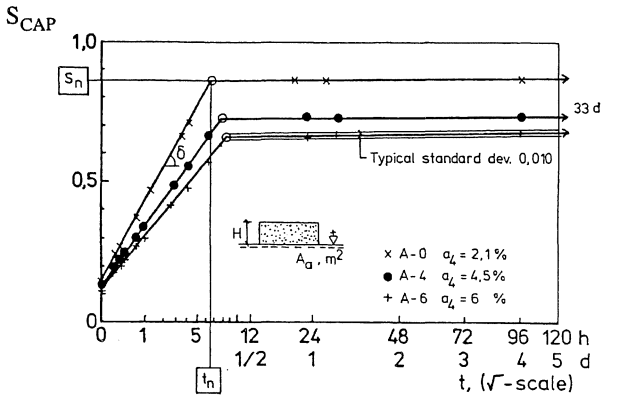

Figure 6. Example of a determination of S_{CAP} for the same concrete as in Figure 4. (The lowest of the three curves is valid. The other curves are valid for other concretes).

4.4 Determination of the frost resistance and the potential service life

Frost resistance is defined according to eq (4´´). For the concrete in Fig 4 and 6 it is valid

$$F(t)=0.845 -\{0.66+3.81\cdot10^{-3}\cdot t^{0.42}\}$$

The potential service life is:

$$t_{p,life} = \{(0.845-0.66)/3.81\cdot10^{-3}\}^{1/0.42} = 1.03\cdot10^4 \text{ hours (431 days)}$$

4.5 The international comparative test of the S_{CR}-method

A comparative test of the S_{CR}-method was performed during the years 1974-1975. Two concretes were produced and cured at our department and thereafter tested at 5 European laboratories. The results of the test have been published, [3]. A short review of the results are given below.

The characteristics of the concretes were as follows:

Concrete Type I:	Non-air-entrained	Fresh air content 2.1%.	w/c-ratio 0.50
Concrete Type II:	Air-entrained.	Fresh air content 7.6%.	w/c-ratio 0.57

The S_{CR}-cylinders (diameter 100 mm, length 200 mm) were stored in saturated lime water for 63 days and then pre-dried at +50°C to interrupt the hydration and cause a certain ageing. Then, they were sent to the laboratories. The slices (thickness 25 mm) were cut from the same type of cylinders as the S_{CR} -cylinders. They were also stored in saturated lime water for 63 days and then pre-dried at +50°C in CO_2-free atmosphere.

The freeze-thaw procedure was carefully prescribed. Despite this, there were rather big differences between the different labotatories. So for example the rate of freezing within the range 0°C to -10°C varied from 1.9°C/h to 7.1°C/h. The minimum temperature varied from -17°C to -24°C; see Fig 7. 6 freeze-thaw cycles were run at each laboratory.

Despite the rather big variation in the freeze-thaw cycle the S_{CR}-value was fairly well-defined as seen in Fig 9 and Table 1. There possibly is a marginal effect of the freezing rate as seen in Fig 8 where the S_{CR}-value is plotted versus the freezing rate.

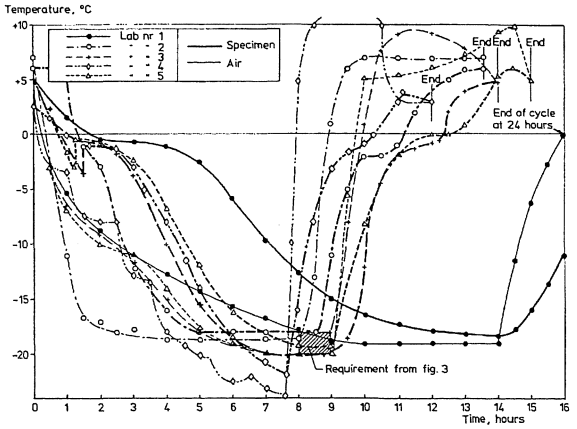

Figure 7. Freeze-thaw cycles used at different laboratories in the cooperative test [3].

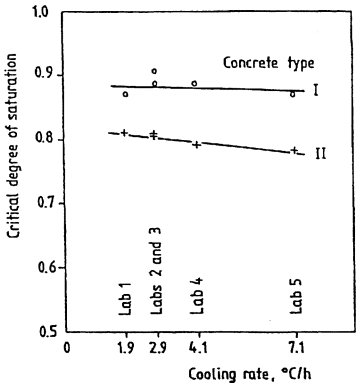

Figure 8. The critical degree of saturation versus the cooling rate between 0 and -10°C [3].

The S_{CAP}-determination was run for 14 to 21 days. The results are shown in Fig 10. S_{CAP} after 2 weeks of absorption are also shown in Table 1. The spread in results is remarkably small.

The frost resistance is calculated by eq (4´´) and plotted in *lin-log scale* in Fig 11. Values of the frost resistance after 2 weeks of water uptake are also listed in Table 1.The difference in service life between non-air-entrained and air-entrained concrete is evident.

Table 1: Results of the International Comparative Test of the S_{CR}-method [3].

Lab No	Δθ/Δt	Concrete Type I			ConcreteType II		
	0→-10°C	S_{CR}	S_{CAP}(14 d)	F(14 d)	S_{CR}	S_{CAP}(14d)	F(14d)
1	1.9°C/h	0.870	0.900	0.030	0.810	0.645	0.165
2	7.1	0.870	0.910	0.040	0.780	0.690	0.090
3	4.1	0.885	0.925	0.040	0.790	0.660	0.130
4	2.9	0.875	0.900	0.025	0.810	0.660	0.150
5	2.9	0.900	0.910	0.010	0.805	0.650	0.155
Mean		0.880	0.910	0.030	0.800	0.660	0.140
Stand. dev.		0.013	0.012	0.012	0.013	0.017	0.030

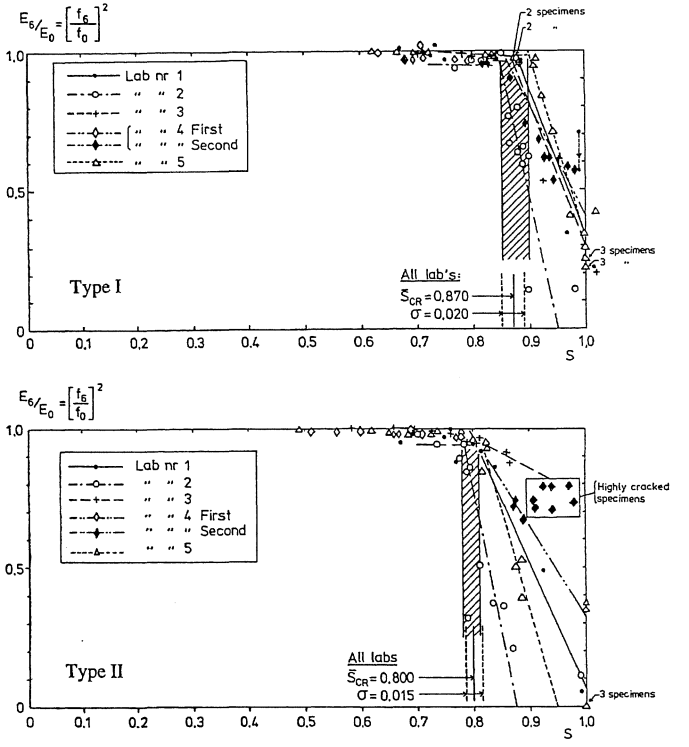

Figure 9. The International Cooperative Test. Results of the determination of S_{CR} [3].

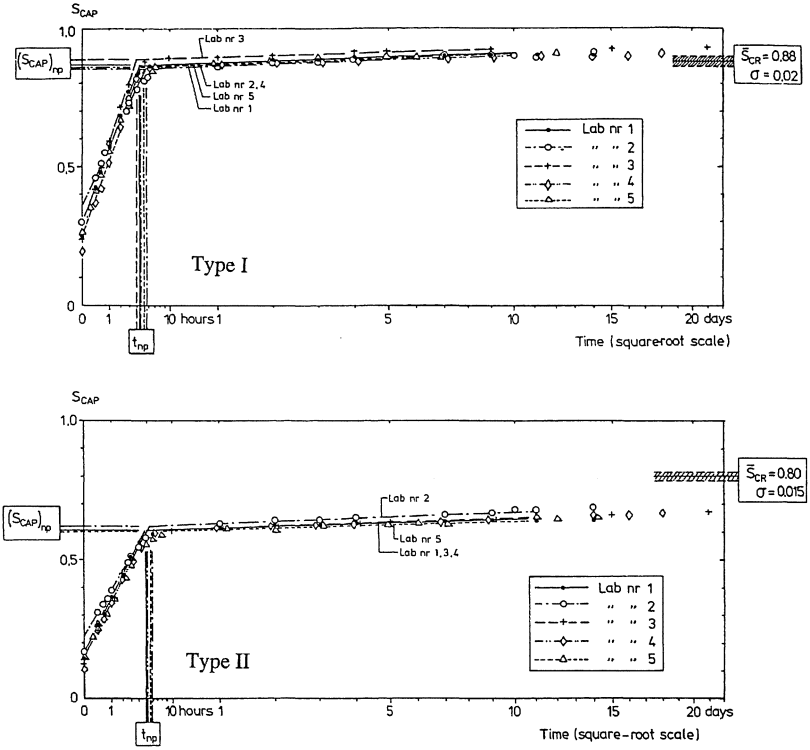

Figure 10. The International Cooperative Test. Results of the determination of S_{CAP} [3].

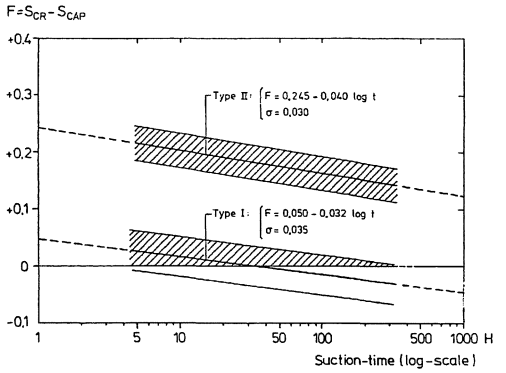

Figure 11.The International Cooperative Test. Results of the determination of "frost resistance" as defined by eq (5')[3].

It is noteworthy that the differences in frost resistance determined at the different laboratories are so small, especially considering the fact that 4 of the laboratories had never used the SCR-method before. There are few (or no) international comparative investigations of frost testing methods that have given so small differences between different laboratories. This indicates that the SCR-value is a fairly "insensitive" property, which is not so much influenced by deviations in the test procedure. The same is valid for the capillary absorption test.

5 SOME THEORETICAL DIFFICULTIES WITH THE S_{CR}-METHOD

Theoretically, there are some problems with the S_{CR}-method that ought to be considered:

Problem 1:
The drying of cylinders before adjustment to the desired S-value is rather time-consuming. This problem is more pronounced the higher the concrete quality (the lower the w/c-ratio). Normally, more than 1 week is required for normal concrete, and even longer time for high performance concrete.

Problem 2:
The concrete might have a certain variation in its properties from the surface inwards. Thus, a cylinder drilled from the real structure, or cast, will have different air-pore characteristics on different depths from the surface. Thus, the S_{CR}-value determined is not as precise as it might have been, had the air-pore system been exactly the same over the entire specimen volume. The S_{CR}-value is a sort of mean value for the entire, rather big, specimen.

Problem 3:
The slice for determination of S_{CAP} is only representative for the rather thin part of the concrete that it represents. Maybe, therefore, the air-pore structure of the S_{CAP}-slice is somewhat different from that of the S_{CR}-cylinder. This defect can partly disappear if the S_{CAP}-slices are taken from different depths that are representative for the entire concrete; Fig 5.

Problem 4:
The S_{CR}-value almost always corresponds to a certain water-filling of the air-pore system. In the test, the S_{CR}-value is determined on specimens that are *dried* to different S-values while the S_{CAP}-value is determined on specimens that are *moistened.* There might be a hystersis (e.g. due to an "ink-bottle effect") between drying and absorption so that for a given S-value coarser air-pores are water-filled at desorption than at absorption. If so, it is theoretically wrong to compare the S_{CR}-value and the S_{CAP}-values as is done in the S_{CR}-method. The hysteresis is visualized in Fig 12. A discussion of the mechanism behind hysteresis phenomena in the "over-capillary" range is performed in [8].

Problem 5:
During drying to the desired water content before freeze-thaw, some moisture gradients over the cross-section might arise. Therefore, the average S-value of the specimen is not necessarily representative for the entire volume. Some parts might be drier and some wetter. The effect has been investigated for other materials than concrete and turned out to exist, but not to be so big [1]. Most of the gradients disappear when the concrete cools down, first to room-temperature, and finally to the freezing point. The effect will lead to a somewhot lower S_{CR}-value than the real value, that is valid for a small unit volume with no moisture gradients.

Problem 6:
In the general definition of frost resistance by eq (4) no consideration is taken to how water enters the concrete. In the test, however, only isothermal capillary water uptake is considered.

In reality, under certain circumstances, some more water might enter the concrete. Examples of such circumstances are:

1: Repeated freeze-thaw under very moist conditions. Then, water might be forced in by other, more forceful, mechanisms than these acting during isothermal water uptake.
2: Condensation of moisture under dense surface layers due to temperature gradients.

These water uptake mechanisms are not considered in the test as it is designed now.

Problem 7:
Absorption in the air-pore system during the S_{CAP}-test is assumed to take place simultaneously and evenly over the entire specimen volume, i.e. absorption is not assumed to take part as a moving boundary from the water surface inwards. This can be questioned because it should be more easy for dissolved air to escape from pores that are closer to a free surface. An analysis performed in [4] on the rate of dissolution of air in an air-pore and the rate of water absorption from the water surface filling the emptied pore, indicates, however, that it is reasonable to assume a more or less uniform absorption if the S_{CAP}-slice is sufficiently thin. Studies of the effect of slice thickness on the long-term absorption ought to be performed, however, in order to verify the hypothesis. Probably, there will be a deviation from uniform absorption when the specimen reaches a certain critical thickness which might be rather small for concrete with low water/binder ratio.

Problem 8:
The pre-drying before adjusting specimens to different S-values before the S_{CR}-test and before the absorption test is started can be questioned. Drying has two effects, one positive and one negative. The positive effect is that water-filled pockets in the concrete, or water-filled coarse aggregate pores are dried-out and are then very difficult to resaturate by normal means. The negative effect is that the amount of freezable water tends to increase substantially when a concrete is dried once. There are many observations that the positive effect is dominating over the negative in a traditional freeze-thaw test. In the S_{CR}-method, however, these emptied pockets are re-saturated more or less completely during the vacuum-treatment before the frost test. Therefore the positive effect shoud be very much reduced at determination of S_{CR}. On the other hand the negative effect of increased amount of freezable water will still be there. Thus, the net effect might be that the S_{CR}-value measured is a bit lower than the value valid for undried concrete. On the other hand, also the S_{CAP}-value is a bit lower due to the problem of filling emptied pockets.

Besides, it is not unlikely that a concrete surface in a real structure will reach both +50°C and higher temperatures during hot summerdays. Therefore, the drying phase used in the S_{CR}-method is not necessarily unnatural for field concrete.

In the following paragraphs procedures are outlined to avoid, or diminish, the first six of the problems. The other two problems are discussed above.

(NOTE: It must be observed that the problems presented above are not bigger than different problems related to other freeze-thaw tests in use today.)

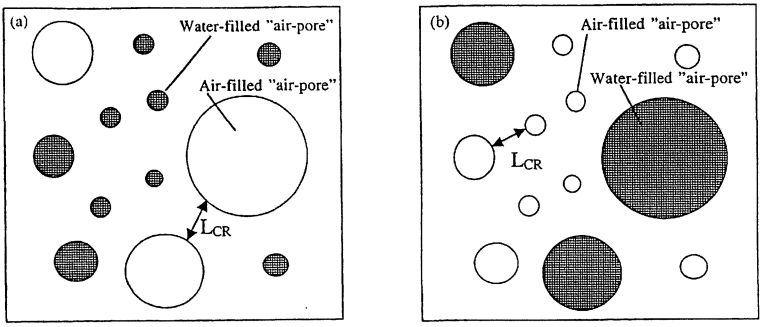

Figure 12. Illustration of moisture hysteresis in the air-pore system. (a) Absorption giving the lowest possible value of S_{CR}. (b) Desorption giving the highest possible value of S_{CR} [7]

6 THIN SPECIMENS FOR DETERMINATION OF S_{CR}

6.1 Principles

Problems 1, 2 and 3 can be solved more or less completely if S_{CR} is determined on the same type of specimens as S_{CAP}, i.e. on thin slices with the same diameter and thickness, and taken from the same location inside the concrete as the S_{CAP}-slices.

Problem 1: Long drying time
The ratio of drying time between a 15 mm or 25 mm thick slice, and a 100 mm diamer cylinder is about 0.10 and 0.25. This means that if the drying time for a 100 mm cylinder is 2 weeks it will be less than 2 days for a 15 mm thick slice and less than 4 days for a 25 mm thick slice. In addition, all determinations of volume and S-value will be considerably less time-consuming when slices are used.

Problem 2: Less well-defined value of S_{CR}
If all specimens for determination of S_{CR} are thin and taken from the same depth from the surface the spread in air-pore structure between different specimens and inside the same speci-

men will be reduced. Consequently, also the S_{CR}-value will be determined with a higher precision. Besides, by taking series of specimens from different depths, the spatial varaiation in S_{CR} over the concrete volume can be determined; Fig 13.

Problem 3: Different air-pore structure in specimens for S_{CR} and S_{CAP}
Since the S_{CR}-slices and the S_{CAP}-slices can be taken at the same depth from the concrete surface the air-pore structure in the two types of specimens are the same. Consequently, the S_{CR}-value and the S_{CAP}-value can be directly compared in a more safe way. Besides, one can determine the *variation in frost resistance* within a structure by comparing S_{CR} and S_{CAP} for the same depth in the concrete: Fig 13.

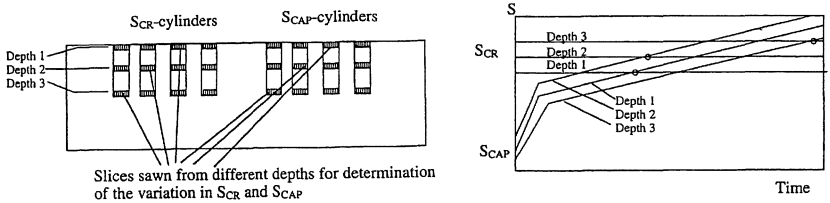

Figure 13. Distribution of S_{CR}, S_{CAP} and potential service life within the concrete.

(NOTE: If the plate is thinner than the coarsest aggregate grain, this will be cut exposing both its interface to the cement paste and its interior structure. This means that if the aggregate contains pores these might take up more water during the saturation phase before freeze-thaw than what should have been possible had the grain been completely embedded in cement paste. Besides, the interface might absorb more water than is possible in the real situation. On the other hand, this excess water can easily escape through the aggregate surface when the slice freezes. The net effect of the saw-cut is not possible to estimate without making tests, for example by comparing S_{CR} determined on slices with S_{CR} determined on cylinders. Possibly, the effect is marginal for most concretes. For safety reasons one should avoid to use thin plates for concrete with porous aggregate until this question has been clarified. Normally, one should also use slices that are at least 1.5 times the size of the coarsest aggregate so that some coarse aggregate grains are completely "sealed" by cement paste.)

6.2 Method for determination of S_{CR} using thin plates

The experimental technique for determination of S_{CR} using thin plates is exactly the same as for determination of S_{CR} on cylinders. The pre-drying, the resaturation, the adjustment of the S-level, the freeze-thaw procedure, and the final determination of the dry weight and pore volume are exacly the same as for cylinders.

As for the cylinders, damage is best judged on basis of the fundamental frequency of transverse vibration. There are many possibilities to do this. The following procedure has been used with success. The slice is placed with one flat side on a foam-rubber plate. The edge of the slab (or centre depending on the vibration mode) is activated by a vibrator driven by a tone-generator. The response from the specimen is catched by a piezoelectric pic-up attached to the edge of the slice. The signal from the pic-up is amplified and shown on an oscilloscope screen. The input frequency is varied until resonance is reached as seen as a maximum in the pic-up amplitude. The corresponding fundamental frequency is proportional to the square-root of the dynamic E-modulus, [9]:

$$f=(\alpha/r^2)\{E\cdot h^3/(12(1-\nu^2)\cdot m\}^{1/2} = \text{Const}\cdot E^{1/2} \quad \text{or} \quad E=\text{Const}\cdot f^2 \qquad (8)$$

where f is the fundamental frequency [Hz]
r is the radius of the plate [m]
E is the E-modulus [N/m^2]
h is the plate thickness [m]
ν is Poisson´s ratio
m is the mass per square-meter of the plate [kg/m^2]

The coefficient α depends on the mode in which the plate vibrates. For the lowest mode consisting of two perpendicular node diameters and no node circle α=5.251. For the higher mode where there are no node diameters but only one node circle α=9.076. In this case the pic-up (or vibrator) can also be put at the central part of the plate. The node giving the highest and most sharp response is used. Normally the fundamental frequency is very well defined making it fairly easy to detect the S_{CR}-value.

6.3 Experimental results

A series of 23 different concretes were produced. The w/c-ratio varied from 0.35 to 0.64 and the air content varied from natural to more than 9%. Different air entraining agents and different superplasticizers were used. A number of cylinders (diameter 100 mm, length 200 mm) were cast from each batch. After water curing for at least 28 days, 15 mm thick slices were cut from the centre part of the cylinders. 16 slices were used for determination of S_{CR} and 5 slices for determination of S_{CAP}.

S_{CR} was determined according to the method described in [4]. In all cases rather distinct values of S_{CR} were identified. Results for two of the concretes are shown in Fig 14. The S_{CR}-values are:

w/c 0.46, fresh air content 6.0%: S_{CR}=0.89
w/c 0.58, fresh air content 3.6%: S_{CR}=0.95

(NOTE: Theoretically, the maximum possible *effective* critical degree of saturation is 0.917 based on the fact that there must be room for the 9% volume expansion when water is transformed into ice. However, the fact that S_{CR}>0,917 for one of the concretes above is no contradiction to this requirement, because all of the pore water is not freezable; compare the two different definitions of degree of saturation according to eq (1) and (2).)

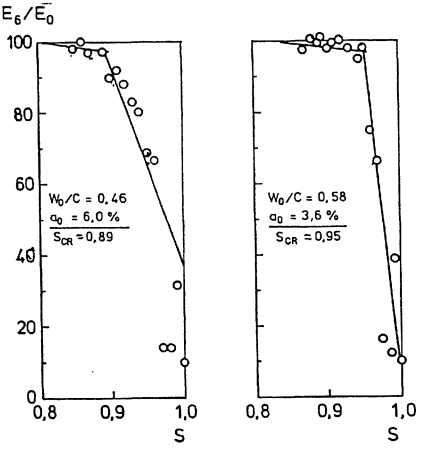

Figure 14. Determination of the degree of saturation of two types of concrete using 15 mm thick plates.

S_{CAP} for these two concrete was also determined, Fig 15. The long-term absorption can be described by.

w/c 0.46: $S_{CAP}=0.63+1.74\cdot10^{-3}\cdot t^{0.5}$ (t in hours)
w/c 0.58: $S_{CAP}=0.74+1.35\cdot10^{-3}\cdot t^{0.5}$

This means that the frost resistance after 1 month of uninterrupted water absorption is (as defined by eq (4´)):

w/c 0.46: $F(1\text{ month})=0.89-\{0.63+1.74\cdot10^{-3}(30\cdot24)^{1/0.5}\}=0.213$
w/c 0.58: $F(1\text{ month})=0.95-\{0.74+1.35\cdot10^{-3}(30\cdot24)^{1/0.5}\}=0.173$

Consequently, the risk of frost damage is lowest for the concrete with the lowest w/c-ratio and the highest air content.

After 1 year of continuous water absorption the corresponding values of the frost resistance are:

w/c 0.46: F(1 year)=0.097
w/c 0.58: F(1 year)=0.083

The difference between the two concretes is now smaller which depends on the fact that the rate of long-term absorption is a bit higher in the concrete with the highest air content. This is reasonable since diffusion of air through air-filled pores is much more rapid than diffusion through water-filled pores.

The potential service life as defined by eq (7) is:

w/c 0.46: $t_{p,life} = \{(0.89-0.63)/1.74\cdot10^{-3}\}^{1/0.5}=2.2\cdot10^4$ hours (930 days)
w/c 0.58: $t_{p,life}= \{(0.95-0.74)/1.35\cdot10^{-3}\}^{1/0.5}=2.4\cdot10^4$ hours (1000 days)

The difference between the concretes is almost negligible.

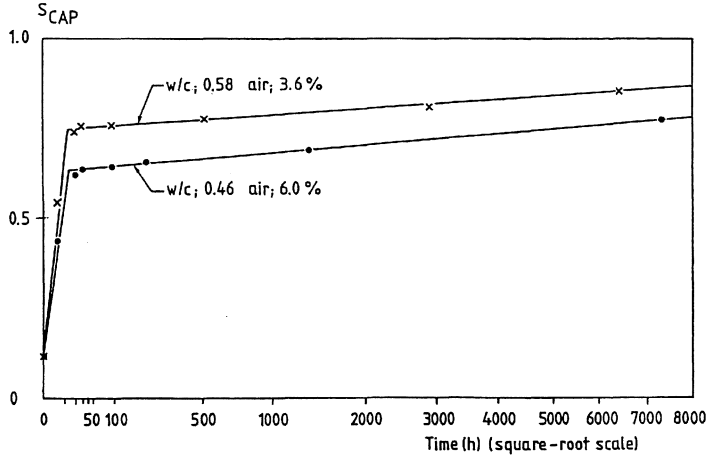

Figure 15. Determination of S_{CAP} for the same concretes as in figure 14.

7 ADJUSTMENT OF THE DEGREE OF SATURATION BEFORE FREEZE-THAW USING AN ABSORPTION PROCEDURE

Problems 4 and 5 described in paragraph 4 can be avoided by adjusting the S_{CR}-specimens before freeze-thaw by absorption from a dry stage instead of by drying from a saturated stage. Therefore, instead of saturating a pre-dried specimens completely before adjustment to the desired S it is evacuated to a certain *residual* air pressure. Then, water is let into the vacuum chamber containing the specimen. The lower the residual air pressure the higher the degree of saturation reached. Theoretically, according to Boyle´s law and neglecting the air-pore pressure created by capillary forces, the following relation exists between the residual air pressure and degree of saturation.

$$S=1-(1-V_w/V_p)\cdot(p_r/p_o) \qquad (9)$$

where V_w is the initial water volume after pre-drying but before vacuum treatment [m^3]

V_p is the total pore volume [m^3]

p_r is the residual air-pressure during vacuum pumping [Pa]

p_o is the atmospheric pressure [10^5 Pa]

According to this equation, S=0 when no vacuum is applied. Of course this is erroneos and depends on the fact that capillary action is neglected in eq (9). In reality $S\approx 1-V_a/V_p$ after such a treatment where V_a is the effective air-pore volume in the specimen. However, eq (9) can be used for selecting the residual air pressure to be used at adjusting specimens to different desired S-values. For $V_w=0$ the following relations between residual pressure and S are valid:

p_r= 2 torr (260 Pa):	$S\approx 0.997$
p_r= 20 torr (2630 Pa)	$S\approx 0.974$
p_r= 50 torr (6580 Pa)	$S\approx 0.934$
p_r=100 torr (13150 Pa)	$S\approx 0.869$
p_r=200 torr (26300 Pa)	$S\approx 0.737$

Consequently, since normal values of S_{CR} lies between 0.75 and 0.95 the residual pressures to be used should be between about 2 torr and 200 torr.

By using absorption and not drying for adjusting the specimen to the desired value of S, moisture gradients are avoided more or less completely.

8 ALTERNATIVE WAYS OF DETERMINING S_{ACT}

As said before in paragraph 5, there are situations where the capillary water uptake gives moisture levels that are lower than those reached in the real structure. Then, the definition of frost resistance by eq (4´´) is not directly applicable, unless it is possible to translate a given real environment into a certain point on the capillary absorption-time curve.

This difficulty will not reduce the possibility of using the S_{CR}-method as described by the general eq (4). S_{CR} is not affected by the manner by which water enters the concrete. Therefore, it is determined in the same way irrespectively of the use of the concrete. The actual degree of saturation S_{ACT} is now instead determined by a method that represents the real situation and not by a simple capillary water uptake test. Imaginable possibilities for determination of S_{ACT} are:

1: Water absorption during freeze-thaw cycling. Thin specimens (e.g. the same as the normal S_{CAP}-specimens) are constantly exposed to water on one side. They are also exposed to representative uni-directional freeze-thaw cycles starting from the moist side. The water absorption (expressed as S_{ACT}) is measured as a function of the number of cycles.

(NOTE: Test results after the concrete has started to deteriorate cannot be used because then S_{CR} is transgressed over an unknown portion of the specimen. It is the absorption *before* cracking that is of interest in the S_{CR}-test. Results after cracking are meaningless.)

2: Water aborption during temperature variation: The normal S_{CAP}-test is performed under varying temperature simulating natural temperature variations

3: Water absorption during internal moisture redistribution and condensation: Concrete plates are sealed on one side by epoxy or any other dense material. The uncovered surface is placed in contact with water of constant temperature. The covered surface is exposed to repeated rapid temperature lowering simulating natural cooling (e.g. cooling by radiation towards a dark winter sky). The moisture uptake and moisture distribution is measured and expressed in terms of degree of saturation.

There are many other possibilities of determining values of S_{ACT} that are more realistic for the real field conditions than the values given by the simple S_{CAP}-test. These S_{ACT}-values can then be used in eq (4) for a quantitative estimation of the frost resistance of a given concrete in a given situation.

9 FINAL REMARKS

As described above, the S_{CR}-method could probably be rationalized and also improved as compared to the original procedure described in [2]. By using thin specimens for determination of S_{CR} and by shortening the S_{CAP}-test, making use of a reasonable extrapolation of the observed water uptake curve, the total test time can be reduced considerably. No more than 2 or maximum 3 weeks would be needed which makes the S_{CR}-method just as rapid as other methods for determination of internal frost resistance. In the method ASTM C666, 300 freeze-thaw cycles are used with a total test time from 3.5 weeks to 9 weeks depending on the freeze-thaw rate used.

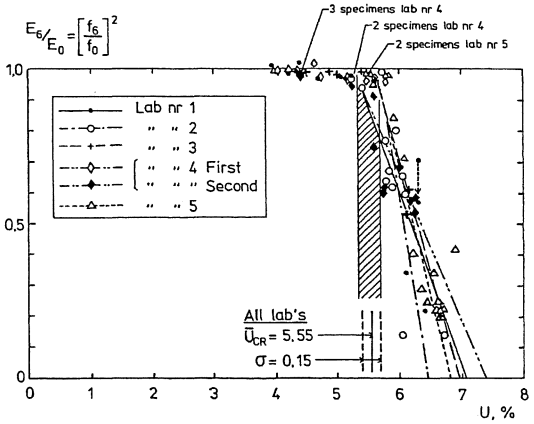

Figure 16. Determination of the critical moisture ratio, U. Concrete 1 in figure 9[3]

The somewhat laborious work required for determination of the degree of saturation of all specimens can be reduced considerably if the moisture ratio is used instead. Examples of the use of moisture ratio for determination of the critical moisture content is shown in Fig 16 where results from the international cooperative test are plotted.

The method of determining capillary water uptake described in [2] can be very much simplified; the first absorption when the water front is penetrating the specimen is neglected since it is not relevant for defining frost resistance. Besides, the weight increase might be measured a couple of times only during the week (or weeks) that the experiment is run.

Finally, it can be mentioned that EMPA in Switzerland has for a long time used a somewhat simplified version of the S_{CR}-method as its standard frost-test method [10].

10 REFERENCES

References without author name are written by the present author.

[1] *Critical Degrees of Saturation in Connection with Freezing of Porous and Brittle Materials.* Division of Building Technology, Lund Institute of Technology, Report 34, 1972. (In Swedish with English Summary).

[2] RILEM Tentative Recommendation: *The Critical Degree of Saturation Method of Assessing the Freeze/Thaw Resistance of Concrete.* Materials and Structures, Vol 10, No 58, 1977.

[3] *The International Cooperative Test of the Critical Degree of Saturation Method of Assessing the Freeze/Thaw Resistance of Concrete.* Materials and Structures, Vol 10, No 58, 1977.

[4] Prediction of the service life of concrete exposed to frost action. In *"Studies on Concrete Technology"*, Swedish Cement and Concrete Research Institute. Stockholm 1979.

[5] Service life with regard to frost attack. A probabalistic approach. In *"Proceedings of the Eighth International Conference on Durability of Building Materials and Components"*. NRC Research Press, Ottawa 1999.

[6] Predicting the Service Life of Concrete exposed to Frost Action through a Modelling of the Water Absorption Process in the Air-pore System. In *"NATO Conference on Modelling of Microstructure and its Potential for Studying Transport Processes and Durability"*. Kluwer Academic Publishers, 1996.

[7] *Influence of Environmental Factors on the Frost Resistance of Concrete.* Div. Building Materials, Lund Institute of Technology, Report TVBM-3059, 1994.

[8] *On Hysteresis between Pore Water Pressure and Moisture Content. Consequences for Drying Shrinkage and Frost Resistance.* Div. Building Materials, Lund Institute of Technology, Report TVBM-7138, 1999. (In Swedish)

[9] S Timoshenko: *Vibration Problems in Engineering.* D. Van Nostrand, New York 1937.

[10] EMPA. *Test Method SIA 162/1, §309 "Critical Degree of Saturation"* combined with *Test Method SIA 162/1, §305 "Water Conductivity"*. EMPA, Dübendorf, 3rd Revision, Edition 1989.

USING LOW-TEMPERATURE CALORIMETRY WHEN STUDYING INTERNAL FROST RESISTANCE OF CONCRETE

— Part of a research project on Internal Frost Resistance of Concrete

Katja Fridh
Division of Building Materials, Lund Institute of Technology
Box 118
221 00 Lund, Sweden

1 INTRODUCTION

1.1 Measuring techniques

When studying ongoing internal frost deterioration there are some measuring techniques available. The techniques can be divided into two types. One type is based on measurements of internal cracking by sending a signal or pulse through the material like ultrasonic pulse transmission or using acoustic measurements. The other type measures the response of the material by detecting the length-change. The later technique is more sensitive because the material does not have to be damaged to be able to detect response. In this paper it will be shown how this technique combined with calorimetry can give even more information. This is based on ideas of Verbeck and Klieger [1].

2 CALORIMETRY

2.1 Ice-formation releases heat

When water is transformed into ice 333 J/g of heat is released. Therefore, if the amount of heat can be measured the amount of ice that is formed at different temperatures can be calculated. To measure the heat developed a low-temperature SETARAM BT 2.15 II calorimeter is used in our laboratory. To control the low temperatures liquid nitrogen is supplied to the calorimeter from a tank next to the calorimeter (fig.1). Bager and Sellevold have used this technique with great success in series of investigations [2,3,4].

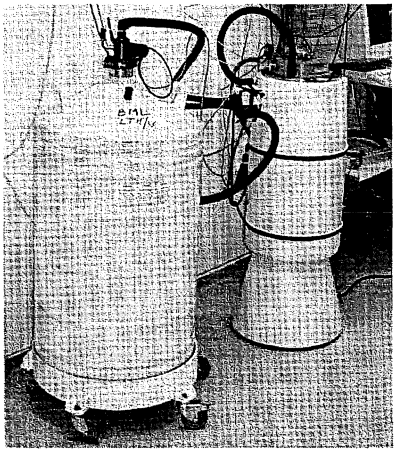

Figure 1. The SETARAM calorimeter with the liquid nitrogen tank.

2.2 Low-temperature calorimeter

The calorimeter (fig.2) consists of (from the outside) a layer of insulation consisting of mineral powder in vacuum. Inside of the insulation there is a liquid tight tank, which contains the liquid nitrogen. The level of the liquid nitrogen is kept constant during measurement to obtain the best stability. Inside the liquid nitrogen tank is the calorimetric chamber. It is a liquid tight chamber with controlled atmosphere to avoid low temperature condensation. It consists of the calorimetric block and two inlets, one to the specimen cell and one to the reference cell. Between the calorimetric block and the casing is the thermostat and peripheral resistor winding. These together with the control thermosensor enable the regulation of the block. The cells are completely surrounded by heat flow detectors. These measure the heat exchange difference between the two cells, which correspond to the heat exchange of the sample corrected for disruption from the regulation of the block. The temperature of the block can be controlled to be constant or in scanning mode. The temperatures can vary between 200°C - (-196°C) and the scanning rates are within the range 0.06-60°C/h.

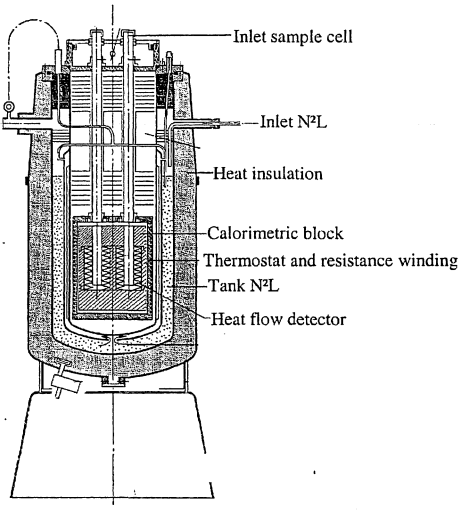

Figure 2. Cross-section of the calorimeter

2.3 Calculating ice-formation

The ice formation process releases heat in proportion to the amount of ice. This heat can be measured by the calorimeter described above and the ice formed at different temperatures can then be calculated. A typical result from freezing of a cement mortar can be seen in fig 3. The large super-cooling occurring as a result of the lack of nucleating agents results in a large first peak when water of the largest pores freezes. The other two peaks can also be a result of local super-cooling in isolated pores and do therefore not necessary reflect the pore size distribution. Therefore the freezing curve is not suitable for determination of the pore size distribution. New results using cholesterol as a crystallisation agent [5] show very little super-cooling. Therefore will this be tried in the following work.

The calorimeter measures the heat flow. That signal contains contributions from everything inside the specimen cell but the significant contributions are from the sample, water, ice and the transformation between water and ice. The area beneath the graph represents the amount of ice, and to determine this area a baseline has to be determined. This baseline has to be adjusted for the decrease in heat capacity of the system during cooling because of the

formation of ice. Ice has lower heat capacity than water. That can be done with a simple program, for example using Matlab.

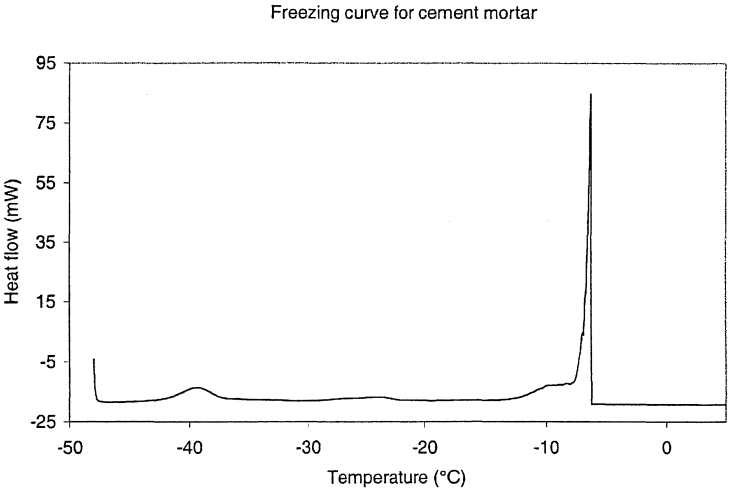

Figure 3. Heat flow from a cement mortar in the SETARAM calorimeter during freezing.

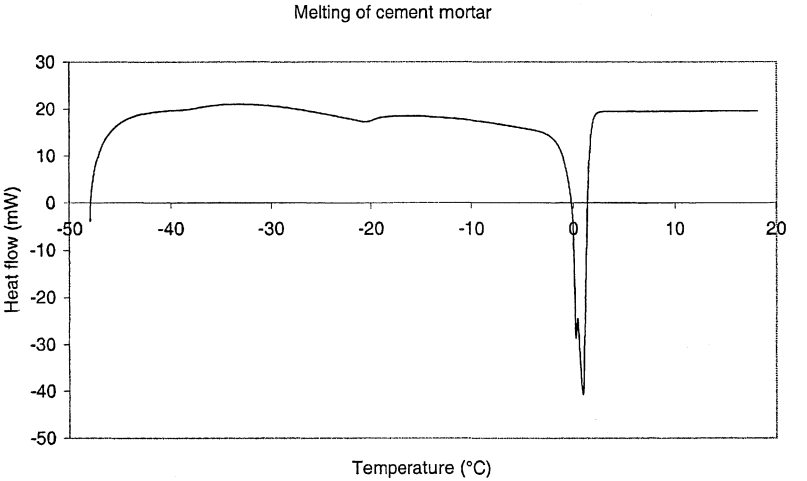

Figure 4. Heat flow from the same cement mortar as in fig 3 in the SETARAM calorimeter during melting.

The calculations are done by dividing the graph into appropriate temperature steps where the heat flow in every step is adjusted for the amount of ice formed or melted before the actual step.

3 LENGTH-CHANGE MEASURING EQUIPMENT

3.1 General

When measuring the length-change curve during freezing and thawing on rather big samples a rig of a material which have a small thermal movement like invar and a LVDT-sensor is used. When investigating freeze/thaw phenomena which involve moisture and moisture transport it is very important to minimise the specimen preparation time. That is possible using LVDT-sensors. The specimen is placed in the rig where the sensor is fastened (fig.5). The whole device is then placed in a freeze cabinet for the test (fig.6).

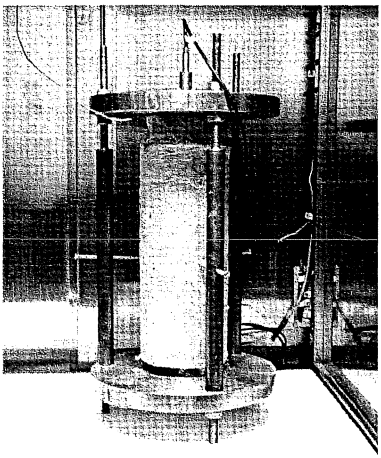

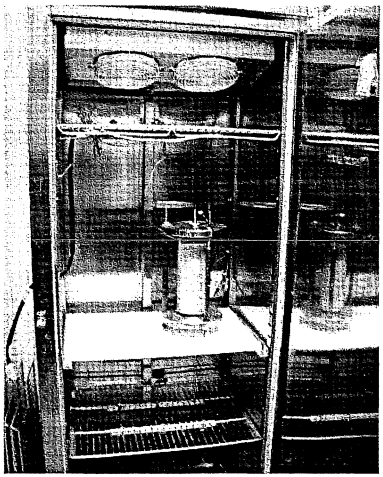

Figure 5 and 6. Measuring length-change on large samples.

3.2 Dilation measurements in a low-temperature calorimeter

When trying to measure the length-change curve in a calorimeter using a LVDT-sensor a somewhat different technique has to be used. There is no place for a rig so the equipment has to be hang inside the calorimeter. That is done to secure that the sensor only measures the movement of the specimen and not movements of the calorimeter itself.

The calorimeter cell is hung in a quartz glass tube that is fastened in the calorimeter lid. A quartz glass rod runs inside the tube. It is supported by the specimen in its lower end and supports the moving LVDT-"piston" on its upper end. The device is seen in fig. 7.

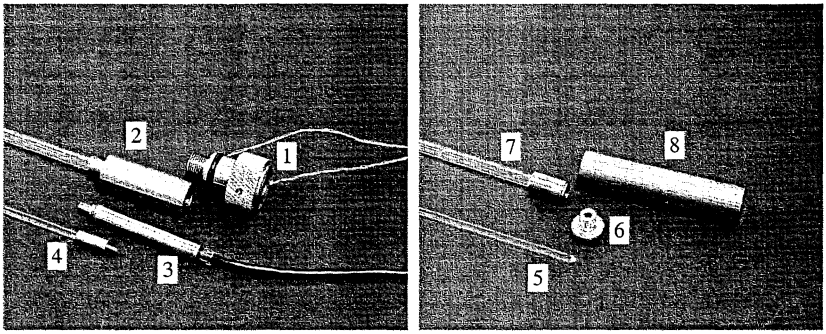

Figure 7. (1) Lid to the specimen inlet at the calorimeter lid. (2) Upper part of the glass tube. It is screwed in the lid. (3) LVDT-sensor. (4) Upper part of glass rod. Screws on the LVDT-sensor. (5) Lower part of the glass rod. (6) Lid to the specimen holder. Screws on the glass tube. (7) Lower part of the glass tube. (8) Specimen cell.

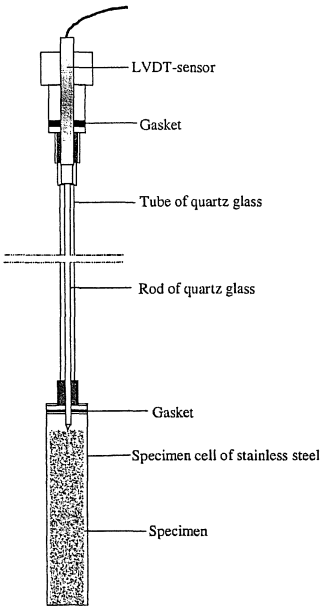

Figure 8. The length-change detecting equipment inside the calorimeter.

Calibration measurements are in progress. A result from a measurement on a cement mortar can be seen in fig 9. The calorimeter and the LVDT-sensor detect the ice-formation at the same time. When the ice-formation ends the specimen contracts. The small movements at the lower temperatures (~-35°C) derive from the controlling of the calorimeter.

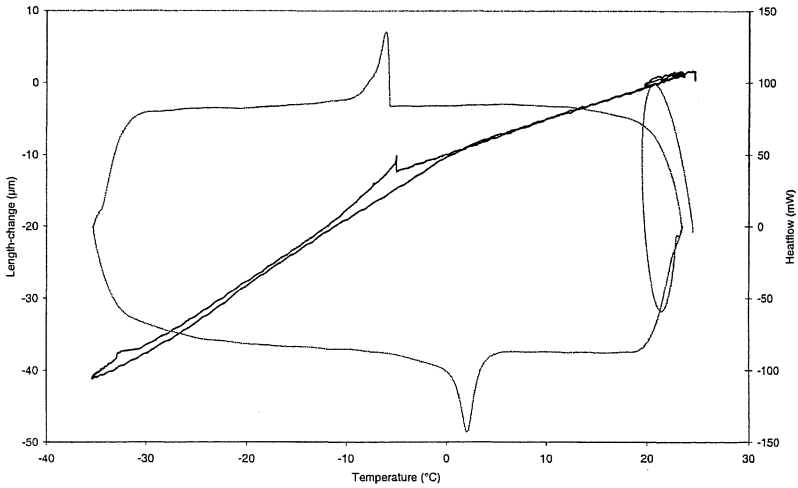

Figure 9. Result from calibration measurement using cement mortar specimen.

4 RESEARCH PROGRAMME

This measuring technique is part of a PhD-project that includes studies of cement mortar of ten different recipes regarding internal frost resistance. The material studied has water cement ratio between 0.40 and 0.60 and air contents from natural to 10%. The measuring technique will be used to simultaneously study the ice-formation and the length-change with different freeze/thaw cycles. The cycles will have different freezing rates, duration and lowest temperature. The response in the material of these cycles together with supplementary investigations regarding water absorption and the critical degree of saturation will give important information of the mechanism behind the internal destruction due to frost action.

5 REFERENCES

1. Verbeck, G., Klieger, P.," Calorimeter – Strain Apparatus for Study of Freezing and Thawing Concrete", *Highway Research Board*, Bulletin 176, 1958
2. le Sage de Fontenay, Carl and Sellevold, E.J., "Ice Formation in Hardened Cement paste – I. Mature Water Saturated Pastes", *Durability of Building Materials and Components, ASTM STP 691*. P.J. Sereda and G.G. Litvan, Eds., American Society for Testing and Materials, 1980, pp. 000-000
3. Bager, D.H. and Sellevold, E.J.,"Ice Formation in Hardened Cement Paste – II. Steam cured Pastes with variable Moisture Contents", *Durability of Building Materials and Components, ASTM STP 691*. P.J. Sereda and G.G. Litvan, Eds., American Society for Testing and Materials, 1980, pp. 439-454
4. Bager, D.H. and Sellevold, E.J.,"Ice Formation in Hardened Cement Paste, Part I – Room Temperature Cured Pastes With Variable Moisture Contents" *Cement and Concrete Research,* vol 16, 1986, pp. 709-720
5. Kaufmann, J., Nordstrom, R.A. and Studer, W.,"Damage Mechanisms in Frost Deicing Salt Resistance Tests", *Proc. of Int. Conference on Concrete under severe conditions, CONSEC '98,* vol , pp 272-281

ON THE NEED FOR DATA FOR THE VERIFICATION OF SERVICE LIFE MODELS FOR FROST DAMAGE

Mette Geiker, Associate Professor
Institute of Structural Engineering and Building Materials
The Technical University of Denmark
Building 118
DK 2800 Lyngby
Denmark
e-mail: mge@bkm.dtu.dk

Svend Engelund, Senior Engineer
COWI Consulting Engineers and Planners
Parallelvej 15
DK 2800 Lyngby
Denmark
e-mail: sen@cowi.dk

1 INTRODUCTION

The purpose of this paper is to draw the attention to the need for the verification of service life models for frost attack on concrete and the collection of relevant data. To illustrate the type of data needed, the present paper presents models for both internal freeze/thaw damage (internal cracking, including de-lamination) and surface scaling.

Several service life models for reinforcement corrosion of steel in concrete are being applied, both for the design of new structures and assessment of the service life of existing structures e.g. [1, 2, 3].

Service life models for frost attack have been proposed, e.g. [4, 5]. However, compared to reinforcement corrosion service life models for frost damage lack verification. In a recent project [6] attempts were made to provide such verification, but the need for further data for the statistical quantification was identified.

1.1 Probabilistic Based Service Life Modelling

A probabilistic service life model provides a rational tool for decision making based on available data taking into account the random variation of the model parameters and the model uncertainty.

Probabilistic modelling of the deterioration of concrete has been dealt with by several authors in recent years, e.g. [7, 8, 9]. By probabilistic modelling the probability that a given structure will be subject to the considered damage at a given time is estimated, ref. *Figure* 1.

The starting point is a deterministic model for the deterioration mechanism(s) considered. The relevant parameters are modelled as stochastic variables, and on the basis of available data the physical uncertainty related to these parameters is estimated. Due to the limited amount of data the distribution parameters of the stochastic variables describing the physical uncertainty will be subject to statistical uncertainty. This uncertainty has also to be estimated. A Bayesian approach may be used to estimate the statistical parameters and their associated uncertainty. Finally, the uncertainty related to the considered models should be estimated, i.e. the accuracy by which the models can predict the performance of a given structure.

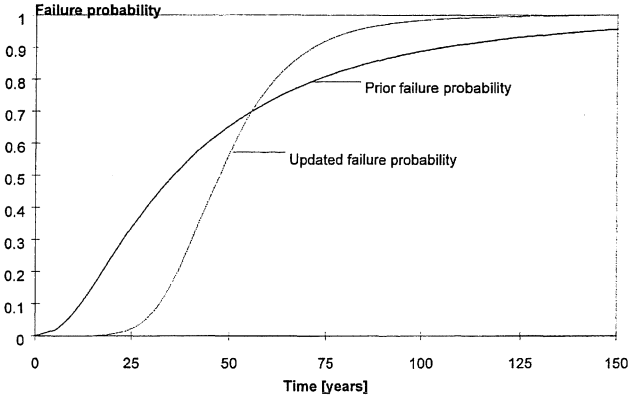

Figure 1. Failure probability as a function of time.

By a sensitivity analysis the most important parameters, i.e. the parameters which give the largest contribution to the probability of damage, can be identified. Together with information on the cost of testing and the influence of the statistical uncertainty of the data the sensitivity analysis provides a rational tool for planning of supplementary investigations on the basis of which the probability of failure can be updated, ref. Figure 1.

2 INTERNAL FROST DAMAGE

Internal frost damage of concrete occurs when the water content (i.e. degree of saturation) in a volume larger than a critical volume is higher than the critical degree of saturation for the actual concrete and freeze/thaw exposure (e.g. freezing temperature and rate). Frost damage of a critically saturated concrete is likely to occur at temperatures below -2.5°C. The freezing-point depression of the pore liquid held in large pores is caused by soluble salts. The pore liquid held in small pores will only freeze at lower temperatures, due to a combination of soluble salts and a lower pressure. That is, not all the pore liquid will freeze at the same time, and the amount of freezable pore liquid increases with decreasing temperature.

2.1 Probabilistic Model

The probability of failure at a given location, $\mathbf{x}$, within a given reference period of time from t to $t+\Delta t$ is given by

$$P_f(t,\Delta t,\mathbf{x}) = 1 - P\left(S(\tau,\mathbf{x}) < S_{cr} \cup T(t,\mathbf{x}) > T_{cr} \;\forall\, \tau \in [t,t+\Delta t]\right) \tag{2.1}$$

where $S(\tau)$ is the actual degree of saturation of the concrete at the time τ, S_{cr} is the critical degree of saturation, i.e. the degree of saturation which is necessary for frost damages to occur, $T(t)$ is the temperature of the water, and T_{cr} is the temperature necessary for the water in the concrete to freeze.

Internal frost damages usually occurs in concrete where the temperature necessary for the water in the concrete to freeze, T_{cr}, is relatively high. This implies that if the actual degree of saturation at

some time during a winter exceeds the critical degree of saturation failure is almost certain to occur. Therefore, the failure probability is given by

$$P_f(t,\Delta t,\mathbf{x}) = 1 - P\left(S(\tau,\mathbf{x}) < S_{cr}\,\forall\tau \in [t;t+\Delta t]\right) = P\left(S_{\max}(t,\Delta t,\mathbf{x}) \geq S_{cr}\right) \tag{2.2}$$

where $S_{\max}(t,\Delta t,\mathbf{x})$ is the maximum degree of saturation at the location, $\mathbf{x}$, within the reference period. It has naturally been assumed that the structure is located in an environment where freezing is certain to occur.

If the considered time period is chosen as 1 year, i.e. $\Delta t = 1$ year, and if there is no systematic variation of the degree of saturation between different years, the failure probability will not depend on time, t. This is based on the assumption that the material properties of the concrete are independent of time. Usually this assumption is not fulfilled, and the problem depends on t as well as Δt.

As mentioned earlier, failure is assumed only to occur when the degree of saturation within a given volume of concrete is larger than the critical degree of saturation. It has been observed that delamination occurs at intervals of approximately 10 mm. This leads to the assumption that for internal damage to occur if the *local average* of the degree of saturation within a volume with minimum dimension of 10 mm exceed the critical value.

The variable $S(\tau)$ will now be defined as the maximum value within the considered structure of the local average of the degree of saturation. This implies that the probability of failure is given by

$$P_f(t,\Delta t) = 1 - P\left(S(\tau) < S_{cr}\ \forall\ \tau \in [t,t+\Delta t]\right) \tag{2.3}$$

The critical degree of saturation can for different types of concrete be determined on the basis of experiments using test specimens obtained from the considered structure. Also the local average of the actual degree of saturation in a given structure can be determined by core drilling and testing of slices of the core. However, it is complicated to predict the development with time of the local average of the actual degree of saturation in a given structure. A simple model for the time-dependency of the local average of the actual degree of saturation has been suggested by Fagerlund [10]

$$S(\tau) = S_0 + h(\tau) \tag{2.4}$$

where S_0 is the initial degree of saturation and where $h(\tau)$ is a function describing the moisture ingress as a function of time, τ. The rate of moisture ingress depends on the permeability of the concrete and the exposure. However, in order to determine the degree of saturation at a given time it is also necessary to take into account the external climatic conditions as e.g. the effective lengths of periods of wetting and drying of the concrete on a micro-climate level.

The ingress of water into concrete can be described by a set of partial differential equations. These equations can be solved by using the Finite Element Method. However, the effort involved in such computations is usually excessive. Further, such computations must always be calibrated on the basis of measurements from the considered structure. For a more detailed discussion of moisture ingress in concrete see [11].

Fagerlund [10] suggests to determine the local average of the actual degree of saturation on the basis of the following expression

$$S(\tau) = a + b\tau^c + \varepsilon \tag{2.5}$$

where a, b and c are constants which must be determined on the basis of laboratory tests of capillary suction and ε is an error term. By this test a thin test specimen (thickness 25 mm) is placed such that one of its two surfaces is below water. The capillary suction of this test item is now measured as a function of time. By fully saturating the specimen after a period of capillary suction the test results can be given as degree of saturation. The result of such a test will usually have the form shown in Figure 2.1. It should be noted that this type of curve consisting of two distinct lines is not obtained for dense concretes.

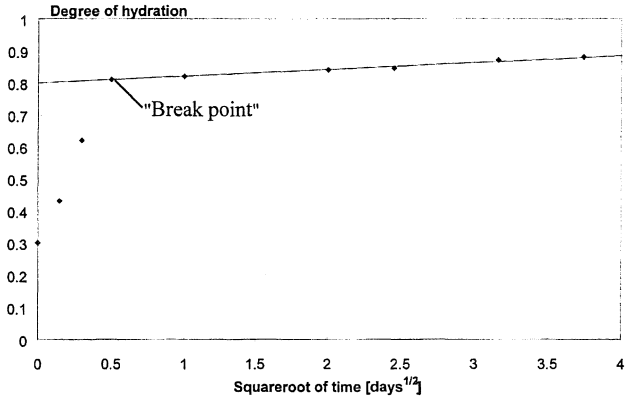

Figure 2. Results of capillary suction test.

The degree of hydration at the "break point" in Figure 2, S_k, will be reached after a relatively short period of time. It must be assumed that this period is short in relation to the time necessary to reach the critical degree of saturation. If it is assumed that the initial degree of saturation, S_0, is lower than S_k then

$$S(\tau) \approx S_k + b\tau^c + \varepsilon \tag{2.6}$$

where b and c can be estimated on the basis of the test results where $S(\tau) > S_k$.

It is assumed that this test represents the ingress of water for an existing structure. The test must be performed using test specimens from the given structure or test specimens made from the same cast of concrete mix cured and conditioned similarly. If the maximum value of the degree of saturation within a given time period can now be determined as

$$S_{\max}(t, \Delta t) = S_k + bt_{\max}(t, \Delta t) \tag{2.7}$$

where $t_{\max}$ is the length of the longest wetting period of the structure within the considered time period, $[t, t + \Delta t]$. To determine $t_{\max}$ it may be necessary to distinguish between three different environments.

1. An environment where the drying of the concrete is negligible. In this case the longest period of wetting is equal to the age of the structure. However, it is difficult to assess the initial value of the degree of saturation of the structure. Alternatively, a measurement of the actual degree of saturation can be performed. The measured degree of saturation can be used as S_0 and the longest period of wetting is equal to the length of the period of time since the measurement was performed.
2. An environment where the drying of the concrete always brings the degree of saturation below the "break point", S_k. In this case the longest period of wetting can be estimated on the basis of meteorological data and the initial degree of saturation can be chosen as S_k.
3. An environment where the drying of the concrete is not always able to bring the degree of saturation below the "break point", S_k. Therefore, an equivalent period of wetting must be determined. The most simple model for the period of wetting is to assume that it is equal to a variable, *K,* multiplied by the age of the structure. In this case the initial degree of saturation may

have to be determined on the basis of measurements where the actual degree of saturation in the structure is determined.

The third case is clearly the most difficult to handle. However, by letting the variable, K, be equal to one it is at least possible to obtain some upper limit for the probability of failure.

The model presented above is mainly based on simple laboratory experiments and data fitting. Very little information about water ingress in existing structures is available. The model is, therefore, subject to substantial uncertainty.

The model uncertainty is taken into account by introducing the model uncertainty m. Because the maximum degree of saturation cannot exceed 1.0 it is difficult to associate this quantity with a model uncertainty. The model uncertainty is, therefore, introduced as the uncertainty related to the prediction of the relation between $S_{\max}(t,\Delta t)$ and S_{cr}.

The evaluation of the probability of freeze-thaw damage can be performed FORM/SORM-analysis. The limit state function which is less than zero if and only if failure occurs can be defined as

$$g(\mathbf{x},t,\Delta t) = 1 - m\frac{S_{\max}(t,\Delta t)}{S_{cr}} \tag{2.8}$$

In eq. (2.8) the model uncertainty is taken into account. It is seen that the model uncertainty must be larger than or equal to zero. Alternatively, the model uncertainty can be modelled by a stochastic variable whose probability of outcomes less than zero is negligible.

2.2 Needed Input data

To determine the probability of frost damage the following parameters must be quantified

S_{cr}	Critical degree of saturation
S_k	"Break point" for the degree of saturation as a function of time
m	Model uncertainty
b, c	Regression parameters for the moisture ingress
$t_{\max}$	Longest period of wetting
K	Factor for the equivalent period of wetting.

It is essential that the same method of saturation is used for determining the critical degree of saturation and the actual degree of saturation. It has recently been found the vacuum saturation is not sufficient for the saturation of dense concrete specimens of some size (w/c=0.4, 10 mm, the limit is not determined). For saturation of such specimens a pressure must be applied.

2.2.1 Moisture Ingress

The quantification of the uncertainty related to the parameters given in Section 2.2 must be performed on the basis of the available data. The longest period of wetting is an environmental parameter which must be quantified on the basis of data concerning the micro and macro climate of the considered structure.

The equivalent period of wetting, i.e. the factor K, cannot be observed and, therefore, the distribution and distribution parameters of K cannot be determined by analysing a number of outcomes of K. However, if an observation of the actual degree of saturation is available the distribution of K can be estimated by performing a Bayesian updating of a FORM/SORM analysis, see e.g. Duracrete [3]. The observation is modelled by the event

$$h(\mathbf{x},\tau) = S(\tau) - S_{obs} \tag{2.9}$$

where $S(\tau)$ is the degree of saturation predicted on the basis of the model and S_{obs} is the observed degree of saturation.

The parameters S_k, b and c can be determined on the basis of experiments. By the use of Bayesian statistics also the statistical uncertainty related to the parameters can be estimated, see appendix A. According to Fagerlund, the parameters may also be determined on the basis of information about the air void structure in the concrete, see e.g. Fagerlund [10] and Fagerlund [12].

2.2.2 Critical Degree of Saturation

The critical degree of saturation is normally determined experimentally, ref. e.g. Fagerlund [10]. However, models for estimation of the critical degree of saturation have been proposed, ref. e.g. Fagerlund [13] and Hansen [14]. For ordinary concrete the normal range for the critical degree of saturation is 0.75 - 0.90. No information about the standard deviation of results is available. However, Fagerlund claims that the critical degree of saturation exhibits a very small variation.

2.2.3 Model Uncertainty

The model uncertainty, i.e. the accuracy of the model and the bias, can be estimated on the basis of simultaneous observations of the degree of saturation of a test specimen and the degree of saturation of a given in-situ structure made of the same type of concrete as the test specimen. At present no such data is available. The estimation of the model uncertainty, therefore, has to be based on expert opinion. Like the factor K also the model uncertainty can be updated on the basis of observations.

3 SURFACE SCALING

In some cases, freeze-thaw attack causes external frost damage, also called surface scaling. According to Pigeon and Pleau [15] this type of frost damage only occurs on surfaces covered by a salt solution.

3.1 Probabilistic Model

A structure is said to fail when the amount of scaled concrete has reached a given limiting value. The limit can be expressed as the loss of a given weight of concrete per unit surface area. The limit must be chosen on the basis of considerations of the thickness of the cover and the aesthetics of the structure.

The failure probability as a function of time, t, is

$$P_f(t) = P\left(s(t) \geq s_{cr}\right) \tag{3.1}$$

where $s(t)$ is the weight of scaled concrete as a function of time and s_{cr} is the limit. In order to solve this problem a probabilistic model for $s(t)$ must be formulated. The model is based on the assumption that the amount of scaling which can be observed on a given structure in situ is correlated to the amount of scaling which can be measured by accelerated tests made using test specimens made of the same concrete as the considered structure. This can be formulated as

$$s(N) = \alpha s_{test}(N) \tag{3.2}$$

where N is the number of standardized freeze-thaw cycles (according to the given test method) m takes into account the model uncertainty and $s_{test}(N)$ is the mean of the amount of scaling of the

test items as a function of the number of freeze-thaw cycles, N. The variable, α, is modelled by a stochastic variable whose distribution and parameters can be determined on the basis of observations of the amount of scaling on a number of structures where also test results are available. If no such information is available the distribution of α may be determined on the basis of expert opinion.

An expression for $s_{test}(N)$ is determined on the basis of the test results. Usually a relation of the following form is assumed

$$s_{test}(N) = aN^b \tag{3.3}$$

where a and b are constants. Fagerlund [10] describes scaling to progress in three different ways:

1. Retarded (b<1), lower quality of outer surface , e.g. due to bleeding, separation, lack of curing, lower air content
2. Linear(b=1), homogeneous concrete
3. Accelerated (b>1)

Examples of retarded, linear and accelerated scaling are shown in Figure 3.

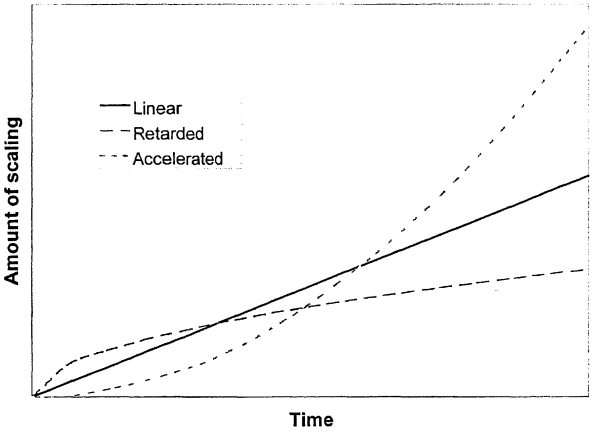

Figure 3. Examples of retarded, linear and accelerated scaling

Using test results the parameters in the model can be estimated using Bayesian linear regression. It is also necessary to determine the number of freeze-thaw cycles, N, as a function of time, t. It must be taken into account that the regression parameters are estimated using test results where the lowest temperature in each freeze-thaw cycle is a constant reference temperature, e.g. $T_{ref} = -20\ ^{\circ}C$. The amount of scaled material depends on the lowest temperature reached in a given cycle. The fact that a given structure in situ is subject to a number of cycles where the lowest temperature varies is taken into account by defining N as an equivalent number of cycles given by

$$N = \sum_{i=1}^{n(t)} \frac{T_i^2}{T_{ref}^2} \tag{3.4}$$

where $n(t)$ is the number of freeze-thaw cycles where the water content in the surface layer of the concrete is high enough for damages to occur as a function of time and T_i is the lowest temperature reached in the ith cycle. This model has been suggested by Fagerlund [4].

Assuming that the number of freeze-thaw cycles occurring in a given year is independent of the number of freeze-thaw cycles occurring any other year the number of freeze-thaw cycles within a year can be described by a Poisson distribution. Each time a freeze-thaw cycle occurs the equivalent number of cycles in increased by $\frac{T_i^2}{T_{ref}^2}$. If it is assumed that $T_i, i = 1,2,\ldots n(t)$ all are independent and identically distributed it can be shown that the mean and variance of the equivalent number of cycles are given by

$$E[N] = E[P]E[n(t)]$$
$$Var[N] = E[P^2]E[n(t)]$$

where P denotes the magnitude of the increase of N for each cycle, i.e. $P = \frac{T_i^2}{T_{ref}^2}$.

Because the equivalent number of cycles is a sum of independent contributions the variable N will follow a Normal distribution (according to the Central Limit Theorem).

It should here be noted that the assumptions that all T_i are independent and identically distributed generally is not fulfilled. However, the error made by this assumption is assumed to be negligible.

The number of freeze-thaw cycles where the water content in the outer layer is high enough for frost damages to occur, $n(t)$, depends on the micro-climate of the structure. E.g. in the splash zone of a bridge in a marine environment the degree of saturation of the outer layer is likely to be high. In other structures in a more protected environment the number of cycles where the degree of saturation is high will be substantially lower than the number of freeze-thaw cycles. It is assumed that the number of cycles where the degree of saturation is high enough for damage to occur, $n(t)$, can be determined as

$$n(t) = km(t) \tag{3.5}$$

where k is a parameter describing the environment and $m(t)$ is the number of freeze-thaw cycles. Depending on the amount of knowledge the parameter, k, can either be modelled as a deterministic parameter or as a stochastic variable.

On the basis of the model presented here the failure probability can now be determined by

$$P_f = P(s(t) > s_{cr}) = P(\alpha aN(t)^b > s_{cr}) \tag{3.6}$$

This problem can be solved using FORM/SORM-analysis, see e.g. Duracrete [16] or Thoft-Christensen and Baker [17].

The model presented here is based on the assumption that the accelerated laboratory experiments can be used to predict the behaviour of the concrete in situ. An investigation by Eriksen et al [18] indicates that there in general is a fair agreement between the observed and predicted damage on a structure on a structure. No exact measurements of the amount of scaling on the given structures have been performed but the structures which on the basis of the experiments were predicted to be most sensitive towards freeze-thaw damage generally also showed the largest amount of deterioration.

3.2 Assumptions and Limitations

Blast furnace slag concrete has been observed to obtain increased porosity due to carbonation. As carbonation is likely to occur in-situ, but normally not included in laboratory testing, such laboratory tests may provide too positive results.

3.3 Needed Input data

The following variables must be quantified

a,b	Regression parameters
α	Model uncertainty
$N(t)$	Equivalent number of freeze-thaw cycles.

3.3.1 Data

No general model for the evaluation of the regression parameters on the basis of the concrete composition is known to the authors. In general, the regression parameters, a and b, must be determined on the basis of experiments. Further, the equivalent number of freeze-thaw cycles, $N(t)$, can be evaluated using meteorological data. Only the model uncertainty, α, must be specified here.

To estimate the model uncertainty standardised tests must be conducted on the basis of which the regression parameters a and b can be estimated. Further, the amount of spalling must be measured from an in situ structure made from the same concrete as the test specimens. By comparing test results from these tests the model uncertainty can be estimated. Petterson [19] and [20] have performed a series of tests where the so-called Borås test method, SS 13 72 44 [21], was used.

For the evaluation of the spalling of the concrete in situ Petterson used test specimens of the dimensions $50 \times 150 \times 150$ mm. The amount of spalling of the in situ test items was measured as the reduction in % of the weight of the test specimens. During a four year period a number of test items placed in a marine environment and a number of test items placed close to a roadway were investigated. In a laboratory the amount of spalling was determined using the Borås test method.
In Figure 3.2 the reduction of the weight of the in situ test specimens is shown as a function of the amount of spalling measured using the Borås method. The results shown in Figure 3.2 are for the test specimens placed close to a roadway.

In Figure 4 it is seen that for concrete with a low *w/c*-ratio (a *w/c*-ratio between 0.37 and 0.45) there is in general a poor agreement between the in situ observations and the results of the Borås test, independent of the amount of entrained air. This is a critical observation because most modern concrete have a relatively low *w/c*-ratio.

It is difficult on the basis of the results given in Figure 4 to specify the model uncertainty. The model uncertainty will in general have to be assessed for each type of concrete, depending on the amount of entrained air and the *w/c*-ratio. Even in this case the model uncertainty is likely to exhibit a substantial scatter.

4 SUMMARY AND CONCLUSIONS

In conclusion, there exists limited data on the basis of which a probabilistic service life model for freeze/thaw damage can be developed. Parameters to be quantified for determination of the probability of frost damage include materials properties (obtained from compliance testing), in-situ performance, and the environmental exposure. Presently, the models proposed for freeze/thaw damage must be considered as personal belief and experience formulated within the framework of Bayesian statistics.

A service life model would not only be applicable for estimation of the lifetime of a considered structure, but also for reliability updating using observations from the structure. This implies that the probabilistic model is updated providing more accurate predictions about the lifetime of the structure.

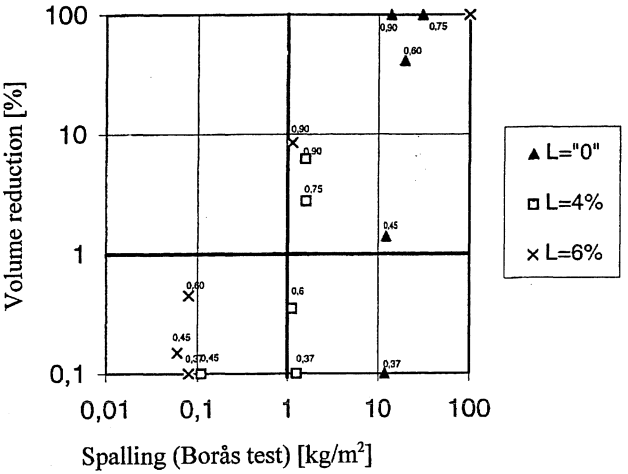

Figure 4. Results of in situ tests as a function of results of Borås testing together with commonly used acceptance limits (L denotes the air content and the number indicated by each measurement is the w/c-ratio), Petterson [19].

5 ACKNOWLEDGEMENTS

The paper has been prepared based on work undertaken under the European Community Brite/EuRam Project BE95-1347 at COWI Consulting Engineers and Planners.

6 REFERENCES

1. Fredriksen, J.M. and Poulsen, E. (1997) *HETEK, Chloride penetration into concrete - guide.* Report No. 123, Danish Road Directorate
2. COWI Consulting Engineers (1999) *DuraCrete. General guidelines for durability design and redesign.* Task 7 Report, BE95-1347/R14.
3. Geiker, M. and Vincentsen, L.J. (1999) *Strategies for improved ageing management.* RILEM-ACI-OECD Int. Conf. On Life prediction and ageing management of concrete structure, Bratislava
4. Fagerlund, G. (1996) *Livslängdsberäkninger för betongkonstruktioner.* Lunds Tekniska Högskola, Lund (in Swedish).
5. Vasikari, E. (1996) *Modelling of frost attack for service life design of concrete structures.* Proceedings of a Nordic Research Siminar in Lund on Frost resistance of building materials. Edt. Lindmark
6. COWI Consulting Engineers (1999) *DuraCrete. Statistical quantification, frost attack.* Task 4 Report, The European Community Brite/EuRam Project BE95-1347/internal report T4_9
7. Engelund, S., Sørensen, J. D., and Sørensen, B. (1999) *Evaluation of Repair and Maintenance Strategies for Coastal Bridges on a Probabilistic Basis,* ACI Materials Journal, 96, pp. 160-166

8. Hergenröder, M. (1992) *Zur Statistischen Instandholtungsplanung für bestehende Betonbauwerke bei Karbonatisierung det Betons und möglicher Korrosion der Bewehrung*, Berichte aus dem Konstruktiven Ingenieurbau 4/92, Technische Universiät München
9. Hoffmann, P. C., and Weyers, R. E., *Probabilistic Analysis of Reinforced Concrete Bridge Decks*, in: Frangopol, D. M., and Grigoriu, M. D. (eds.) (1996) Probabilistic Mechanics and Structural Reliability, ASCE, New York, pp. 290-293
10. Fagerlund, G.(1993) *Frostangrepp - beskrivning av verkande mekanismer.* Marina betongkonstruktioners livslängd, Cementa and Euroc, Sweden, pp. 23-70
11. Chalmers University of Technology (1997) *DuraCrete, Models for Environmental Actions on Concrete Structures*, The European Community Brite/EuRam Project BE95-1347, Task 2 Report
12. Fagerlund, G. (1995) *The required Air Content of Concrete.* Int. Workshop on Mass-Energy Transfer and Determination of Building Components - Models and Characterisation of Transfer Properties, pp. 591-609
13. Fagerlund, G. (1979) *Prediction of the Service Life of Concrete Exposed to Frost Action.* In "Studies on Concrete Technology". Swedish Cement and Concrete Research Institute, Stockholm, 1979 (referred to in private communication by Fagerlund)
14. Hansen, E. de Place 1996) *Byggematerialers frostbestandighed. Modellering af kritiske vandmætningsgrader (Frost resistance of Building Materials. Modelling of Critical Degree of Saturation).* SBI Report 268
15. Pigeon, M. and Pleau, R. (1995) *Durability of Concrete in Cold Climates.* E & FN SPON
16. Siemes, T. and Faber, M.H. (1998) *DuraCrete. Short Course on Probabilistic Methods for Durability Design,* The European Community Brite/EuRam Project BE95-1347, Internal report
17. Thoft-Christensen, P., Baker, M. J. (1982) *Structural Reliability Theory and Its Applications,* Springer, Berlin
18. Eriksen, K., Geiker, M., Grelk, B., Laugesen, P., Pedersen, E.J. and Thaulow, N. (1997) *Methods for Test of the Frost Resistance of High Performacne Concrete. Performence Testing versus In Situ Observations.* The Danish Road Directorate, Report No. 93
19. Petersson, P.-E. (1995) *Betongs saltfrostbestandighet - Fältförsök.* SP Report 1995-73, 1995.
20. Petersson, P.-E (1996) *Scaling Resistance of Concrete Field Exposure Tests.* Durability of Concrete in Saline Environment, Cementa
21. SS 1372 44 (1995) *Concrete Testing - Hardened Concrete - Scaling at Freezing.* Swedish Standard

RECYCLED AND POROUS AGGREGATE IN WET FROST TESTING

Stefan Jacobsen, dr.ing
The Norwegian Building Research Institute
P.O.box 123 Blindern
0314 Oslo, Norway
stefan.jacobsen@byggforsk.no

1. INTRODUCTION

Some investigations have been carried out in our laboratories on the freeze/thaw deterioration of recycled aggregate (RCA). These are part of a four-year project in Norway on implementation of recycled aggregate in the construction industry [1-3]. In this project various unbound (roads, fill around flexible pipes) and bound applications (mainly cement based materials) are being considered. The use of RCA is fairly new in Norway and the scepticism against the product has been difficult to overcome for the producer, which is a new actor on the market with a new product – normally a difficult combination. One reason for the scepticism towards RCA in Norway is that we from nature side have a lot of good quality rock. There should, however, be many possibilities for use of recycled and/or porous aggregate, even under winter conditions.

There should be no doubt as to the positive effect recycling has on the environment by reduced outtake of primary raw materials and at the same time reducing the amount of waste generated. This positive effect holds even if energy consumption during crushing is almost the same as in production of crushed rock.

The object of the present investigation has been to study the durability of various types of bulk RCA, for example when exposed to de-icers in unbound road construction, and also to assess the usefulness of the new European frost testmethod [4] for RCA. For this purpose RCA of different composition (pure concrete, concrete/brick/asphalt-blends, pure brick) have been tested. Also one artificial LWA has been tested for comparison. Frost testing has been carried out both with the prescribed pre-drying for 24 hours at 105 °C, and with no predrying. It is well known that pre-drying can alter the pore structure and frost durability of cement based materials [5,6]. The severe pre-drying procedure of [4] might therefore be more unrealistic to cement based materials than to other materials, and this is particularly important to find out. Also the deteriorating effect of salt solution has been investigated for various materials (both cement based and others).

It should also be mentioned that it is well known that the aggregate behaviour in an unbound (bulk) frost test does not necessarily relate to the behaviour in bound use, for example concrete [7-9]. Testing of unbound aggregate as such, however, has relevance to practice since most aggregates are used for other purposes than concrete.

2. THE BULK AGGREGATE FROST TEST METHOD

The test method [4], which is based on the German DIN test, is fairly simple in both design and execution. The aggregate (8 – 16 mm, 16- 32 mm, ..) is washed, sieved and dried at 105 °C for 24 hours. After drying, 2 kg samples (1 litre in the case of LWA) are prepared and submerged in de-ionised water for 24 hours. Then each aggregate sample is frozen and thawed during 10 cycles in an open topped metal can. The can diameter is 120 - 140 mm, the height is 170 - 220 mm and the volume is about 2 litres. The water level is adjusted to 10 mm above the aggregate before freezing.

Figure 1 shows one 24 hour frost cycle measured in the centre of a can. A lid is put on top of the can to prevent evaporation. After 10 cycles the frost deterioration is measured by sieving wet and by hand the material passing half the initial minimum size (4 mm when testing the 8 – 16 mm fraction). The frost deterioration, F, is then expressed as

F (%) = dry mass < 4 mm after frost / total dry mass before frost

Damage can also be expressed as loss of mechanical properties of the aggregate by performing some kind of strength test before and after frost exposure.

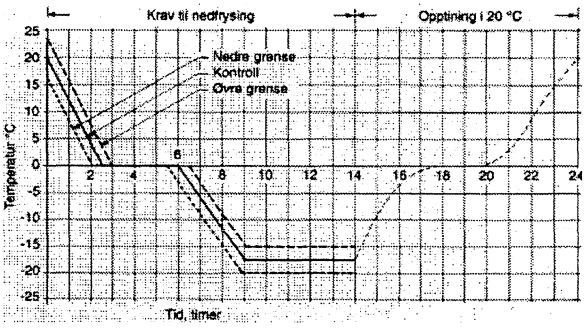

Figure 1: Frost cycle in bulk aggregate test [4]

Similarly to wet concrete tests, the method can be criticised for being quite different from most natural exposure situations and too accelerated. This is mainly due to the accelerated liquid uptake in wet freeze/thaw ("pumping effect") caused by ice forcing water inwards and migration of unfrozen water towards ice in the material, [10]. The degree of saturation is the main parameter for the severity of most frost tests [11].

The actual test is in the authors opinion creating a significant hydraulic pressure. By observing the cans during freezing, it can be seen that ice is forming first on the can walls and on the surface of the liquid. This creates an ice-box in the metal can. The hydraulic pressure or confinement inside this ice-box has caused several of our solid welded stainless steel cans to get rounded bottoms. When using a horizontal mesh and weight placed on top of the LWA in the can during test to prevent LWA from floating, the mesh is bended upwards in the centre since it is restrained by the first ice formed along the inside of the vertical can walls. The hydraulic pressure probably depends on can design, -strength/stiffness and confinement ability. In addition to the hydraulic pressure there is of course the ability of ice lens growth due to migration of unfrozen water towards ice formed in the porous material. This water uptake effect will depend on material and exposure condition. Cement based materials, particularly those exposed to de-icer salt during freezing and thawing, will have the largest uptake due to ice lens growth and vapour migration.

It should also be noticed that some kind of salt segregation probably is taking place during test when using salt solution since the water is less salt in the top of the can at the end of test. The heat flow and rate of ice formation is also important for testing in both pure water and salt solution [12]. For large differences in sample density and porosity the heat flow and degree of saturation will probably vary largely. This could give different frost cycles for different materials.

In the work of CEN there have been discussions whether aggregates should be tested using salt solution. Salt solution can have a very negative effect on aggregate frost durability in practice [13], as for concrete. Investigations have also shown that the increased salt frost deterioration of many natural porous aggregates in field can be reproduced in the laboratory, and with correlation to their field behaviour [14]. It has even been found that the reliability of frost testing is improved when using 1 % salt solution compared to testing in fresh water [15]. These are reasons to include the use of salt normatively in [4]. All these findings, however, were made on natural aggregates.

3. MATERIALS

The materials tested were mainly recycled aggregates produced from crushed building debris at the recycling plant of BA Gjenvinning at Grønmo in Oslo. These are mainly pure concrete or blends of concrete, brick, asphalt, LWA, gas concrete etc. In addition, one pure crushed tile and one artificial LWA (Norwegian expanded clay produced in a rotating kiln) were tested. All aggregates were in the fraction 8 – 16 mm. Table 1 shows the materials and their characteristics.

Table 1. Aggregates (8-16 mm) tested and their characteristics

Aggregate	dry particle dens. (kg/m^3)	24 h abs. (% dry mass)	description – main materials *
Blend 1	2240	6,3	70 % concr, 20 % rock, 7 % brick
Blend 2	2280	5,7	74 % concr, 17 % rock, 8 % brick
Blend 3	2330	4,4	35 % concr, 42 % rock, 14 % brick, 10 % asphalt
Blend 4	2520	2,7	30 % concr, 62 % rock, 4 % brick, 4 % asphalt
Blend 5	2140	7,6	mainly concrete
Brick	1920	12,8	only crushed brick
Concrete 1	2370	4,5	only concrete
Concrete 2	2280	5,3	only concrete
LWA	≈500	≈10 - 12	expanded clay

*: not including small quantities of gas concrete, LWA, glass, metal, organic material etc.

To study the effect of pre-drying and salt solution, four combinations of predrying and test liquid were used:

- 105 W: pre-dried at 105 C for 24 h, tested in de-ionized water (standard [4])
- 105 S: pred-ried at 105 C for 24 h, tested in 1 % NaCl solution
- W: no pre-drying, tested in de-ionized water
- S: no pre-drying, tested in 1 % NaCl solution

All aggregates were tested using three individual samples (2 kg or 1 litre for LWA) according to [4]. The volume was measured after 24 h absorption using a wire basket. When calculating the frost deterioration of non dried material the 2 kg absorbed mass of the initial sample was corrected for its 24 hour absorption.

4. RESULTS AND DISCUSSION

Table 2 shows frost test results as mean of the three parallel samples for each aggregate and combination of pre-drying and test liquid.

Table 2: Frost deterioration – F (%)

Aggregate	105 W [4]	105 S	W	S
Blend 1	8,3	40,4	5,8	27,2
Blend 2	14,6	34,7	10,6	28,5
Blend 3	4,2	14,9	4,2	9,8
Blend 4	2,7	21,4	-	-
Blend 5	7,7	25,4	2,4	18,2
Brick	3,2	6,4	-	-
Concrete 1	8,0	37,6	3,7	30,9
Concrete 2	13,9	36,8	3,1	30,3
LWA	3,9	1,1	8,7	2,0

From table 2 we see first of all that the deterioration in general is quite high for most aggregates. According to the standard test [4] with pre-drying and water the deterioration varies largely: from 2,7 – 14,6 %. The Norwegian standard aggregate for concrete testing [16] is a gneiss-granite with typically 0,2 – 0,4 % absorption and particle density of about 2670 kg/m^3. This aggregate has been tested in our laboratories from at least 12 different quarries according to this bulk aggregate test. These tests were performed both with water and 1 % NaCl after 105 °C pre-drying and always gave very low deterioration with F in the range 0,1 – 0,5 %. There were no differences between tests with water and 1 % NaCl.

Table 2 also clearly shows the negative effect of salt for cement based materials, as expected. The deteriorating effect of salt tends to be smaller when there is less cement based material present in the aggregate. For pure brick aggregate the increased deterioration due to salt is lower than for any of the blends. For LWA there is actually more damage with water than with salt both with and without pre-drying. This has also been observed on very porous natural LWA (Icelandic pumice) [17,18]. The reason is not yet understood but is probably related to the coarse pore structure of the LWA and a low degree of saturation. In LWA, hydraulic effects are probably mainly responsible for the damage. The salt in LWA is presumably mainly resulting in reduced ice formation and hence reduced damage. Many natural rocks, however, show the same negative effect of salt as cement based materials do [13-15]. Today we are still missing the basic research telling precisely which pore structure properties of the aggregates that are making them susceptible to frost/salt deterioration. We suspect, however, that aggregates with a high share of very fine gel-type porosity are susceptible to frost/salt damage.

Omitting the pre-drying at 105 °C reduces the damage for aggregates with cement based materials, whereas there is no such effect for LWA, as expected. In fact, LWA has higher damage without pre-drying for both water and salt. The explanation can be that the drying mainly results in lower degree of saturation in the LWA after 24 hours of absorption compared to non-dried materials. (Pore structure coarsening due to drying is probably very weak, if at all present, in LWA and brick compared to in cement based materials.) The non-dried LWA presumably contained some moisture before absorption. It therefore had a higher degree of saturation than the dried LWA after 24 hours of absorption before frost exposure started. This effect is probably smaller for the other materials that will have a larger portion of their total porosity (= larger degree of saturation) filled during 24 hours compared to the LWA.

Due to the results RCA should be used were salt is not present . Furthermore, the aggregate should not be able to freeze while submerged, i.e proper drainage should exist.

The usefulness of the test method is, as for most wet frost test methods, difficult to establish. For ranking of various materials the test is probably similar to other wet frost tests like [19, 20]. This of course depends on statistical data on reliability [15], and on experiments calibrating the deterioration against field performance [14]. Basically, frost durability is a function of how much water that can be absorbed before damage occurs in freezing, and how long absorption time it takes before damage occurs [21,22]. In the present test the degree of saturation obtained after 24 hours of absorption varies largely. To get more information out of the test, the actual degree of saturation after 10 frost cycles can be measured. This could give some additional information on how large the water uptake due to the pumping effect is during freeze/thaw. This additional uptake gives information on the rate of absorption during freeze/thaw conditions. If total porosity is also measured, the degree of saturation can be determined at the various stages of testing.

The importance of the degree of saturation of the RCA for the frost durability of concrete was demonstrated in [3]. Frost dilation tests of concrete were performed on concretes with identical binders made with saturated and rather dry RCA respectively. There was a clear critical increase in frost dilation in the wet RCA concrete compared to the dry RCA concrete. Clearly, a safe area for use of RCA in concrete is in concrete for less aggressive environments [23].

In the present investigation the concrete compositions were not known, but they were presumably non air-entrained. In most cases of demolition, knowledge about the concrete composition is low. Detailed investigations to establish the exact composition does not seem realistic at present. It could be that in the future a simple, inexpensive procedure could be established to determine approximate w/c and air content of the concrete structure before demolition and RCA production. This could for example be done using plane sections to determine the aggregate-, paste- and air content. Then, the PF-method on parallel specimens could be used to determine paste porosity (i.e. w/c ratio) and also air void content and PF. This could be a part of further development of methods to assess the potential frost resistance of the RCA produced from a structure since it is well known that the air voids also improve the frost durability of RCA [24-26].

5. CONCLUSION

Recycled aggregates exhibit rather high frost deterioration when tested in the bulk aggregate test, and the results also vary largely between randomly chosen samples, as expected. Testing with salt increases the deterioration of cement based materials; more the higher the content of cement based material in the RCA. The deteriorating effect of salt is very weak for brick and not present for LWA. Pre-drying of the aggregate at 105 °C before testing reduces the frost test performance of cement based RCA, whereas LWA showed no such effect. When evaluating frost test results of RCA containing cement based material, the severity of the 105 °C pre-drying must be considered since this treatment is very harsh compared to natural ageing.

As a preliminary recommendation, RCA based on concrete should not be exposed to frost when submerged, particularly not in the presence of salt. There are, however, applications where the aggregate is sufficiently drained to function, even under winter conditions.

Some suggestions are given for future development of inspection methods of concrete structures for demolition and RCA production. Also a few simple extra measurements in the bulk frost test to give additional information on frost durability are proposed. Some features of the test method deviating from real exposure have also been discussed.

6. REFERENCES

1. RESIBA – Recycled aggregate for building and construction – 4 year ØkoBygg development project. http://www.byggforsk.no.prosjekter/
2. Jacobsen S. Deklarasjon av egenskaper for resirkulert tilslag – forprsjekt 1998 (foreløpig rapport 10.12.1998), NBI rapport E 7753, 6 s + 6 appendix, 1998
3. Jacobsen S., Rommetvedt O.E., Gjengstø K.T.: Properties and frost durability of recycled aggregate from Oslo Norway, Sustainable construction – use of recycled concrete aggregate (ed. R.K.Dhir et al.), Thomas Telford, London, pp. 189-196 (1998)
4. prEN 1367-1 – Tests for thermal and weathering properties of aggregates – Part 1: Determination of resistance to freezing and thawing, Final draft December 1998, 11 p.
5. Bager D.H and Sellevold E.J.: Cement and Concrete Research, Vol.16 pp.835-844 (1986)
6. Sellevold E.J and Farstad T.: Frost/salt testing of concrete: effect of test parameters and concrete moisture history, NCR Publ. 10 pp. 121-138, 1991
7. Verbeck G, Landgren R.: Influence of physical characteristics of aggregates on frost resistance of concrete, Proc. ASTM, Vol.60, pp.1063-1079, 1960
8. Collins R. Lower grade aggregates in concrete. Long-term durability report, Quarry Management and Products Vol. 20, pp.13-21, 1993
9. Fagerlund G. Frost resistance of conc. with porous aggregates CBI rep 2:78 189 p. 1978
10. Jacobsen S. "Liquid Uptake Mechanisms in Wet Freeze/thaw: Review and Modeling," Draft Proc., Minneapolis Works. Frost Damage in Conc., Rilem/Univ.of Minnesota, D.J.Janssen, M.J.Setzer, M.B.Snyder (eds.), pp.41-51 (1999)
11. Fagerlund G.: Nordic Concrete Research Publ.No.11 pp.20-36, 1992
12. Jacobsen S., Sæther D.H., Sellevold E.J.: Frost testing of high strength concrete: frost/salt scaling at different cooling rates, Materials and Structures, V.30 Jan-Feb. pp.33-42, 1997
13. Höbeda P, Jacobson T. Freeze/thaw tests on stone material using weak solutions of deicers, National Road and Traffic research Institute, report 244, 90 p., 1981 (in Swedish)
14. Petursson P. Frost resistance test for coarse aggregates, Nordic Concrete Research Publication Vol.15 no.27, pp. 47-58, 1994
15. Petursson P. Frost resistance test on aggregates: intercomparison of a new Nordtest method - a base for CEN standardisation, IBRI report 96-18, Iceland 1996
16. NS 3099, Standard aggregate for concrete testing
17. Nordtest project 1440-99
18. Petursson P. Personal communication aug. 1999
19. SS 13 72 44 Concrete testing – hardened concrete – scaling at freezing
20. ASTM C666 Resistance of concrete to rapid freezing and thawing (in water – proc.A)
21. ASTM C671 Critical dilation of concrete specimens subjected to freezing
22. Rilem committee 4 CDC, The critical degree of saturation method of assessing the freeze/thaw resistance of concrete, Mat. and Str. Vol.10, No.58, pp.217-229, 1977
23. Beton med beton i, Dansk beton nr. 1, pp.7-9, Feb. 1999
24. Hansen T.C.(ed.) Recycling of demolished concrete and masonry, Rilem rep 6, E&FN Spon, 316 p., 1993
25. Hilsdorf H.K., Kottas R., Müller H.S. Investigations on freeze/thaw resistance of recycling concrete, Rilem Proc. 34 Frost res. of concrete, E&FN Spon, pp. 61-72, 1997
26. Dillman R. Freeze/thaw resistance of concrete with recycled aggregate, Rilem Proc. 34 Frost resistance of concrete, E&FN Spon, pp. 73-80, 1997

ACKNOWLEDGEMENTS

Ivar Molstad and Steinar Solberg at NBI Materials and structures Dept., and Frode Kleiva from Oslo College are thanked for carrying out frost testing and material characterisation. BA Gjenvinning/Bjørn Vegar Hansen, Veidekke/Ole Skytterholm and the ØkoBygg programme at GRIP-senter are thanked for cooperation and financial support through ØkoBygg development project 6055.

MOISTURE TRANSFER IN CONCRETE AND DEGRADATION BY FROST - EXPERIMENTAL RESULTS AND THEIR ANALYSIS

Hannele Kuosa
MScTech, Research Scientist
VTT Building Technology
P.O. Box 1805, FIN-02044 VTT,
Finland

Erkki Vesikari
Lic.Tech., Senior Research Scientist
VTT Building Technology
P.O. Box 1805, FIN-02044 VTT,
Finland

1 INTRODUCTION

The purpose of this research was to verify the theories and material parameters of moisture transfer in concrete and frost attack to be used in an analytical evaluation of concrete frost resistance and service life. For a reliable simulation of moisture transfer and frost attack in concrete there has been inadequately experimental research. There have been theories at hand but no exact data on the material parameters related with them [3, 4].

This report contains results of moisture transfer and frost resistance tests and results of some further analysis of the test results. The created models and parameters were to be applied in a computer simulation programme by which the service life of a concrete structure can be predicted [1, 2].

2 COMPOSITION OF CONCRETES

The test program included five different concrete compositions. The nominal strength of the test concretes were 35 MPa, 45MPa and 70MPa (denoted as K35, K45 and K70). The concretes K35 and K45 were air entrained by 3% and 5%. Mix proportions including admixtures and measured mass properties are presented in table 1 [3].

Table 1. Mix proportions and measured properties of concrete mass.

Concrete:	A	B	C	D	E
Strength class (MPa)	K35	K35	K45	K45	K70
Consistency grade (VeBe), sVB	2-3	2-3	2-3	2-3	2-3
Target air content, %	3	5	3	5	1
Air entraining agent, % by weight of cement	0.0040	0.0071	0.0035	0.0210	-
Superplasticizer, % by weight of cement	-	-	-	0.603	2.500
w/c ratio	0.58	0.52	0.47	0.42	0.37
Cement content, kg/m^3	305	321	385	405	396
Water content, kg/m^3	177	166	180	170	143
Aggregate content, kg/m^3	1850	1810	1780	1730	1900
Measured air content, %[1)]	3.5	5.0	2.8	5.2	1.0
Mass density, kg/m^3	2326	2305	2376	2314	2476
VeBe/slump, s/mm	60/1.9	40/2.5	50/2.5	40/2.6	45/2.5

The concretes were tested by four tests:

- Air pore analysis
- Capillary water uptake test
- Drying test and
- Critical degree of saturation test

The test results were re-examined by special analysis methods

3 AIR PORE ANALYSIS

3.1 Test and initial results

The air porosity of test concretes was analysed by image analysis using plane sections (75x75 mm^2). Plane sections were ground, died black and air pores were filled with white fine-graded material. In the calculation phase of the analysis, the measured 'plane distribution' of air pores was converted theoretically into a volume distribution [5].

The cumulative volume distributions of air pores are presented in figure 1.

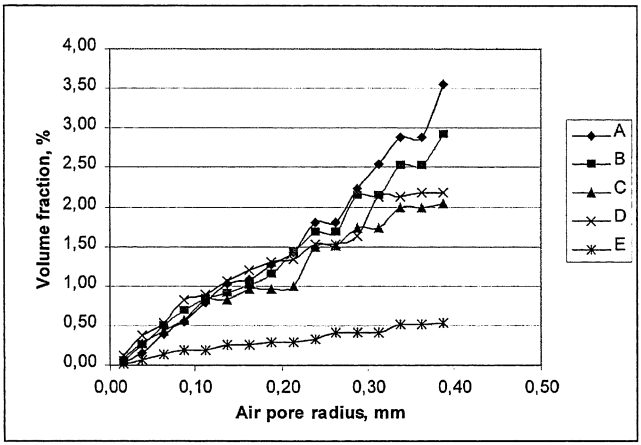

Figure 1. Cumulative volume distribution of air pores as determined by optical analysis.

3.2 Cumulative distribution function

To be able to treat the performance of air pores analytically the distribution of air pores must be presented in a simple mathematical form. Based on the results of the air pore analysis it was decided to use equation 1 as the model of the cumulative volume distribution of air pores.

$$a(r) = a_0 \cdot \left(\frac{r}{r_{max}} \right)^{n_r} \qquad (0 \le r \le r_{max}) \tag{1}$$

where

a(r) is	cumulative volume distribution of air pores, m^3/m^3
a_o	total volume of air pores ($r<r_{max}$), m^3/m^3
r_{max}	maximum air pore radius (usually 0.5 mm)
r	air pore radius ($0< r < r_{max}$), mm
n_r	exponent of the air pore distribution.

The curvature of the air pore distribution is defined by the exponent n_r. If $n_r = 1$, all the air pore size classes include the same amount of air. If $n_r < 1$, the air pore distribution is concentrated on the small air pores, and if $n_r > 1$, the distribution is concentrated on big air pores.

Formula 1 was adjusted to the air pore analysis results above (fig. 1) to find values for the total volume of air pores, a_o, and the exponent of air pore distribution n_r. These parameters are presented in table 2.

Table 2. Parameters a_O and n_r.

Concrete	Air content, a_o, %	Exponent of the air pore distribution, n_r
A	3.56	1.33
B	2.91	1.14
C	2.04	0.85
D	2.63	0.72
E	0.65	0.80

The fit of the theoretical air pore distribution to the experimentally measured distribution was good as presented in figure 2.

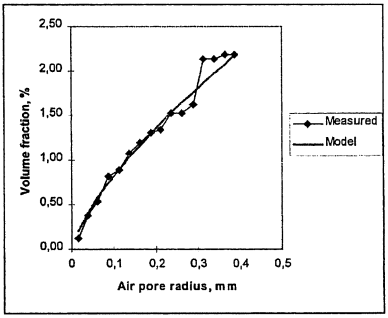

Figure 2. Concrete D. Adjustment of the theoretical and measured air pore distribution.

Air pore parameters calculated using equation 1 and the parameters in table 2 are presented in table 3. The minimum air pore radius r_{min} is 0.010 mm and the maximum radius r_{max} is 0.500 mm.

Table 3. Air pore parameters determined using the theoretical air pore distributions.

Concrete	Total air content, %	Specific surface, mm^2/mm^3	Powers' spacing factor, mm
A	5.0	17	0.28
B	3.9	21	0.26
C	2.4	28	0.25
D	2.5	33	0.21
E	0.6	30	0.40

4 CAPILLARY WATER UPTAKE TEST

4.1 Test and initial test results

The capillary water uptake test was carried out using concrete sections with 25 mm thickness and area of 100x100 mm^2. After drying in +50 °C for a period of 14 days these sections were allowed to absorb water through their bottom surface [6, 7]. There was three sections representing each concrete (A, B, C, D and E). The test was carried out in a relative humidity > 95%. The concrete sections were 3 mm below water surface and they were covered with a plastic foil during the test. The water uptake phase was followed by pressure saturation with 15 MPa water pressure and drying to constant weight in +105 °C. In figure 3 the results of the capillary water uptake test are presented.

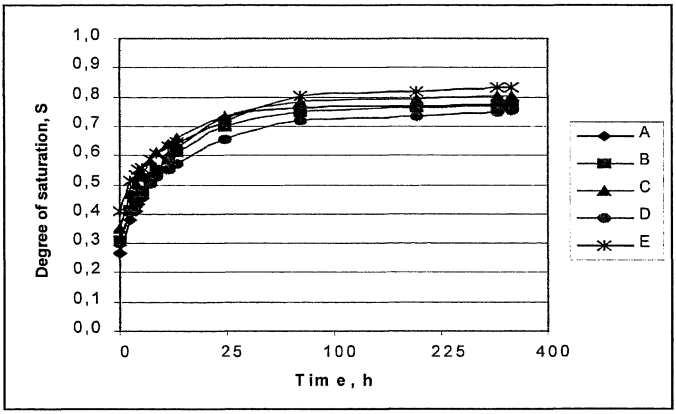

Figure 3. Degree of saturation vs. time.

The determined porosities and permeability parameters based on the capillary water uptake test are presented in tables 4 and 5. P_{tot} (l/m^3) is the total porosity of concrete corresponding to water content w_{tot} (kg/m^3). These values were determined by pressure saturation and drying in +105 °C. The volume of each concrete section was measured by weighing in water and in air. P_a is the total volume of air pores, l/m^3, and P_{cap} is the total volume of capillary pores, l/m^3.

Table 4. Results of capillary water uptake test. Porosity parameters.

Concrete	Total porosity P_{tot} l/m^3	Air pore content P_a l/m^3	Capillary pore content P_{cap} l/m^3
A	170.4	42.2	82.5
B	164.9	43.1	71.0
C	166.0	37.7	70.2
D	171.2	51.2	68.4
E	121.3	26.5	45.2

Table 5. Results of capillary water uptake test. Permeability parameters.

Concrete	Coefficient of water resistance, m 1) s/mm^2	Capillary index k_1 $kg/m^2\sqrt{s}$	"Capillary index" k_2 2) $kg/m^2\sqrt{s}$
A	46.4	0.0121	0.000117
B	48.4	0.0102	0.000135
C	39.9	0.0111	0.000129
D	47.0	0.0100	0.000227
E	51.5	0.0063	0.000171

1) Calculated as $m = \left(\frac{P_{cap}}{1000 \cdot k_1} \right)^2$.

2) Calculated in the same way as k_1, although air pores are not filled by capillary force.

4.2 Capillary moisture diffusion

In simulation computations the rainwater is assumed to be absorbed to the edge zone of the structure by capillary suction and transferred further into the structure by capillary moisture diffusion. To be able to simulate properly the moisture movements in a structure it is essential to establish the relationship between the capillary index and the capillary moisture diffusivity. In this research the relationship is represented by equation 2:

$$D_w = c \cdot k_1 \tag{2}$$

where

D_w is capillary moisture diffusivity (as m^2/s),
k_1 capillary index (as $kg/(m^2 \cdot s^{1/2})$) and
c coefficient.

The relation between k_1, and D_w, was analysed using the above results of capillary water uptake test. This analysis was performed by dividing the 25 mm thick section calculatorily into five slices (3.13 mm + (3 x 6.25 mm) + 3.13 mm). It was assumed that water was absorbed into the first slice that was in contact with free water by the capillary theory. To the next slice and further on the moisture transfer was assumed to occur by capillary water diffusion. The principle of the calculations is presented in figure 4.

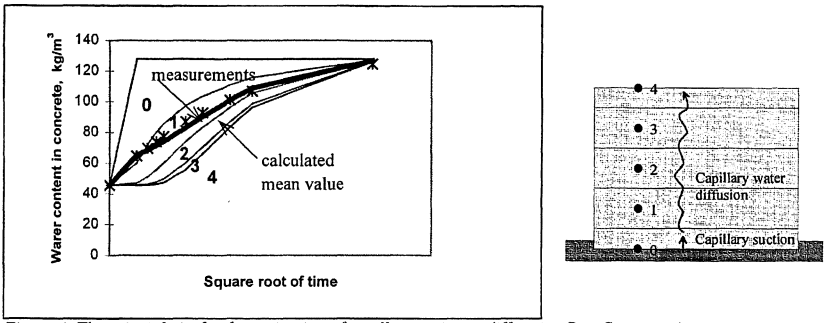

Figure 4. The principle in the determination of capillary moisture diffusivity, D_W. Concrete A.

The curves (0 - 4) in figure 4 express the calculated moisture contents as a function of time at different slices. The calculated moisture content of concrete was compared with the measured moisture contents in the capillary water uptake test. The capillary moisture diffusivity, D_w, was adjusted to give the best fit with the measured moisture content. The results of the analysis are presented in Table 6.

Table 6. Capillary moisture diffusivity, D_W.

Concrete	Capillary moisture diffusivity D_w 10^{-8} m²/s
A	1.2
B	1.2
C	1.4
D	1.0
E	0.7

A statistical connection between the capillary index and the capillary moisture diffusivity was established as:

$$D_w = 1.16 \cdot 10^{-6} \cdot k_1 \qquad (3)$$

where D_w is capillary moisture diffusivity in units m²/s, and capillary index, k_1 in units kg/(m²·s^{½}).

4.2 Air pore absorption and air diffusion coefficient

According to Fagerlund the air pore absorption rate is related to the air pore distribution. The time for an air pore to be completely filled by water can be evaluated from equation 4 [8]:

$$t = 9.35 \cdot 10^{6} \cdot r^3 / \delta_1 \qquad (4)$$

where

t is is the time for an air pore with radius r to be completely filled with water, s
r air pore radius, m, and
δ_1 diffusion coefficient of air in cement paste, m²/s.

The diffusion coefficient of air in cement paste is according to Fagerlund about 10^{-11} to 10^{-12} m^2/s. Equation 4 can be worked out to give the air pore radius r corresponding to time t. At any time t all the air pores having a smaller radius than this value are supposed to be water filled.

$$r = 0.475 \cdot 10^{-2} \cdot (\delta_1 \cdot t)^{\frac{1}{3}} \tag{5}$$

By inserting equation 5 into equation 1 the total air pore absorption can be expressed as:

$$a_w = w - w_{np} = a_0 \cdot \left(\frac{0.00475}{r_{\max}} \right)^{n_r} (\delta_1 \cdot t)^{\frac{n_r}{3}} \tag{6}$$

where

a_w is the amount of water filled air pores, m^3/m^3,
w concrete water content, kg/m^3 and
w_{np} nick point water content, kg/m^3.

The filling rate of air pores was measured by the capillary water uptake test. The value for the diffusion coefficient of air in cement paste, δ_1, was determined by comparing the measured and calculated water content.

In the first analysis a value for the exponent of air pore distribution, n_r, was chosen to yield the best fit with the measured water absorption in air pores. The exponent n_r was however not allowed to be greater than 1.5 as the exponent of time, $n_r/3$, in equation 6 was not allowed to be greater than 0.5.

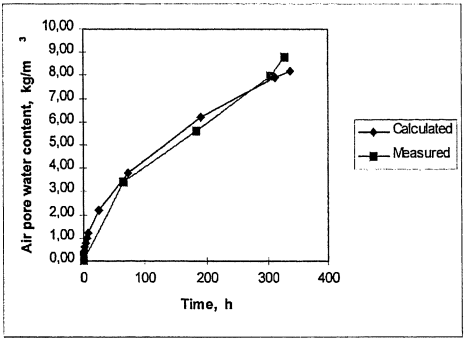

Figure 5. Principle of the determination of diffusion coefficient of air in cement paste, δ_1. Concrete D.

The results of the analysis are presented in table 7.

Table 7. Diffusion coefficient of air in cement paste, δ_1, determined by the 'best fit'-principle ($n_{r;max}$ = 1.5).

Concrete	Air pore distribution exponent, n_r	Diffusion coefficient of air in cement paste, δ_1, x 10^{-11} m^2/s
A	1.5	0.65
B	1.5	1.53
C	1.5	3.33
D	1.5	9.39
E	-[1)]	-[1)]

1) The values for concrete E can be considered incorrect as the amount of air pores < 1 mm in this concrete was very small compared with the amount of compression pores.

Furthermore the same analysis was done using the measured exponent of air pore distribution n_r (see table 2 above). In this case the agreement of the theoretical air pore absorption with the measured water absorption of air pores was not so good, but the variation in δ_1 was smaller. The results of this analysis are presented in table 8. If concrete E is excluded the average value for δ_1, was 0.36 x 10^{-11} m^2/s.

Table 8. Diffusion coefficient of air in cement paste, δ_1,, determined using values for exponent n_r from air pore analysis.

Concrete	Air pore distribution exponent, n_r	Diffusion coefficient of air in cement paste, δ_1 x 10^{-11} m^2/s
A	1.33	0.33
B	1.14	0.38
C	0.85	0.19
D	0.72	0.52
E	-	-

The value recommended for diffusion coefficient of air in cement paste to be used in computer simulation is δ_1 = 1 x 10^{-11} m^2/s. This is slightly greater than the average in analysis above. However, this value is justified by some auxiliary test results, which are not presented here. These results were obtained from 'a sprinkler irrigation test'. In this test concrete samples were exposed to artificial rain and the results were analysed in the same way as in the standard capillary water uptake test [6, 7]. The air pore absorption was faster in the 'sprinkler irrigation test' than in the standard capillary water uptake test.

5 DRYING TEST

5.1 Test and initial results

For the drying test concrete sections (25x100x100 mm^3 - 3 sections per each concrete A, B, C, D and E) were first stored in RH 95-100% for 70 - 80 days. Afterwards the sides of the sections were sealed to allow drying only through the two opposite faces (100x100 mm^2). The weight of the concrete sections was followed for 91 days as they were drying in RH 70%.
The drying of the concrete slices in RH 70% is presented in the figures 6 and 7. In figure 6 the weight loss with time is related to the initial weight. In the figure 7 the weight loss is presented as the degree of water saturation.

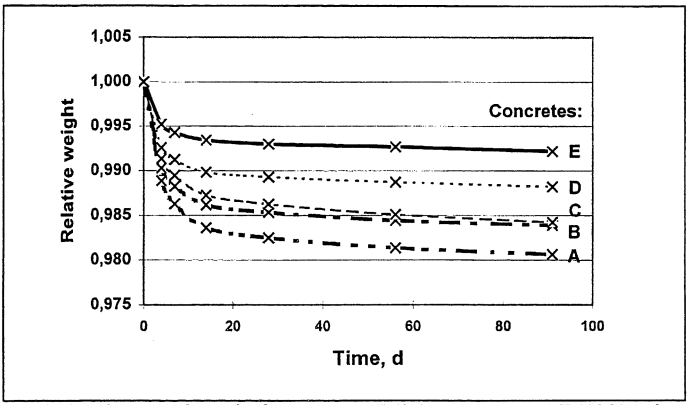

Fig. 6. The relative weights in the drying test in RH 70%. First curing in RH 100 % to the age of 70 - 80 d. Concretes A, B, C, D, and E.

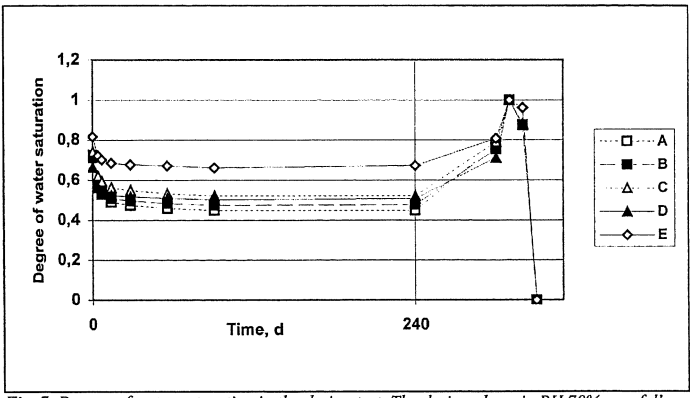

Fig. 7. Degree of water saturation in the drying test. The drying phase in RH 70% was followed by water suction, pressure saturation and drying in 105 °C. Concretes A, B, C, D, and E.

5.2 Water vapour diffusion coefficient

In the computer simulation programme the moisture transfer in concrete takes place by both capillary water diffusion and water vapour diffusion. The water vapour diffusion coefficient was assumed to be in relation to the relative humidity of concrete according to equation 7.

$$\delta_p = \delta_{p0} \cdot (1 + b2 \cdot \varphi^{n2}) \tag{7}$$

where

δ is water vapour diffusion coefficient, kg/(m s Pa)

δ^p_{p0} water vapour diffusion coefficient at a low relative humidity, kg/(m s Pa).

φ relative humidity of concrete and

b2 and n2 are constant parameters.

The water vapour diffusion coefficients for the test concretes were determined by an analysis of the test results. This analysis was done by dividing the thickness of the specimen (25 mm) calculatorily into five slices (figure 8). Inside concrete the moisture was assumed to be transferred both by capillary water diffusion and by water vapour diffusion. At the edges the moisture was assumed to be removed by convection (RH 70% and t = 20°C).

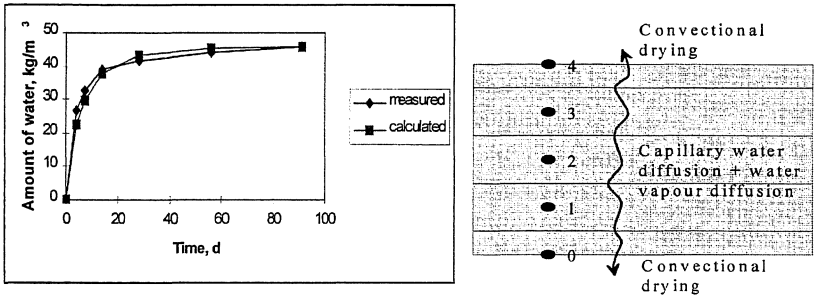

Fig. 8. Measured and calculated drying of concrete A.

As a result of the analysis the water vapour diffusion coefficient could be expressed as:

$$\delta_p = \delta_{p0} \cdot (1 + 10 \cdot \varphi^5) \tag{8}$$

The values of δ_{p0} are presented in table 9.

Table 9. Water vapour diffusion coefficients at a low relative humidity. Concretes A, B, C, D and E.

Concrete	Water vapour diffusion coefficient δ_{p0} kg/(m s Pa).
A	1.9
B	2.0
C	1.6
D	1.7
E	1.5

A statistical connection between water vapour diffusion coefficient at a low relative humidity, δ_{p0}, and the capillary moisture diffusivity D_w could be found:

$$\delta_{p0} = 1.35 \cdot 10^{-5} \cdot D_w \tag{9}$$

In equation 9 the unit of δ_{p0} is kg/(m s Pa) and the unit of D_w is m^2/s.

6 CRITICAL DEGREE OF SATURATION TEST

6.1 Test and initial results

For each concrete A - E 15 concrete sections (50x100x100 mm^3) were prepared. In each series of specimens the degree of water saturation was adjusted so that it ranged from about 0.75 to 1.00. The specimens were wrapped in a plastic foil during the freeze-thaw test. Degradation was determined by measuring the ultrasonic pulse velocity in the specimens after 1, 3 and 6 freeze-thaw cycles. The dynamic modulus of elasticity was assumed to be proportional with the square of ultrasonic pulse velocity.

The results for concretes A and C can be seen in figures 9 and 10. In these figures the reduction of the dynamic modulus of elasticity (E_n/E_o) is presented as a function of the degree of water saturation. From the plotted results the critical degree of saturation was determined.

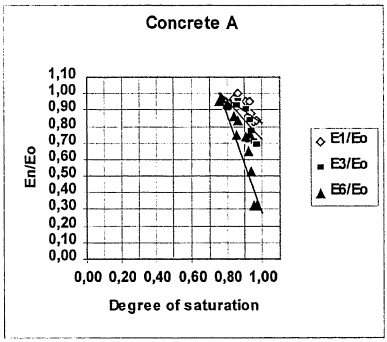

Fig. 9. Concrete A. Determination on the critical degree of saturation and degradation after 1, 3 and 6 freeze-thaw cycles.

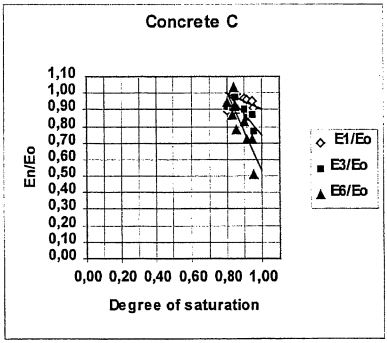

Fig. 10. Concrete C. Determination of the critical degree of saturation and degradation after 1, 3 and 6 freeze-thaw cycles.

The determined values of critical degree of saturation are presented in Table 10.

Table 10. Critical degree of saturation for concretes A to E

Concrete	S_{crit}
A	0.77
B	0.81
C	0.80
D	0.81
E	0.80

6.2 Rate of degradation

The degradation caused by successive freeze-thaw cycles is defined as the reduction of the relative value of dynamic modulus of elasticity. The degradation can be estimated according to Fagerlund by the following equation [8]:

$$D = 1 - \frac{E_N}{E_0} = K_N \cdot (S - S_{crit}) \tag{10}$$

where

D	is degree of degradation of concrete ($0 \leq D \leq 1$)
N	number of critical freezing events (number of freezing events with a moisture content greater than the critical moisture content),
S	degree of saturation at freezing,
S_{crit}	the critical degree of saturation.

K_N is the coefficient of degradation. According to Fagerlund, K_N can be determined from equation 11 [9]:

$$K_N = \frac{A \cdot N}{B + N} \tag{11}$$

where A and B are constants.

In this research the constants A and B were determined experimentally by analysing the results of the critical water saturation test. The results are presented in table 11.

Table 11. Experimentally determined values for constants A and B.

Concrete	A	B
A	13.04	19.00
B	10.22	15.18
C	9.04	17.08
D	9.26	18.55
E	4.11	15.43

The mean value for constant B was 17.1.
For constant A the following formula could be developed:

$$A = 36.2 \text{ w/c} - 8.0 \tag{12}$$

where w/c is the water-to-cement ratio of concrete.

According to formula 11 the degradation of concrete occurs rapidly in the beginning but after some years it stops completely. This kind of degradation is not considered to be in conformity with actual degradation in outdoor conditions. It is also impossible to determine the service life with that kind of degradation curve.

The analysis was continued by assuming a slightly different form for the coefficient of degradation K_N :

$$K_N = \frac{A \cdot N^C}{B + N} \tag{13}$$

As a result of this analysis the following possible solutions for A, B and C could be found:

$$C = 1.33 \qquad A = 8.7 \cdot w/c - 1.9 \qquad B = 4.1 \tag{14}$$

$$C = 1.5 \qquad A = 5.4 \cdot w/c - 1.2 \qquad B = 2.6 \tag{15}$$

The former value (equation 14) for constant C was considered most appropriate. During the service life of a structure the number of critical freezing events is usually some hundreds or thousands. This means that the constant B is very small compared to N and can thus be omitted.

As the concrete specimens were wrapped in a plastic foil during the freeze-thaw cycles the degree of saturation remains constant during the test. This means that the test method does not take into account the so-called 'pumping effect' which normally may substantially increase the rate of degradation. Because of the 'pumping effect' the actual constant A was considered to be multifold compared to the value obtained in the critical degree of saturation test. The final value for A was defined by an enquiry, which was arranged for all the frost resistance researchers in VTT Building Technology. The researchers were asked to compare the calculated rate of degradation to the actual degradation in facade concrete. As a consensus decision the following formulae were recommended:

$$K_N = A \cdot N^{\frac{1}{3}} \tag{16}$$

where

$$A = 34.8 \cdot w/c - 7.6 \tag{17}$$

6.3 Critical spacing factor

The values of S_{crit} were used to determine the critical amount of air filled air pores,

$$a_{r,crit} = (1 - S_{crit}) \cdot P_{tot} \tag{18}$$

where

$a_{r,crit}$ critical amount of air filled air pores at $S=S_{crit}$, m^3/m^3

The critical spacing factor corresponding to $a_{r,crit}$ was determined using the known theoretical air pore distributions and the formula of Powers' spacing factor:

$$L_{r;crit} = \frac{3}{\alpha_{r;crit}} \cdot \left[1.4 \cdot \left(\frac{V_{paste}}{a_{r;crit}} + 1 \right)^{1/3} - 1 \right] \quad (19)$$

where

$L_{r;crit}$ is Powers' spacing factor corresponding to S_{crit}, m
$\alpha_{r;crit}$ specific surface of air filled air pores at $S=S_{crit}$, m^2/m^3
V_{paste} concrete cement paste content (excluding air pores), m^3/m^3 concrete.

The determined values for the critical spacing factor are presented in table 12.

Table 12. Experimentally determined values for constants A and B.

Concrete	$L_{r;crit}$
A	0.434
B	0.599
C	0.347
D	0.525

For the simulation computations a value $L_{r;crit}$ = 0.40 mm was recommended.

8 REFERENCES

1. Vesikari E. Computer simulation technique for prediction of service life in concrete structures. Proc. Int. Conf. Life Prediction and Ageing Management of Concrete Structures, July 1999. RILEM Expertcentrum. Bratislava. pp. 17-23.
2. Vesikari, E. 1999. Prediction of service life of concrete structures with regard to frost attack by computer simulation. Proc. Nordic Res. Sem. on Frost Resistance of Building Materials, Aug. 31 - Sept. 1 1999, Lund. Lund Institute of Technology, Division of Building materials. 17 p.
3. Vesikari, E, Hannele K. 1999. Kosteuden liikkuminen betonissa ja pakkasvaurioituminen koetuloksia ja koetulosten analysointia (Moisture transfer in concrete and degradation by frost - Experimental results and their analysis). VTT Building Technology, Internal Rapport RTE-IR-10/1999, 33p. In Finnish.
4. Kuosa, H. 1998. Betonin ilmahuokostuksen ja pakkasenkestävyyden välinen yhteys (Connection between the air pore structure of concrete and concrete frost resistance). VTT Building Technology, Internal Report RTE 36-IR-18/1998. 42 p. In Finnish.
5. Vesikari, E. 1985. Image Analysis in Determining Pore Size Distributions of Concrete. 1985. VTT Research Notes 437. 31 p.
6. Fagerlund, G. 1977. The critical degree of saturation method of assessing the freeze/thaw resistance of concrete. Tentative RILEM recommendation. Prepared on behalf of RILEM Committee 4 CDC. Materiaux et Constructions 1977 no 58. Pp. 217-229.
7. VTT-TEST 358-86. Betoni, kapillaarisen vedelläkyllästysasteen määritys. 5p.
8. Fagerlund, G. 1996. Livslängdsberäkningar för betongkonstruktioner. Översikt med tillämpningsexempel. Lund, Lunds Tekniska Högskola, Byggnadsmaterial. TVBM-3070. 124 p. In Swedish.
9. Fagerlund, G. 1994. Influence of environmental factors on the frost resistance of concrete. A contribution to the BRITE/EURAM project BREU-CT92-0591 "The residual service life of concrete structures". Lund, Lund Institute of Technology. Division of Building Materials. Report TVBM-3059. 48 p.

SALTFROST SCALING OF PORTLAND CEMENT-BOUND MATERIALS

Sture Lindmark, PhD
Senior Researcher
Lund Institute of Technology
Div. Building Materials
Box 118
S-221 00 LUND
SWEDEN

Abstract

A hypothesis for a mechanism causing salt frost scaling of porous materials is described. It is hypothesised that salt frost scaling mainly is due to the much facilitated osmotic ice body growth, in the surface close regions of a material, which results from the presence of some liquid phase, *e.g.* a salt solution, at the material surface. A short review of the appropriate thermodynamics is given. Several results from salt-frost scaling tests, which have been reported in the literature, are explained.

1 INTRODUCTION

The mechanism(-s) of salt frost scaling of porous, brittle materials is (are) unknown. Consequently, precise prediction of the service life of a certain material in a certain environment cannot be made and thus material qualities cannot be optimised on basis of the environmental conditions in which the material is to be used.

Recently though, a hypothesis describing a major mechanism of salt frost scaling was forwarded[1], which may be used to explain most of the hitherto repeatedly reported observations from tests of salt frost scaling. It is the aim of this paper to describe this mechanism.

2 PROPOSED MECHANISM

2.1 General description

When a porous specimen containing water and some ice is cooled, the vapour pressure of the ice falls below that of the water. Due to the difference in vapour pressure, water starts moving towards the ice bodies, which thereby grow. The pores containing water will be partially drained, by which process the vapour pressure of the remaining water is reduced. After a certain extent of drainage has been reached, the vapour pressures of the ice and the water will again be equal and equilibrium will thus be re-established. Consequently, no further water movement takes place and the ice bodies stop growing. Alternatively, equilibrium may be established if the vapour pressure of the ice is somehow raised, *e.g.* by applying a positive pressure on the ice.

This type of ice body growth, is frequently referred to as osmotic ice body growth and is the cause of both wintertime soil heaving[2] and of frost induced deterioration of cement based materials [3,4].

Since the narrow pores are partially dried due to the osmotic ice body growth, the material is now in a state of suction. In a moisture-isolated specimen, this results in shrinkage. However, if some liquid were present at the material surface, that liquid would be sucked into the pores. The extent of drainage would be reduced and the chemical potential of the water close to the ice bodies would be raised above the value required for equilibrium with the ice. Thus, more water would move from the liquid to the solid phase, *i.e.* the ice bodies would grow. The only way of re-establishing equilibrium now is to raise the ice pressure (or, possibly, add some solute to the water phase, see below). This occurs when the ice bodies have completely filled the pores in which they began growing. However, the required ice pressure is some 1.1 MPa per degree below freezing, *i.e.* already at –5°C, a pressure of 5.5 MPa on the ice is needed. Considering that the tensile strength of cementitious materials is only a few MPa, one realises that this type of ice body growth, *i.e.* ice body growth with almost unlimited access to moisture, readily produces ice pressures which will damage the material.

2.2 Driving force

It was stated above that equilibrium may be re-established by increasing the pressure on the ice, or by adding some solute to the liquid phase. The following is a description of which possibilities are at hand and how each one of them affects the equilibrium. (The reader may alternatively proceed immediately to section 3).

The driving force for the described phase transition and the consequent suction consists of a difference in level of free energy of the solid and the liquid phase at the interface between the two phases. Such a difference may be expressed in terms of level of free energy, chemical potential or, as above, in terms of vapour pressure. Here, the discussion is given in terms of chemical potential and the reader is referred to the literature, *e.g.* Atkins[5], for the relation between chemical potential and vapour pressure.

At the interface liquid water – solid ice, the driving force for osmotic ice body growth may be calculated from the chemical potentials of each phase. Assuming the molar volume and the entropy to be pressure- and temperature independent, respectively, we have for the liquid water phase,

$$\mu_l = \mu_{ref} + V_{m,l}\left(P_l - P_{ref}\right) - S_{m,l}\left(T_l - T_{ref}\right) + RT\ln(X) + \frac{d(A\gamma)}{dn} \qquad (1)$$

in which μ = chemical potential, *i.e.* the change in free energy of the system caused by the addition of one mole of water to the system,
μ_{ref} = chemical potential at the reference state
$V_{m,l}$ = molar volume of the liquid, appr. 18×10^{-6} m³/mole
P_l = pressure
P_{ref} = reference pressure, usually 101325 Pa (1 atm)
$S_{m,l}$ = molar entropy, appr. 63 J/K/mole
T = temperature
X = mole fraction of water in the liquid
r = radius of the pore in which the liquid is confined
$d(A\gamma)/dn$ = change in interface free energy due to addition of n moles of water

A similar expression is valid for the chemical potential of the ice phase, μ_s. Usually though, the ice may be regarded as pure ice and the term $RTln(X)$ thus may be omitted.

Imagine a system consisting of an inert matrix (the concrete specimen) containing both ice and water. The change in free energy of the entire system when the amounts of ice and water are changed is

$$dG_{sys} = \mu_s dn_s + \mu_l dn_l \qquad (2)$$

in which n denotes number of moles of each phase in the system. In a system closed to mass exchange with the surroundings,

$$dn_s + dn_l = const \Rightarrow dn_s = -dn_l \qquad (3)$$

The change in free energy of the entire system when molecules are transferred from the liquid to the solid state therefore may be calculated

$$dG_{sys} = (\mu_s - \mu_l) dn_s \qquad (4)$$

From this expression, it is seen that when the chemical potential of the ice is less than that of the liquid phase, the free energy of the entire system is reduced if molecules are transferred from the liquid to the solid state. The driving potential $\Delta\mu$, or the "driving force", for phase transition thus may be calculated

$$\Delta\mu = \mu_s - \mu_l \qquad (5)$$

Now we shall examine how this driving potential is affected by changes in temperature, pressure, mole fractions and pore sizes.

Effect of temperature
The chemical potential of each phase changes with temperature according to

$$d\mu = -SdT \qquad (6)$$

Since the entropy, S, of water is some 63 J/K/mole and that of ice is some 41 J/K/mole, a decrease in temperature rises the chemical potential of water more than that of ice so that the difference in chemical potential according to eq. (5) is negative. Thus, in a situation where water and ice co-exist at equilibrium (*e.g.* at 0°C and atmospheric pressure) and the temperature is lowered, a driving potential for transfer of molecules from the water to the ice is set up.

Effect of pressure
The chemical potential of each phase changes with pressure according to

$$d\mu = V_m dP \qquad (7)$$

An increased pressure thus rises the chemical potential of both phases. However, since the molar volume of ice, $V_{m,s}$, is slightly larger than that of water, equal pressure changes will rise the chemical potential of ice more than that of water and thus the driving potential for phase transition is reduced.

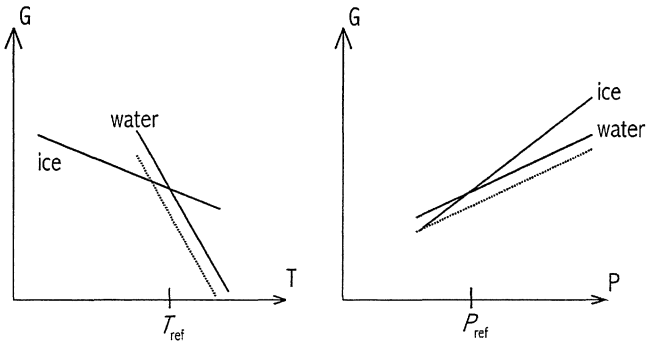

Figure 1: Principal dependence of free energy of water and ice on temperature (left) and pressure (right). Suitable choices of reference temperature and reference pressure indicated. Dashed lines: The addition of some solute to pure water reduces its free energy, eq. (7).

Effect of solutes in the water

If some solute is added to the water, the chemical potential of the water is reduced so that

$$\mu_l = \mu_{l,ref} + RT\ln(X) \qquad (7)$$

in which $\mu_{l,ref}$ is the chemical potential of pure water under equal conditions in terms of temperature, pressure and so on. The term X, the mole fraction, is the fraction of water molecules to the total amount of molecules in the liquid solution, *i.e.*

$$X = \frac{n_{H_2O}}{n_{H_2O} + n_{sol}} \qquad (8)$$

For 1 kg of a 3% b.w. NaCl solution, we have (mole weights 53.5 and 18 g for NaCl and H_2O, respectively)

$$n_{sol} = 30/53.5 = 0.561 \text{ moles}$$

$$n_{sol} = (1000-30)/18 = 53.9 \text{ moles}$$

$$X = \frac{n_{H_2O}}{n_{H_2O} + n_{sol}} = \frac{53.9}{53.9 + 0.561} = 0.9896...$$

At room temperature, T≈298 K, the chemical potential of a 3% NaCl solution is less than that of pure water by an amount of

$$\mu_{solution} - \mu_{purewater} = RT\ln(X) = 8.3145 \cdot 298 \cdot \ln(0.9896) \approx -25.7 \text{ J/K/mole}$$

The effect of an added solute on the level of free energy of water thus is to displace downwards the curves for water in figure 1. There it is seen that the equilibrium is displaced towards a lower temperature and a lower pressure, respectively.

Effect of pore size and interface free energies

In a porous material, there are many interfaces between the different phases, *e.g.* between the solid matrix and the air in its pores. These interfaces contribute to the total level of free energy of the entire system. Any change of the amount of the different phases in such a system will change the amounts and types of interfaces. In fine porous materials, the quantity of these changes may be quite considerable as compared to the entropy and pressure changes attributed to phase changes and therefore the interface changes involved must be taken into consideration when studying the driving forces for phase transition.

When water penetrates the pores in a dry, porous material, the initial interfaces matrix-air are substituted by an interface matrix-water. The change in interface free energy is

$$\Delta\gamma = \gamma_{liq-mat} - \gamma_{air-mat} \qquad (9)$$

For materials in which capillary suction of water is a spontaneous process, $\Delta\gamma$ is negative, *i.e.* the change of type of interface causes a reduction in level of free energy of the system.

The change in free energy of the system is also dependent on how large an interface area is changed per mole of liquid added to the system. This depends on the size and shape of the pore to which the liquid is added. In the case of a cylindrical pore of circular cross section and radius r (fig 2), the term dA in equation (1) is:

$$dA = 2\pi r dx \qquad (10)$$

in which dx is the depth of water penetration. dx is calculated from the volume of water that enters the pore:

$$dV = V_{m,l}\, dn_l = \pi \cdot r^2 dx \qquad (11)$$

with $V_{m,l}$ the molar volume of water and dn_l the change of water content. The change of interface area per mole of water that enters the pore, dA_m, thus becomes:

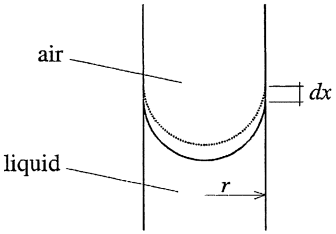

Figure 2: Water meniscus penetrating a distance dx into a cylinder of circular cross section.

$$\frac{dA}{dn_l} = dA_m = \frac{2V_{m,l}}{r} \qquad (12)$$

and the chemical potential of the water is:

$$\mu = \mu_{ref} + \Delta\gamma \frac{2V_{m,l}}{r} \qquad (13)$$

If the pore is not of circular cross section, the factor *2/r* must be replaced by the hydraulic radius of the pore, *i.e.* the ratio of its circumference to its cross section area.

From eq. (13), we see that when the material is almost completely water saturated, so that the radius *r*, of the pores to which any additional water would be added, is very large, the chemical potential of the pore solution is equal to that of the same solution in bulk. Remembering that $\Delta\gamma$ is negative (eq. 9), we also realise that when the pore system is drained, so that the water meniscus moves towards pores of smaller radius, the chemical potential of the remaining water is reduced. Thus drainage is a way of establishing equilibrium between remaining water and existing ice. (The equations also show that the driving force for capillary suction is larger the more narrow the pore.) Of course, if the ice bodies grow so that ice spreads into narrow pores, a term similar to the last one on the right side of eq. (13) should be used also for the ice.

Combined effects

We now have the tools to study how a disturbance of the equilibrium between ice and aqueous solution in a porous material may be re-adjusted.

First, suppose ice formation begins in the large entrained air pores of concrete and that subsequent ice growth takes place through redistribution of water from narrow pores to the (large) ice bodies, *i.e.* through drainage. To what extent, in terms of pore radii, must this drainage be driven in order for equilibrium to be established at –10°C? (Assume no pressure changes take place.)

The reference point is set at T=273.15K and P=101325 Pa. The change in chemical potential of the ice due to the temperature change is

$$\mu_s - \mu_{ref} = -S_{m,s}\left(T_s - T_{ref}\right) \approx -41 \cdot (263.15 - 273.15) = 410 \text{ J/mole} \qquad (14)$$

Correspondingly, the change in chemical potential of the ice due to the temperature change is

$$\mu_l - \mu_{ref} = -S_{m,l}\left(T_l - T_{ref}\right) \approx -63 \cdot (263.15 - 273.15) = 630 \text{ J/mole} \qquad (15)$$

Obviously, the temperature change has created a difference in chemical potential and water will move towards the ice and add to the growth of the existing ice bodies (provided that ice formation does not take place in the form of spreading towards smaller pores, a case which cannot be treated here). To find the radius of the pore at which equilibrium is again estab-

lished, we use the following expression (assuming the pores to be long narrow pores of circular cross section):

$$-S_{m,s}(T_s - T_{ref}) = -S_{m,l}(T_l - T_{ref}) + \Delta\gamma \frac{2V_{m,l}}{r} \qquad (16)$$

The value of $\Delta\gamma$ is estimated to be –0.075 J/m² (see Lindmark[1] for details). With the values given above, we now find r = 12 nm. From pore size distributions of pure Portland cement-pastes, we find that this approximately corresponds to a degree of saturation in the range 0.70 - 0.90 (depending on water-to-cement ratio and degree of hydration).

If drainage is prevented, *e.g.* because an outer liquid phase is present and successively sucked into the pore system, the pressure on the water will remain atmospheric and equilibrium might need to be established in the form of an increased pressure on the ice. What ice pressure is then required? Using the equations above, we may write

$$V_{m,s}(P_s - P_{ref}) - S_{m,s}(T_s - T_{ref}) = -S_{m,l}(T_l - T_{ref}) \qquad (17)$$

with $V_{m,s}$=19.65×10^{-6} m³/mole, we find P_s = 11.3 MPa. Although the exact ice pressure required for damages to occur is unknown, it seems likely that ordinary cement pastes, due to their low tensile strength, are not able to withstand such ice pressures.

Now, if the pore solution close to the interface between the pore solution and the ice is not pure water, *e.g.* because the de-icing agent of the outer solution has penetrated into a certain depth, how is then the required ice pressure affected? At –10°C and with a 3% b.w. NaCl solution present at the interface ice-solution, the ice pressure required for equilibrium to be maintained is reduced from 11.3 MPa (as above) to 10 MPa (insert the last term on the right side of eq. (7) on the right side of eq. (17).)

Thus, the presence of some solute, *e.g.* a de-icing agent, reduces the chemical potential of the liquid and the required ice pressure is reduced. During cooling of the outer solution, the concentration of the remaining outer solution is always adjusted so that the solution is at equilibrium with bulk ice. If that solution reaches the interface between pore solution and ice bodies inside the specimen, the driving potential for osmotic ice body growth will be zero. However, depending on the position of the ice body, *i.e.* its distance from the specimen surface, the outer solution may not reach the interface before the ice body has already grown enough to cause damage. Clearly though, the more time there is for the de-icing agent to penetrate the pore system before freezing sets in, the higher the concentration of solutes in the pore solution and the lower the maximum pressures exerted by the ice bodies.

Summary

To summarise, we conclude that the difference in chemical potential between ice and pore solution constitutes a driving force for flow of pore solution towards the ice bodies *and* indicates the theoretical maximum pressure that the ice may exert on the pore walls. At what depth the ice bodies actually will exert maximum pressure depends on the permeability of the material (in its partly frozen state), the rate of heat flow, the distribution of solutes, and the distribution of initial ice bodies. The first and last of these parameters is highly depending on the pore size distribution of the material, which in turn is highly dependent on how the material has been treated before freezing. The other parameters are highly dependent on how the

test is carried out. Clearly, the mechanism is sensitive to many factors and one realises that small changes in the test procedure, especially those that may affect the pore size distribution of the material, will cause large variations in test results.

Finally, it should be emphasised that the thermodynamics described here should be valid for osmotic ice body growth and consequent redistribution of moisture either the specimen is isolated to exchange of moisture with the surroundings or not. The case of salt-frost induced deterioration differs from that of frost deterioration under conditions of moisture isolation only in that the system is open to the surroundings. The mechanism of salt-frost scaling described here thus is superimposed on the mechanisms of "inner" frost deterioration. Its effect is mainly (possibly only) distinguishable in the surface zone.

3 PREDICTIONS AND COMPARISON TO RESULTS FROM THE LITERATURE

In the literature, some interesting phenomena have been reported which are yet to be explained. The following, which is a shortened version of the text in Lindmark[1] (see the original for full details), shows how the proposed mechanism may be used to explain some of these phenomena.

Reasons for a "3% pessimum"

Most-discussed among the reported phenomena is the apparent existence of a "pessimum" de-icer concentration: Arnfeldt[13] and Verbeck and Klieger[14] reported that a de-icer concentration of about 3% b.w. in the outer solution would cause the most severe damage. According to the present hypothesis, the following factors may be distinguished as those which act to cause such a "pessimum":

From the hypothesis, it is clear that a certain de-icer concentration is needed in the outer solution, since otherwise there will be no liquid phase available during freezing. The higher the de-icer concentration in the outer solution, the larger the amount of moisture available at each temperature during freezing. This "positive" effect of the outer salt concentration is opposed mainly by the following: In tests such as those run by Arnfelt or Verbeck and Klieger, and in modern standard test methods, the outer solution is left on the specimen surface during the period of temperatures above 0°C. During this time, the de-icer may enter the pores of the specimen, and possibly decrease the mole fraction of water in the pore solution (depending on the concentration of the outer solution and the total ion exchanges). During the next freezing, this will make the pore solution in the outermost part of the specimen freeze at a lower temperature than the natural pore solution would. This will reduce the driving force for ice body growth and for moisture flow and will also reduce the maximum possible ice body pressure, thus reducing the risk of damage. The first formed ice bodies will be displaced to a greater depth and their growth will be limited by the increased resistance to moisture flow that the longer flow distance represents. Furthermore, the increased de-icing agent content of the pore solution will reduce the number of (potentially) growing ice bodies, thereby reducing moisture uptake. For further details see Lindmark[1].

Effect of entrained air

Entrained air may prevent, or at least delay, damage, provided the air content is high enough. Upon cooling, air contracts and sucks pore solution into the pore. When this water freezes, the mechanism is activated; moisture flows into the specimen and accumulates in the air pores.

On melting, the air expands and presses out as much water as was sucked in due to its contraction during cooling. Thus in a frost cycle in which the duration of the thawed state is long enough, the air pore system will be completely restored and will have regained its full protective function for the next freezing. If, however, the compressed air can find some way out, the moisture uptake will be permanent and thus the protective effect of the air voids will be reduced in the next frost cycle. Also, because, in several test methods, the duration of cooling is longer than that of heating, there is simply more time for absorption (both due to thermal contraction of enclosed air and due to cryo-suction) than there is for desorption.

If the frost cycle is changed so that temperature oscillates between the freezing point of the pore solution and some lower temperature, say -3° and -10°C, the ice in the air pores never melts and more and more ice will gather in the air pores. After several cycles, the air pores will be completely filled and the material surface will deteriorate.

It follows naturally that the required air content is higher in a specimen subjected to combined salt and frost attack than in one subjected to pure frost attack. While the air pores in the latter will need only to protect the material against freezing of its original water content, the air pores in a specimen subjected to salt frost attack also must provide ample space for accumulation of the ice which forms from incoming moisture. Whether the required true spacing between air voids needs to be shorter than in ordinary, pure water frost attack, cannot be said.

Effect of carbonation

According to some reports, carbonation has a limiting effect on surface scaling[6,7]. The effect of carbonation is probably due mainly to its effect on the permeability of the surface zone. Different effects on the surface layer are obtained depending on cement type and admixers. For ordinary Portland cement-based materials, carbonation causes a denser pore structure[8], while cements containing ground, granulated blast furnace slag (GBFS) become coarser[9]. According to what was reported by Powers *et al* [10] on the dependence of permeability on pore size distribution and total porosity, it thus seems that carbonation will cause a reduction of the permeability of pure Portland cement materials, while that of materials containing GBFS will be increased. The role of permeability was discussed above: Portland cement material will probably benefit from carbonation while GBFS material will become more sensitive to salt frost attack.

In Lindmark[1], the following summary of results reported in the literature was made:

1. Surface scaling almost never appears in the absence of an outer solution which to some extent remains liquid at temperatures lower than the normal freezing point of the pore solution of HCP. It may even be noted that in the two reports in which scaling is reported when the outer solution was pure water, either the outer water was rich in naturally occurring ions[11] or the specimen surface had been exposed to a salt solution prior to testing so that the pore system did contain some salt[12] [S 1965].
2. Portland cement-bound materials with proper air void systems are able to withstand combined salt and frost attack, at least in laboratory tests.
3. The chemical composition of the de-icing agent seems to be of no importance.
4. Without actual freezing temperatures, no scaling occurs.
5. Use of a lower minimum temperature will produce more scaling, at least for minimum temperatures in the interval $0°C > \theta > -20°C$.
6. Coarse porous materials are more sensitive to salt frost attack than dense materials.
7. Purely chemical mechanisms are of little importance in comparison to physical mechanisms.

The explanation of the first point should be rather obvious from the above reasoning. The role of the high amounts of naturally-occurring ions in the outer water will be the same as that of salt in a salt solution; these ions will serve to depress the freezing point of the outer solution. Considering the low quality of the materials used in their study (a w/c ratio 0.60 concrete without air entrainment), the scaling reported by Stark and Ludwig[11] must be regarded as very small: after 28 frost cycles, the accumulated scaling obtained with a water quality containing the highest amounts of solutes was only 0.49 kg/m² for the concrete made with pure Portland cement. In a traditional salt frost scaling test, using a 3% NaCl solution, such a low quality concrete would be expected to be very much more damaged (see, for example, the tests reported in the next chapter). In Snyder's results[12], scaling was obtained when the specimen was covered with pure water after first having been exposed to a salt solution. It seems reasonable that this previous exposure to a salt solution must have resulted in some salt being left in the pores close to the specimen surfaces. During the subsequent freezing tests, this salt may have served to provide a liquid phase during at least a part of the frost cycle.

The second point concerns the effect of entrained air voids and was discussed above.

The third point also follows logically from the described mechanism, since the important role of the de-icing agent is to provide a liquid phase. However, in the results by Arnfelt[13] and Verbeck and Klieger[14], it can be seen that optimum scaling is actually dependent on the de-icing agent used to bring about a freezing point depression of approximately 2°C. This may be because the rate of diffusion of different de-icers into the pore system varies, and/or because the eutecticum, below which there will be no liquid phase remaining on the specimen surface, varies by type of de-icer.

The fourth needs no further comment.

The fifth point: The driving force for moisture absorption increases with decreasing temperature (eq. ()). This is likely to result in increased scaling. However, at temperatures below –20°C though, it might be that the pore system of Portland cement bound materials is clogged with ice to such an extent that the permeability is too much reduced to allow any more ice body growth.

Point six is mainly explained by the effect of micro pore structure on intrinsic permeability and on the amount of ice formed at a given temperature.

The final point stands on its own.

Finally, there are other phenomena, which are not straightforwardly explained by the described mechanism. For example, the sudden increase in scaling on high performance concretes containing silica fume, reported *e.g.* by Petersson[15], cannot be explained, unless the described mechanism causes successive accumulation of moisture in the pores of such materials. Further research is needed.

4 CONCLUSION

The proposed mechanism is robust in the sense that it requires no unusual circumstances for it to function. Rather, it will be active as long as permeability is high enough and the heat released on freezing is conducted away at a sufficient rate. Furthermore, the mechanism is sensitive to small changes in material properties and test procedure, a fact which is likely to make final scaling sensitive to such variations. On a qualitative basis, laboratory results found in the literature and results from our own investigations are in accord with predictions made from the hypothesis.

[1] Lindmark, S: Mechanisms of Salt Frost Scaling of Portland Cement-bound Materials, Thesis, Report TVBM-1017, Lund Institute of Technology, Div. Building Materials, 1998
[2]Taber, S: "Mechanics of Frost Heaving", Journal of Geology, 38, 1930, pp. 303-317.
[3] Helmuth, R A: Discussion to Nerenst: Frost Action in Concrete, Paper VI-2, IVth Int. Symp. Chemistry of Cement, Washington 1960, p. 807
[4] Powers, T.C, Helmuth, R A: Theory of Volume Changes in Hardened Portland-Cement Paste During Freezing, Highway Res. Board, 32/1953
[5] Atkins, P.W: "Physical Chemistry, 4th ed.", Oxford University Press
[6] Stark, J, Ludwig, H-M: "Freeze-Deicing Salt Resistance of Concretes Containing Cement Rich in Slag", in "Frost Resistance of Concrete", Eds. Setzer and Auberg, Proc. International RILEM Workshop, University of Essen, Sept. 1997, pp 123-138
[7] Petersson, P-E: "Scaling Resistance of Concrete - Field Exposure Tests", Swedish National Testing and Research Institute, SP Report 1995:73, Sweden, 1995, In Swedish, Summary in English
[8] Kropp, J: "Struktur und Eigenschaften Karbonatisierter Betonrandzonen", Bautenschutz-Bausanierung, heft 2, Juni 1986
[9] Matala, S: "Effect of carbonation on the pore structure of granulated blast furnace slag concrete", Helsinki University of Technology, Faculty of Civil Engineering and Surveying, Concerete Technology, Report 6.
[10] Powers, T.C, Copeland, L.E, Hayes, J.C, Mann,H.M 1954: "Permeability of Portland Cement Paste", Proc.Am. Concrete Inst. 51
[11] Stark, J, Ludwig, H-M: "The Influence of the Water Quality on the Frost Resistance of Concrete", RILEM TC-117 meeting, Trondheim, Norway, June 1994
[12]Snyder, M.J: "Protective Coatings to Prevent Deterioration of Concrete by deicing Chemicals", National Cooperative Highway research Program Report 16, Highway Research Board of the Division of Engineering and Industrial Reserach, National Academy of Sciences - National Research Council, 1965
[13] Arnfelt, H: "Damage on Concrete Pavements by Wintertime Salt Treatment" Meddelande 66, Statens Väginstitut, Stockholm 1943 (In Swedish)
[14] Verbeck, G.J, Klieger, P: "Studies of "Salt" Scaling of Concrete" Highway Research Bulletin, Bull. 150, Washington D.C, 1957
[15] Petersson, P-E: "Scaling Resistance of Concrete - Field Exposure Tests", Swedish National Testing and Research Institute, SP Report 1995:73, Sweden, 1995, In Swedish, Summary in English

FROST RESISTANCE OF PREFABRICATED FAÇADE ELEMENT - STABILITY OF THE AIR-VOID SYSTEM

Jouni Punkki, Dr.Ing., Research Engineer
Parma Betonila Oy, P.O. Box 76, FIN-03101 Nummela
jouni.punkki@parmabetonila.fi

Klaus Juvas, Lic.Tech., Laboratory Manager
Addtek Research & Development Oy Ab, P.O. Box 23, FIN-20601 Parainen
klaus.juvas@addtek.com

1 INTRODUCTION

This paper reports a series of experiments made at the precast concrete factories of Parma Betonila Oy, Finland to analyse the frost resistance of façade elements produced by standard techniques.

It has been speculated that the intensive compaction used in the precast concrete production may affect the quantity and quality of air-voids. Therefore, the focus was mainly on the stability of the air-voids in the concrete. In addition to the analyses of the air-voids, the experiments included some direct freezing and thawing tests.

2 TEST PROGRAMME

2.1 Test concretes

Test concretes were cast at four Parma Betonila factories. The factories selected the concrete types according to their needs. Altogether, eight test concretes were selected for façade elements, as well as, one test concrete for balcony elements. Four of the façade element concretes were made by using portland cement (rapid hardening) while the other four were made by using white portland cement.

In the case of façade elements, the outer layer of the sandwich element was simulated. The size of the test element was approximately $1 \cdot 1$ m^2 and its thickness was 80 mm. The test elements were manufactured by standard factory routines. The façade elements were compacted by table vibration, in some cases also by poker vibration (with or without table vibration). The elements were cast horizontally, so that the outer surface was against the vibrating table, which is the normal procedure in the production of sandwich elements.

The balcony elements were compacted by a poker vibrator.

Since the main object was to study the stability of the air-void system, it was considered important to analyse the sensitivity of the air-void system to compaction. Three different power levels were used. The normal level was chosen according to the factory´s practice and the type of concrete. The power was altered by changing the vibration time. The amplitude and the frequency of vibration were kept constant. The accelerations of the vibrating tables were measured before the elements were cast.

In addition to the compacting power, it was considered necessary to analyse the air-void system in different parts of the elements, i.e. close to the mould (outer) surface vs. close to the back surface. Table 1 shows the experimental variables.

Altogether 29 test elements were prepared including 26 façade elements and 3 balcony elements. A large number of cores (diameter: 100-150 mm) were drilled out of the elements for testing.

Table 1. Experimental variables.

Variable	Level
Compaction power	Low level; a short compaction time, approx. 50% the normal time Normal level; a normal compaction time High level; a long compaction time, approx. 200% the normal time
Position in the element	Mould surface; within 30 mm of the mould surface Back surface; within 30 mm of the back surface

2.2 Test methods

Since the main object was to study the stability of the air-void system, most of the tests were concerned with the content and the quality of the air in the concrete. In addition, direct frost resistance tests were carried out. The test methods are listed in Table 2. All tests were performed at Addtek Research & Development (ARD), Parainen, Finland except for the thin section analyses which were made by VTT, Finland. In addition to the frost resistance test, the study included normal testing of fresh and hardened concrete.

Table 2. Test methods for frost resistance.

Test method	Measured parameters
Air content of fresh concrete [1]	Air content of fresh concrete.
Pressure saturation, protective pore ratio [2]	Air content of hardened concrete.
Freeze-thaw resistance [3]	Frost resistance after 100 (and 300) cycles.
Thin section analysis [4]	Air content of hardened concrete, specific surface area and spacing factor of protective pores.

In the protective pore ratio test, the test specimens are first water-saturated at normal air pressure. Next, the specimens are fully saturated at an overpressure (15 MPa for 24 hours). The additional saturation through the pressure treatment is considered to correspond to the volume of the protective pores. This is a simple and reliable test method for determining the air content of hardened concrete. The size of the test specimens was: h ≈ 30 mm and ⌀ = 100-150 mm, three replicate specimens were used.

In the freeze-thaw resistance test, the specimens were freezing in air at -20 °C while thawing took place in water at +20 °C. The test consisted of 100 cycles, with some test concretes also 300 cycles. The tensile splitting strength ratio of the specimens subjected to freezing-thawing to the reference (water-stored) specimens was used as an indicator of frost resistance. Three replicate test specimens were used. The test results may not be absolutely reliable because of the small size of the specimens (h ≈ 30 mm and ⌀ = 100-150 mm).

Thin section analyses were made by using the modified point counting method. The analysed area was 1500 mm^2 / sample. The limit value between the protective pores and the compaction pores was 0.8 mm, i.e. the size of the protective pores was 0.020 - 0.8 mm and the size of the compaction pores was > 0.8 mm. The specific surface area of the pores as well as the spacing factor were calculated from the protective pores (< 0.8 mm). It is important to bear in mind that the thin section measurement of the air content may not be very reliable, the proportion of the aggregate in the thin section directly affects the test results.

Protective pore ratio tests were performed with all combinations (altogether 58) and the freeze-thaw tests were carried out with 34 combinations (100 cycles) and additionally with 6 combinations (300 cycles). In all, 25 thin section analyses were made.

3 TEST RESULTS

The average test results are given in Appendix A.

3.1 Air content of concrete

The air content was measured of the fresh concrete and also determined of the hardened concrete (pressure saturation and thin section analyses). The air content of fresh concrete indicates "an air content potential", but the effects of the actual compaction are not taken into account. Therefore, the air content of fresh concrete is normally slightly higher than that of hardened concrete.

The differences in the air contents of fresh concrete and hardened concrete, measured by pressure saturation, are shown in Table 3. Table 4 gives the average effects of the compacting power on the air content of hardened concrete.

Table 3. Average air content of concrete [%]. The air content of hardened concrete was measured by means of pressure saturation.

	Average	Mould surface	Back surface
Fresh concrete	5.73	(1	(1
Hardened concrete	4.90	4.52	5.28
Difference; fresh - hardened	0.83	1.21	0.45

(1 = not possible to divide the mould surface and the back surface.

Table 4. Average air content of hardened concrete [%] as a function of the type and power of compaction. The air content of hardened concrete was measured by pressure saturation.

Vibration	Average	Mould surface	Back surface	Difference; back - mould
Table vibration., low level	5.48	5.16	5.80	0.64
Table vibration, normal level	5.11	4.74	5.48	0.74
Table vibration, high level	4.78	4.26	5.30	1.04
Poker vibration	3.83	3.58	4.08	0.50

The results showed that some air escaped from the concrete due to compaction. On the average, the air content of fresh concrete was 0.8 percentage units higher than that of hardened concrete. Furthermore, a difference can be observed between the mould surface and the back surface: in the mould surface, the air content was, on the average, 0.8 percentage units lower than in the back surface.

The compacting power also had an effect on the air content of hardened concrete. The longer the compaction time, the lower the air content of hardened concrete. However, the effect was not as big as one might assume: also the 200% compaction time appears to give an adequate air content.

The air content of hardened concrete, determined by the pressure saturation test, does not give any information of the type of air pores that disappeared. Therefore, the effects on frost

resistance cannot be estimated directly on the basis of these results.

Figures 1 and 2 show the relationships between the air content of fresh concrete and that of hardened concrete measured by means of pressure saturation and thin section analyses. As can be seen, there is a rather great variation in the test results.

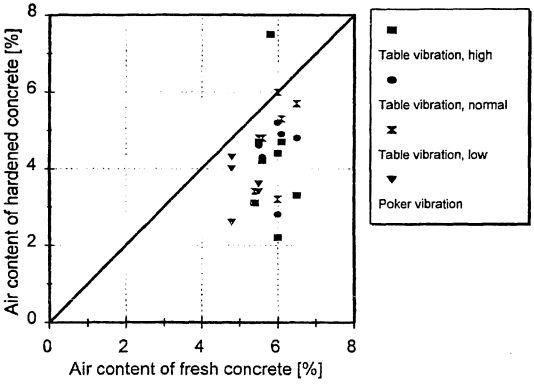

Figure 1. Relationship between the air content of fresh concrete and hardened concrete as a function of the type and power of compaction. The air content of hardened concrete is measured by means of pressure saturation from the mould surface.

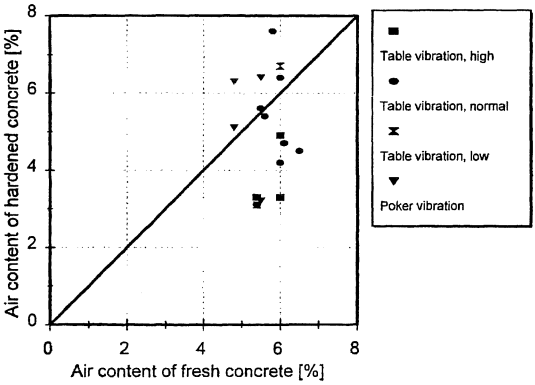

Figure 2. Relationship between the air content of fresh concrete and hardened concrete as a function of the type and power of compaction. The air content of hardened concrete is measured by means of thin section analyses. The total air content was used (protective + compaction pores). The specimens were taken from the mould surface.

3.2 Pore size distribution of air-voids

The quality of the air-void system was evaluated by thin section analyses. The average effects of the position in the element (mould surface vs. back surface) are shown in Table 5 and the average effects of the compacting power in Table 6. A large proportion of the thin sections were taken of only from the mould surface combined with the normal compacting power. Therefore, the comparisons had to make based on a limited amount of data. Only the directly comparable pairs are included.

Table 5. Average effects of the position in the element on the results of the thin section analyses.

Position	n	Protective pores (< 0.8 mm) [%-vol]	Compaction pores (> 0.8 mm) [%-vol]	Specific surface area [mm²/mm³]	Spacing factor [mm]
Mould surface	6	3.13	0.27	39.7	0.150
Back surface	6	3.25	0.88	44.7	0.140
Difference; back-mould	6	0.12	0.61	5.0	-0.01

Table 6. Average effects of the compacting power on the results of the thin section analyses.

Position	n	Protective pores (< 0.8 mm) [%-vol]	Compaction pores (> 0.8 mm) [%-vol]	Specific surface area [mm²/mm³]	Spacing factor [mm]
Table vibration, low level	6	3.56	1.17	41.0	0.140
Table vibration, normal level	6	3.71	0.83	43.3	0.132
Table vibration, high level	6	3.38	0.82	43.3	0.140

According to the results, a small difference can be found between the mould surfaces and the back surfaces. The back surfaces contained more compaction pores, but the differences in the quantity or the quality of the protective pores were small.

The effect of the compacting power was even smaller than that of the position in the element. The normal compaction power produced the best quality, however, the differences are insignificant.

The dependencies of the quality parameters of the air-void system as a function of air content of fresh concrete are shown in Figures 3 and 4. As can be seen, all of the results are very good. There are no commonly accepted requirements for the air-void quality parameters of façade elements, but in Finland spacing factors below 0.27 mm and specific surface areas above 25 mm^2/mm^3 are generally considered to ensure an adequate frost resistance of façade structures.

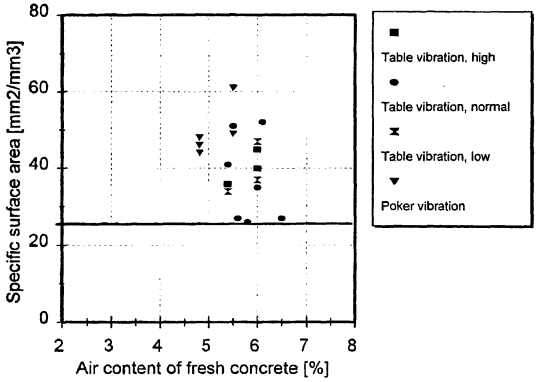

Figure 3. Dependence of the specific surface areas of the protective pores (< 0.8 mm) on the air content of fresh concrete. Specimens were taken from the mould surface.

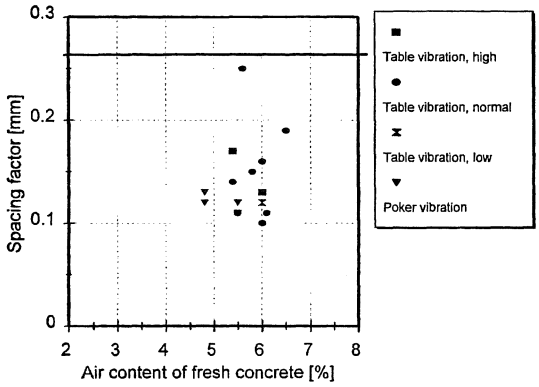

Figure 4. Dependence of the spacing factors of the protective pores (< 0.8 mm) on the air content of fresh concrete. Specimens were taken from the mould surface.

3.3 Freeze-thaw tests

The air contents of concrete and the results of the thin section analyses suggested that all the test concretes would have a very good frost resistance. Therefore, no big differences were expected in the direct freeze-thaw tests. Besides, relatively small test specimens and tensile splitting strength test were used and, thus, the variations of the test results would probably cover the real differences.

A tensile strength ratio (between freezing and thawing and reference specimens) of 0.67 after

100 cycles is normally considered to be the limit value for adequate frost resistance. In these tests, the average ratio after 100 cycles was 0.990 and the lowest value 0.71. The same concrete showed a ratio of 1.00 after 300 cycles, i.e. frost resistance was very good.

Figure 5 shows the dependence of the tensile splitting strength ratio on the air content of fresh concrete. Because of the very good frost resistance of the test concretes and the obviously great variation of the test results, it was not considered necessary to analyse the test results more closely.

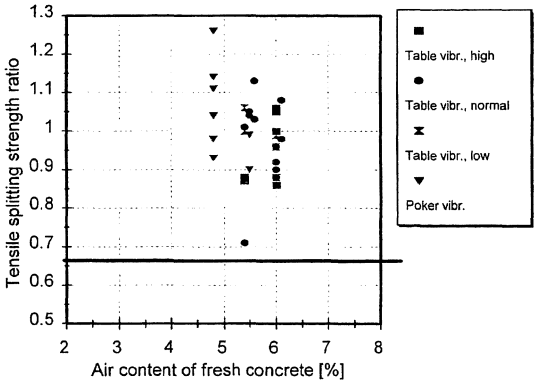

Figure 5. Dependence of the tensile splitting strength ratio after 100 cycles on the air content of fresh concrete. Specimens both from the mould surface and the back surface are included.

4 CONCLUSIONS

The test results proved that some air escapes from fresh concrete during the compaction of façade elements. On the average, the air content of hardened concrete was 0.8 percentage unit lower than that of fresh concrete. Besides, the air is moving inside the concrete due to the compaction. The air content of the mould surface (30 mm layer) was, on the average, 0.8 percentage unit lower than that of the back surface (30 mm layer). The compacting power (compaction time) also affected the difference between the mould surface and the back surface.

Although some air escaped from fresh concrete due to the compaction, the frost resistance of the concrete was not affected significantly. The thin section analyses showed that the content of the largest pores (compaction pores; > 0.8 mm) was higher in the back surface and it was affected by the compacting power. However, the quantity and the quality of the air-voids essential to frost resistance (protective pores; < 0.8 mm) were not affected significantly by compaction.

The test results also showed that the present production technology of Parma Betonila ensures a good frost resistance for façade elements. With a proper air-entraining, the air-void system is not sensitive to the compaction of the concrete.

5 REFERENCES

1. SFS 5287 (1987) *Standard. Fresh concrete. Air content.* Suomen Standardoimisliitto. Helsinki.

2. SFS 4475 (1988) *Standard. Concrete. Frost resistance. Protective pore ratio.* Suomen Standardoimisliitto. Helsinki.

3. SFS 5447 (1988) *Standard. Concrete. Durability. Freeze-thaw resistance.* Suomen Standardoimisliitto. Helsinki.

4. ASTM C457 - 82a (1982). *Standard Practice for Microscopical Determination of Air-Void Content and Parameters of the Air-Void System in Hardened Concrete.* Annual Book of ASTM Standards, Vol. 04.02. (modified according to NTBuild 381).

Appendix A, Table A1. Average test results.

Code	Concrete type	w/c	Air of fresh concrete [%]	Vibration (table vibr. if not other mentioned)	Position in the element	Air of hardened concrete [%]	Thin section results				Freeze-thaw ratio	
							Specific surf. area [mm²/mm³]	Spacing factor [mm]	Prot. pores [%]	Comp. pores [%]	100 cycles	300 cycles
A-1	façade, grey	0.54	6.0	low	mould	3.2	47	0.13	3.1	0.2	1.00	0.99
				low	back	4.5	46	0.14	3.0	2.8	0.99	1.09
				normal	mould	2.8	35	0.16	3.5	0.7	0.88	1.16
				normal	back	3.6	51	0.11	3.2	1.0	0.92	1.11
				high	mould	2.2	45	0.13	3.1	0.2	1.06	1.09
				high	back	4.0	53	0.12	3.7	0.1	1.05	1.00
A-2	façade, white	0.53	5.4	low	mould	3.4	34	0.17	3.0	0.1	1.06	0.97
				low	back	4.7	38	0.15	3.7	0.7	1.00	0.91
				normal	mould	3.1	41	0.14	3.1	0.1	1.01	1.07
				normal	back	4.3	40	0.16	2.9	0.1	0.71	1.00
				high	mould	3.1	36	0.17	3.0	0.3	0.88	0.90
				high	back	4.5	40	0.16	3.0	0.6	0.87	0.89
B-1	façade, grey	0.52	5.5	low	mould	4.8						
				low	back	4.9						
				normal	mould	4.6	51	0.11	4.5	1.1	1.04	
				normal	back	4.5					1.05	
				high	mould	4.7						
				high	back	4.8						
				table + poker	mould	3.4	61	0.11	2.8	0.4		
				table + poker	back	3.8						
				poker, norm.	mould	3.6	49	0.12	3.9	2.5	0.99	
				poker, norm.	back	4.0					0.90	

Appendix A, Table A2. Average test results.

Code	Concrete type	w/c	Air of fresh concrete [%]	Vibration (table vibr. if not other mentioned)	Position in the element	Air of hardened concrete [%]	Thin section results				Freeze-thaw ratio	
							Specific surf. area [mm^2/mm^3]	Spacing factor [mm]	Prot. pores [%]	Comp. pores [%]	100 cycles	300 cycles
B-2	façade, white	0.49	6.0	low	mould	6.0	37	0.12	5.5	1.2	0.88	
				low	back	7.0					0.96	
				normal	mould	5.2	45	0.10	6.0	0.4	0.96	
				normal	back	6.8					0.90	
				high	mould	4.4	40	0.13	4.0	0.9	1.00	
				high	back	6.3					0.86	
B-3	balcony, grey	0.49	4.8	poker, low	mould	2.6	44	0.13	3.1	2.0	1.26	
				poker, low	back	3.4					1.11	
				poker, norm.	mould	4.0	48	0.12	3.6	2.7	1.14	
				poker, norm.	back	4.2					1.04	
				poker, high	mould	4.3	46	0.13	3.5	2.8	0.98	
				poker, high	back	5.0					0.93	
C-1	façade, grey (black pigment)	0.51	5.6	low	mould	4.8						
				low	back	4.8						
				normal	mould	4.3	27	0.25	2.8	2.6	1.03	
				normal	back	4.1					1.13	
				high	mould	4.2						
				high	back	4.2						

Appendix A, Table A3. Average test results.

Code	Concrete type	w/c	Air of fresh concrete [%]	Vibration (table vibr. if not other mentioned)	Position in the element	Air of hardened concrete [%]	Thin section results				Freeze-thaw ratio	
							Specific surf. area [mm²/mm³]	Spacing factor [mm]	Prot. pores [%]	Comp. pores [%]	100 cycles	300 cycles
C-2	façade, white	0.51	6.1	low	mould	5.3	52	0.11	3.7	1.0	0.98	
				low	back	5.4					1.08	
				normal	mould	4.9						
				normal	back	5.5						
				high	mould	4.7						
				high	back	5.2						
D-1	balcony, grey	0.50	5.8	poker, low	mould	8.1	26	0.15	5.7	1.9	1.10 [1]	
				poker, low	back	8.4						
				poker, norm.	mould	8.2						
				poker, norm.	back	8.8						
				poker, high	mould	7.5						
				poker, high	back	8.1						
D-2	façade, white	0.49	6.5	low	mould	5.7	27	0.19	3.7	0.8	0.92 [1]	
				low	back	6.7						
				normal	mould	4.8						
				normal	back	6.2						
				high	mould	3.3						
				high	back	5.3						

[1] the mould surface and back surfaces were not separated

MOISTURE ABSORPTION DURING FREEZE-THAW AND RELATION TO DETERIORATION

Terje F. Rønning
Norcem A.S
P.O.Box 38, N-3991 Brevik, Norway.

1 INTRODUCTION

1.1 General

Many researchers have recognised the significance of differences in thermodynamic potential when concrete is subjected to freeze-thaw for increasing the degree of saturation. The redistribution of moisture within the concrete is believed to activate suction forces causing moisture, if available, to penetrate from the outside. Such potential forces are capillary or osmotic forces – or the thermodynamically potential differences – or a combination of these. The thermodynamics will not be further dealt with in this paper, it may be found in [1]. Absorption tests and examination of the effect of the salt content of pre-storage conditions on the scaling level were performed [2].

1.2 Saturation

Fagerlund [3] performed a series of tests of actual degree of saturation. It was found that 2,5% to 5% NaCl in the testing liquid during freeze-thaw provided the highest degree of saturation in the concrete – compared to isothermal conditions and other salt concentrations. Bager & Jacobsen [4] related the water uptake to scaling and dilation and found a close correlation to both.

1.3 Significance of research

The objective of the present study was to carry out a limited investigation of the absorption properties with different curing regimes – and to compare these to both scaling and internal deterioration.

2 EXPERIMENTAL

2.1 Principles

Concrete of different proportions were subjected to standard and modified pre-testing procedures, compared to SS 13 72 44. This comprised time of sawing, exposure to drying and carbonation as well as re-saturation by pure water or by 3% NaCl. The freeze-thaw testing proceeded with the same two types of liquid as freezing medium on the top surface.

The weight of the specimens was recorded during the pre-treatment and at the end of the testing procedure. For series with low scaling, the mass and the moisture of the scaled material were taken into account. It was not considered relevant to include series with substantial scaling or frequent need for refilling of freezing medium. Consequently, for the short description given here, only a few series are included.

Scaling and ultrasonic pulse velocity was recorded at the normal intervals. However, some series had to be rejected before 56 cycles due to damage and/or frequent need for maintenance or re-filling, which disturbed the significance level of the series.

2.2 Material

The two series included in this paper are :

Table 1. Key properties of the concrete mix design.

Parameter	Mix 1	Mix 2
w/c-ratio	0,55	0,70
Air content	4 %	Natural (No AEA)

Both mixes contained a CEM I 42,5 R cement and a very good frost resistant aggregate.

2.3 Curing regimes

Main data are given below :

- Standard Curing : Water curing until 7 days, then in controlled air climate with sawing at 21 days. Preparation at age 22-24 days.
- Modified Standard Curing : As above, but sawing already at 7 days.
- Plastic Curing : Stored in solid plastic bags until time for re-saturation.
- Intensive Drying (in some cases) : Like standard curing until sawing at 21 days, then subjected to 40 °C, with controlled "evaporation rate potential" (evaporation from a defined water surface).

Re-saturation by water or 3% NaCl. Start of freeze-thaw with water or 3% NaCl at 28 days (not 31 days) for all series.

3 RESULTS AND DISCUSSION

3.1 Absorption during freeze-thaw

The dependence of absorption on the preceding weight loss due to drying has been dealt with elsewhere and is not further commented on here. Fig.1 displays equal absorption when tested with water or 3% NaCl. The scaling, of coarse, was different, but at a level which did not disturb the results. Fig. 2 contains values coinciding with the hypothesis described.

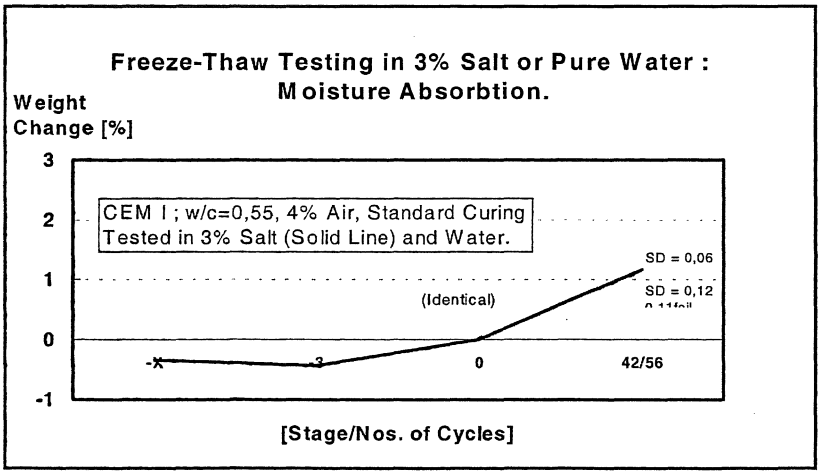

Figure 1. Identical absorption when tested with water or 3% NaCl.

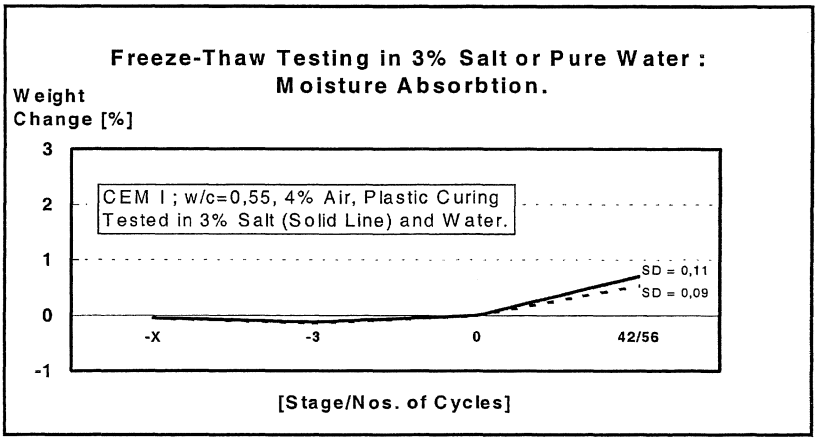

Figure 2. Slightly higher absorption with 3% NaCl testing when cured in plastic.

3.2 Testing in water ; different re-saturation

A relevant question would be whether re-saturation with water or 3% NaCl, respectively, results in systematically different patterns. Figs. 3 and 4 display different results for the two mix designs. A closer investigation shows various results depending on the curing regime. In fact, this tended to coincide with larger scatter (see SD in the figures).

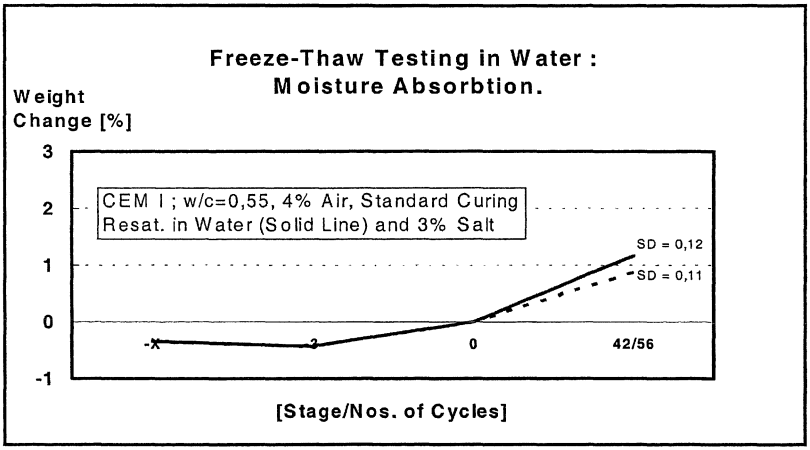

Figure 3. Tested in water, re-saturated by water caused larger absorption.

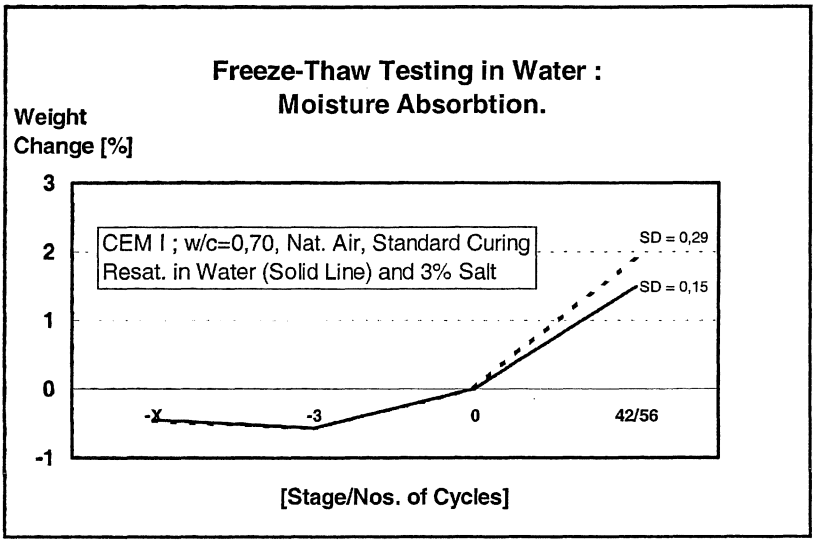

Figure 4. Increased absorption when re-saturated by 3% NaCl – the opposite of Fig. 3.

3.3 Absorption and relation to deterioration

When tested in water, the scaling is normally quite low. It is difficult to achieve adequate scaling levels and still be able to differentiate. The differences are insignificant. The UPV results on the other hand show distinct results. The relative velocity starts to drop, for Mix No. 2, around 14 cycles. It has been shown by non published material within the project

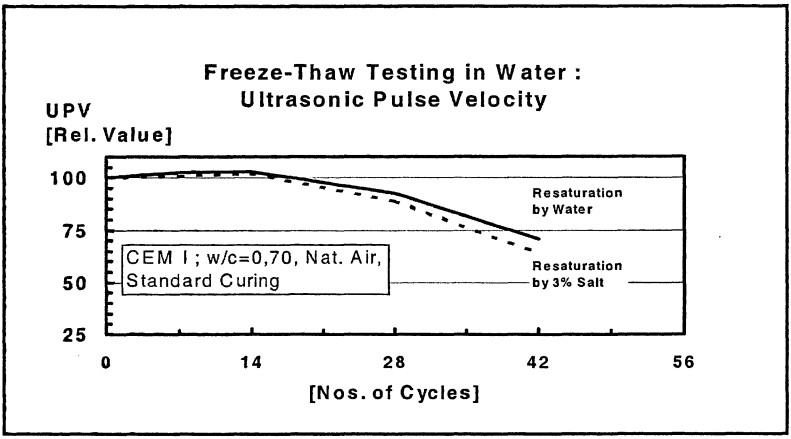

Figure 5 : UPV measurements performed on SS 13 72 42 specimens provide distinct data.

that a pattern of cracks occurs throughout the specimen in such cases, even if the scaling remains very low. For comparison, UPV has been plotted together with the accumulated and

"differentiated" scaling in Fig. 6. This illustrates very well the statistical correlation of the weakening of the structure and the reduced attack on the surface.

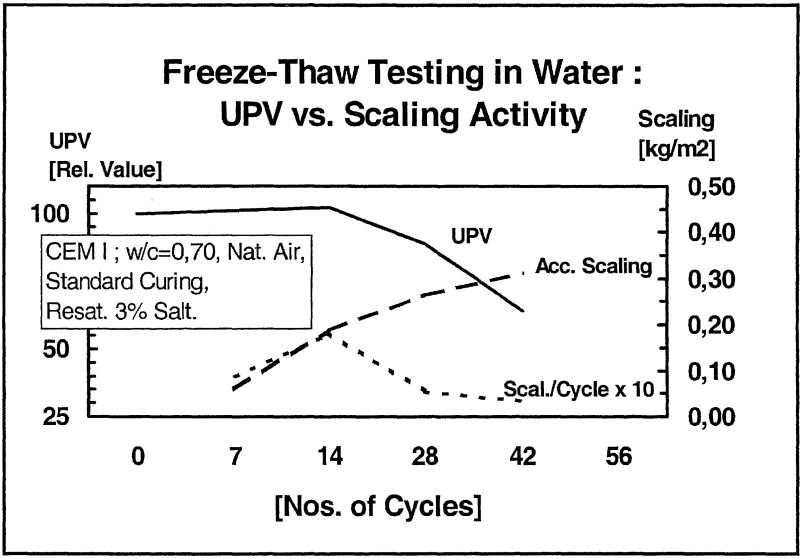

Figure 6. The UPV drop coincides with the reduced scaling activity.

The practical implementation of this phenomenon for laboratory testing is probably that the internal cracking intensity arrives at a stage where it is difficult to maintain the prescribed 3 mm thick testing medium at the top surface, due to percolation. Sealing of the specimens' lateral sides and bottom will only introduce a dimension dependent parameter, which hardly is relevant to in-situ service life conditions.

However, most probably – but not yet proven – the progressive damage will depend on the amount of liquid available at this stage. Hence, the frequency of maintaining 3 mm testing liquid may directly influence the acceleration of the deterioration. Though – this may also remain an academic question .....

4 CONCLUSIONS

The results tend to confirm that moisture absorption increase when tested according to SS 13 72 44 in 3% NaCl, compared to testing in pure water, but the results are not significant in all cases.

A tendency of reduced absorption and scaling when re-saturated by 3% NaCl (and tested in the latter) was confirmed.

When testing in water, the effect of type of re-saturation is still of some significance to the scaling level. However, the scaling seems to be directly limited to the time of percolation of the testing medium. The existence of local defects may control the progression and is more easily detectable by UPV, which drops significantly at this stage.

5 REFERENCES

1. Setzer, M. J. (1999) Micro ice lens formation and frost damage. Rilem TC IDC Workshop on Frost Damage in Concrete, University of Minnesota, Minneapolis, MN, USA, pp. 1-15.
2. Sellevold, E. J. (1987) Betongens Funksjonsdyktighet, Rapport 26 og 27. "The Serviceability of Concrete", Report nos. 26 & 27. Sintef Report Nos. STF65 A88089 & STF65 A88090, Trondheim. (In Norwegian).
3. Fagerlund, G. (1991) Studies of the scaling, the water uptake and the dilation of specimens exposed to freezing and thawing in NaCl solution. Report TVBM 3048, Lund Institute of Technology, Sweden. pp. 37-66.
4. Bager, D. H., Jacobsen, S. (1999) A model for the destructive mechanism in concrete caused by freeze/thaw action. Rilem TC IDC Workshop on Frost Damage in Concrete, University of Minnesota, Minneapolis, MN, USA, pp. 17-40.

Detecting Freeze/Thaw Cracking in Concrete Slabs by Using Ultrasonic Pulse Velocity Methods

L. Tang[1], D. Bager[2], S. Jacobsen[3] and H. Kukko[4]

1 INTRODUCTION

It is well known that freeze/thaw action can result in two types of frost damage in concrete structures: 1) surface damage (scaling) and 2) internal damage (cracking). In the Nordic countries, owing to their long coastlines and the extensive use of de-icing salts in the winter periods, great efforts have been made in developing methods for testing the resistance of concrete to both these types of frost attack. The Swedish standard SS 13 72 44 for scaling (1), the Finish standard SFS 5448 for dilation (2) and the measurement for critical degree of saturation (3) are some examples. Owing to its simplicity and inexpensive test equipment, the Swedish standard SS 13 72 44, also called the slab test, has found a wide application in the Nordic countries and also in some other countries for differentiating concrete qualities with respect to salt scaling resistance. The method is a draft RILEM recommendation (4). The important character of the slab test is that the test conditions (one-dimensional freeze/thaw and slow cooling rate) are close to real climate conditions. Experience from the past ten years shows that the slab test works very well in practical applications (5).

In the slab test only scaling measurement is involved. With the development of high performance concrete with low water-cement ratios, it has been found that very good freeze/thaw scaling resistance can be obtained even without entraining air bubbles in concrete (6). High freeze/thaw scaling resistance, however, does not mean no freeze/thaw cracking (internal damage). In order to ensure a durable structure, the resistance to freeze/thaw cracking should also be examined.

There are different methods to detect the internal cracking. A method commonly used in North America is ASTM C 666. In this method, however, the test conditions (three-dimensional freeze/thaw and rapid cooling rate) are far away from the reality. Besides, the method needs expensive equipment and big specimens.

A simple way to detect the internal damage in a material is to monitor the ultrasonic pulse velocity (UPV) across the specimen, although it is less sensitive than resonance frequency (6). It is readily possible to introduce the UPV measurement into the slab test to examine the internal cracking, because the one-dimensional freeze/thaw condition in this test gives the chance to measure UPV on the unexposed surfaces of the specimen.

In order to evaluate this ultrasonic method so as to find a practically applicable test procedure for detecting the freeze/thaw cracking in concrete, a Nordtest project was carried out in four of the Nordic countries. This paper presents some of the results from this project. The detailed report of the project is available elsewhere (7).

[1] SP Swedish National Testing and Research Institute, Borås, Sweden
[2] Cement and Concrete Laboratory, Aalborg Portland A/S, Aalborg, Denmark
[3] Norwegian Building Research Institute, Oslo, Norway
[4] VTT Building Technology, Finland

2 SPECIMEN MANUFACTURE

2.1 Concreting

The mixture proportions and physical properties of concrete used in this study are listed in Table 1.

All the concrete specimens were produced at SP in Sweden. Each concrete was mixed in one batch by using a 250-liter paddle mixer. The concrete cubes of size 150 mm were cast in steel molds. The molds with the fresh concrete were covered with thick plastic films to prevent evaporation from the concrete surface. One day after casting the cubes were demolded and cured in water until the age 7 days, and then stored at 20 °C and about 65%RH until the 21-day age for sawing for specimens. Three cubes of each mixture were continuously stored until the age 28 days for testing compressive strength.

Table 1. Concrete mixture proportions and physical properties.

	Mixture I	Mixture II	Mixture III
Cement type	Sulfate resistant portland cement (CEM I 42.5R)		
Cement content, kg/m^3	500	375	285
Water-cement ratio	0.32	0.50	0.70
Aggregate, 0~8 mm, kg/m^3	839	910	1041
Aggregate, 8~16 mm, kg/m^3	946	840	818
Water reducer: Dose, wt% of cement	Naphthalene based 0.017	None	None
Air entraining agent: Dose, wt% of cement	None	Tall-oil derivative 0.007	None
Air content, vol% of concrete	1.2	3.4	1.1
Slump, mm	140	70	65
Cube strength at 28 d, MPa	105.1 ± 1.2	51.0 ± 1.5	33.6 ± 2.6

2.2 Specimens

At the age 21 days, two slab specimens of size 150×150×50 mm were sawn from each of the concrete cubes. The sawing direction is illustrated in Fig. 1. Directly after sawing, the specimens were washed with water and the excess water on the surfaces of the specimen was wiped off with a moist sponge. The specimens were then returned to the climate chamber of 20 °C and 65%RH for overnight. On the next day the specimens were separately sealed in plastic bags and were assorted for four laboratories. The assorted specimens were then packaged and transported in frost-free container (temperature above 0 °C) to different laboratories.

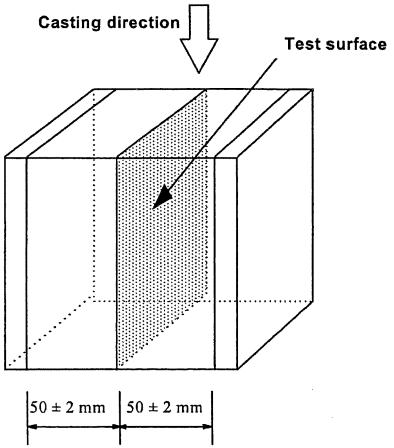

Figure 1. Illustration for sawing of slab specimens from a concrete cube.

2.3 Preconditioning

After receipt, the package containing specimens was kept unopened at each laboratory until a specified age. At the age 28 days, all the specimens were taken out of the plastic bags and placed in a climate chamber of 20 °C and 65%RH for preconditioning according to the standard SS 13 72 44. Non-absorptive solid rubber sheet of 1.5 ± 0.5 mm thick was used to seal the non-freeze surfaces of the specimen. Demineralized water was used for pre-wetting the test surface of a specimen. After preconditioning the UPV measurement was conducted for the initial UPV values.

2.4 Freeze/thaw cycles

After preconditioning, the specimens were subjected to freeze/thaw cycles according to the standard procedure described in SS 13 72 44, but after each collection of the scaled material the weight of each specimen was determined and the UPV measurement was conducted. For Mixtures I and II the 3% NaCl solution was used as a surface liquid, while for Mixture III the demineralized water was used as a surface liquid.

3 MEASUREMENT METHODS

The scaling measurement after specified freeze/thaw cycles, i.e. 7, 14, 28, 42, 56, 70, 84, 98 and 112 cycles in this study, was carried out in accordance with the Swedish standard SS 13 72 44. After the scaling measurement, the weight of the whole slab specimen including the glued rubber was measured under the saturated surface dry condition, that is, the excess water should be wiped away with a moist sponge or similar material prior to weighing. The UPV was measured halfway along the side surfaces of a slab specimen at the positions as shown in Fig. 2. Two readings from two parallel positions, 50 mm apart, were made for each measurement. Three different types of transducers, conic 54 kHz, standard (cylindrical) 54 kHz and 150 kHz, were used for UPV measurement.

In this study some extra specimens were used for destructive measurements such as strength, degree of capillary saturation, porosity, etc., after the specified number of

freeze/thaw cycles. The detailed procedures for these destructive measurements were described elsewhere (7).

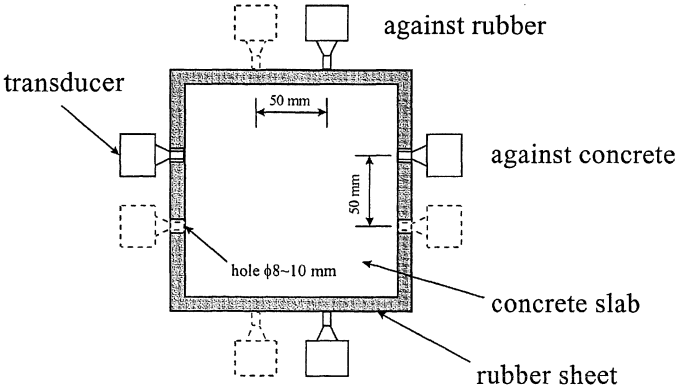

Figure 2. Placement of the transducers in a UPV measurement.

4 TEST RESULTS AND DISCUSSIONS

4.1 Freeze/thaw scaling

The results of average accumulative scaling after different freeze/thaw cycles are shown in Fig. 3. Concrete Mixture I reveals significant scaling damage even though its W/C is as low as 0.32. Concrete Mixtures II and III show very low scaling, either due to good air pore system (Mixture II) or due to the absence of salt solution in the frost test (Mixture III).

4.2 Water uptake

The results of water uptake are summarized in Fig. 4. It can be seen that all types of concrete take up water during the frost test. An interesting thing is that the dense concrete (Mixture I) takes up the largest amount of water. Similar findings were also observed by Jacobsen (6). It can be noticed that the greatest increment in water uptake for Mixture I occurred between 14 and 28 freeze/thaw cycles, similar to the reduction in UPV as will be seen later.

Another important observation is that the concrete without internal damage (Mixture II) takes up even more water than Mixture III (with internal damage). Consequently, it seems as if the measurement of water uptake alone cannot indicate whether there is internal damage.

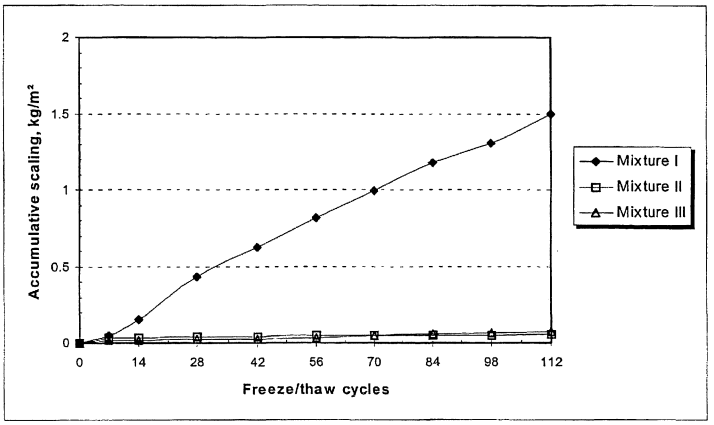

Figure 3. Results from scaling measurement.

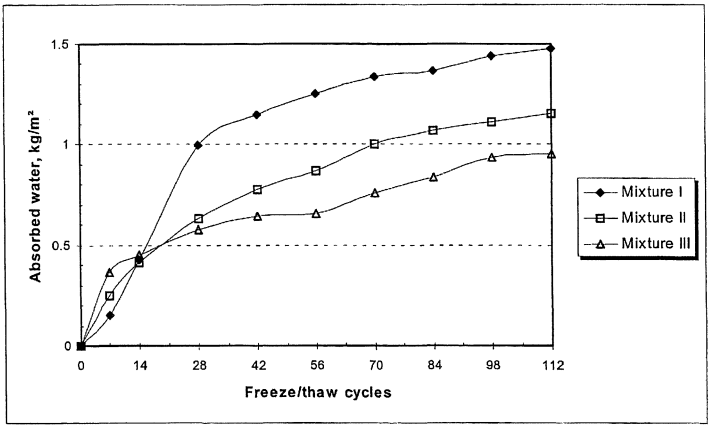

Figure 4. Results of water uptake.

4.3 Degree of capillary saturation and porosity

The measured degree of capillary saturation and porosity are shown in Figs. 5 and 6. It can be seen that most of the capillary pores in concrete Mixture III were already filled with water at the start of the frost test, and that the changes in the degree of capillary saturation throughout the period of freezing and thawing are not so significant.

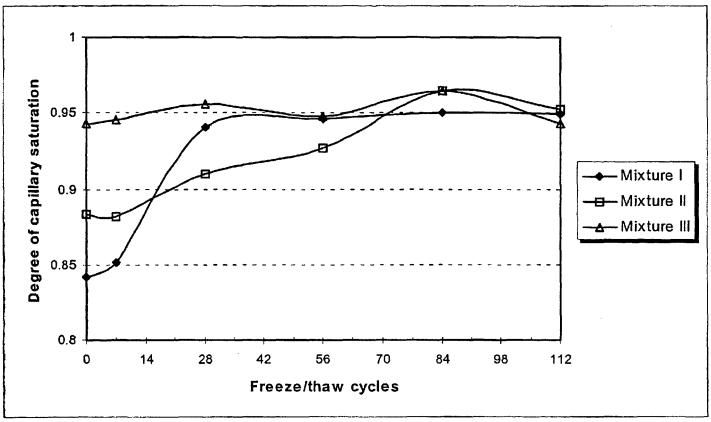

Figure 5. Measured degree of capillary saturation.

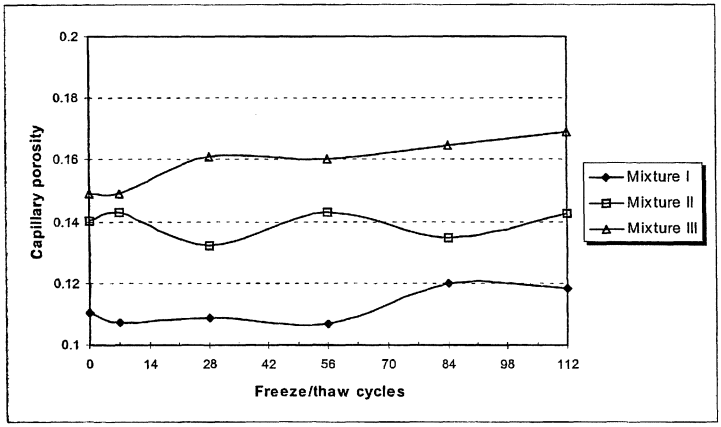

Figure 6. Measured capillary porosity.

The initial degree of capillary saturation in concrete Mixture I was very low at the start of the test, indicating that the pre-wetting procedure is not sufficient to saturate the whole specimen, presumably due to a disconnected pore system. It increased dramatically between 14 and 28 freeze/thaw cycles, in accordance with its water uptake (see Fig. 4). This is an indication of interconnection within the pore system, so that the water outside could flow into inner capillaries and/or air voids.

The degree of capillary saturation in concrete Mixture II gradually increased with the number of freeze/thaw cycles. A low initial degree of capillary saturation for this mixture may be explained by the insulating effect of air pores on the capillary pore system. During the freeze/thaw cycles, the water may be further transferred into the inner capillaries.

The porosity of concrete Mixtures I and III increased with freeze/thaw cycles, indicating that cracking has happened in these types of non-air entrained concrete. The fluctuation in porosity of concrete Mixture II might be attributed to the inaccuracy of porosity measurement.

4.4 Compressive strength

The results of compressive strength are summarized in Fig. 7. It was found that the compressive strength for concrete Mixtures I and III were significantly reduced after the frost test, indicating that substantial internal damage had occurred in these concrete specimens, but not in the air-entrained concrete (Mixture II).

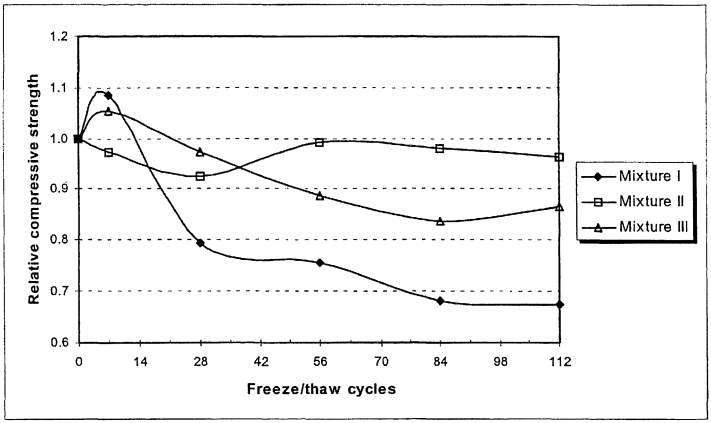

Figure 7. Changes in compressive strength.

4.5 Changes in UPV

The results of the initial and relative UPV measured by using different transducers are summarized in Table 2 and Figs. 8 to 11. It can be seen from Table 2 that the absolute values of UPV measured from different laboratories vary very much, probably owing to different types of equipment, different calibrations and different operators. Nevertheless, only the relative values could be used for comparison. It can be seen that, no matter what type of transducers was used, the significant changes in UPV for Mixture III have been detected, implying severe internal damage.

Table 2. Summary of the measured UPV in km/s.

Type of transducers / Measurement surfaces		Conic 54 kHz Concrete	Conic 54 kHz Rubber	Std. 54 kHz Rubber	Std. 150 kHz Rubber
Mixture I	Lab 1	3.0	2.8	3.8	3.5
	Lab 2	4.4	3.0	-	-
	Lab 3	-	-	4.4	-
	Lab 4	3.1	3.1	4.1	4.4
Mixture II	Lab 1	2.9	2.7	3.6	-
	Lab 2	4.1	2.9	-	-
	Lab 3	-	-	4.1	-
	Lab 4	3.0	2.9	3.7	3.9
Mixture III	Lab 1	2.8	2.7	3.5	2.7
	Lab 2	4.1	2.9	-	-
	Lab 3	-	-	4.0	-
	Lab 4	2.9	2.9	3.8	3.9

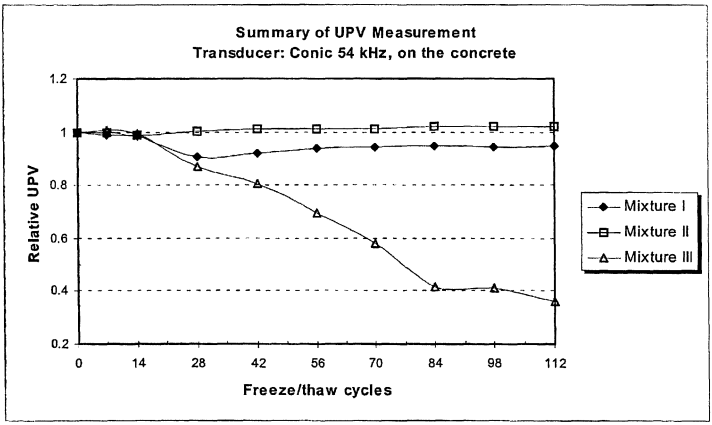

Figure 8. Changes in UPV, using conic 54 kHz transducers on the concrete surfaces.

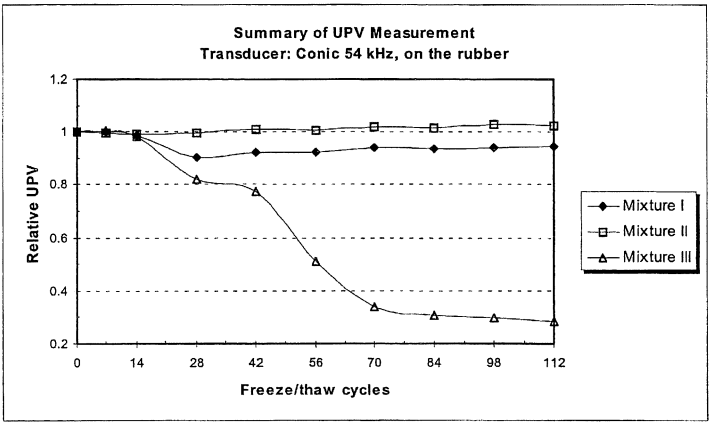

Figure 9. Changes in UPV, using conic 54 kHz transducers on the rubber surfaces.

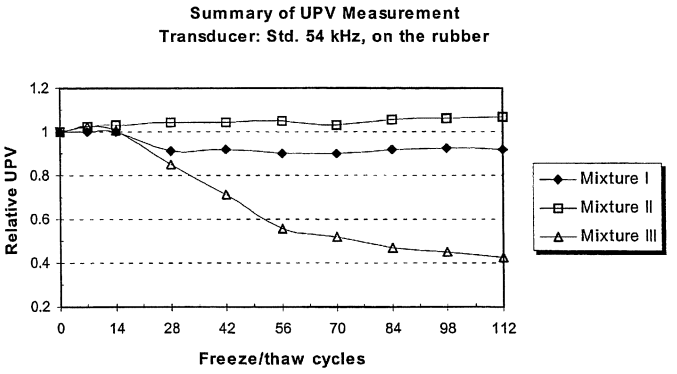

Figure 10. Changes in UPV, using standard 54 kHz transducers on the rubber surfaces.

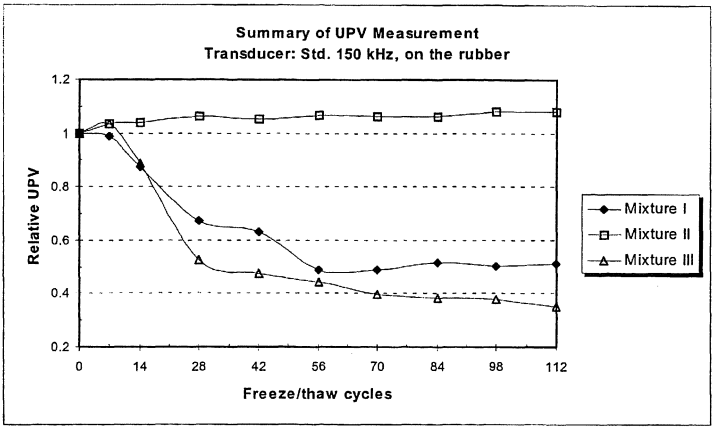

Figure 11. Changes in UPV, using standard 150 kHz transducers on the rubber surfaces.

When using 150 kHz transducers the changes in UPV for Mixture I seem similar to those for Mixture III, but the measurement deviation is very large, as will be shown later in Fig. 14.

When using the 54 kHz transducers, the reduction in UPV for Mixture I does not seem to be very large (only about 10 %), but almost the entire 10 % reduction occurred between 14 and 28 freeze/thaw cycles. The UPV measurements from three different laboratories showed similar results as shown in Fig. 12, that is, the drop in UPV occurs between 14 and 28 cycles. This is in accordance with changes in other parameters, such as water uptake (Fig. 4), degree of capillary saturation (Fig. 5) and compressive strength (Fig. 7). Something must have happened at this stage of freezing and thawing. From the petrographic photograph shown in Fig. 13, it can be seen that the porous transition zones or cracks around the aggregates have been connected by very fine cracks crossing the paste between aggregate particles. Although these fine cracks might result in only a slight change in pore volume or in UPV, they function as connective channels for the water outside to be transferred into pores, cracks, voids and/or transition zones around aggregates, resulting in substantial water uptake as shown in Fig. 4.

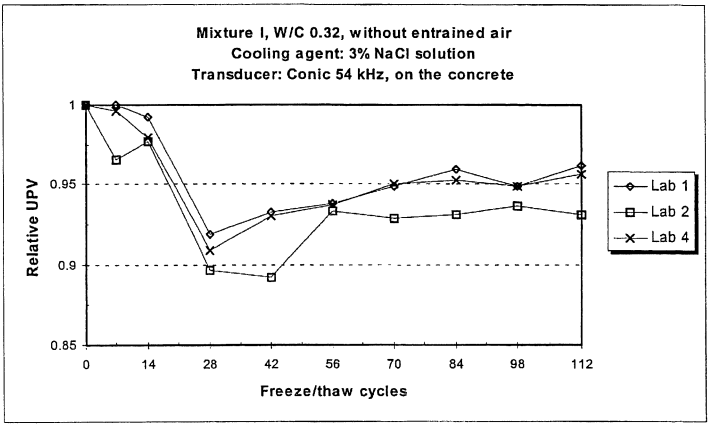

Figure 12. Changes in UPV for dense concrete measured from different laboratories.

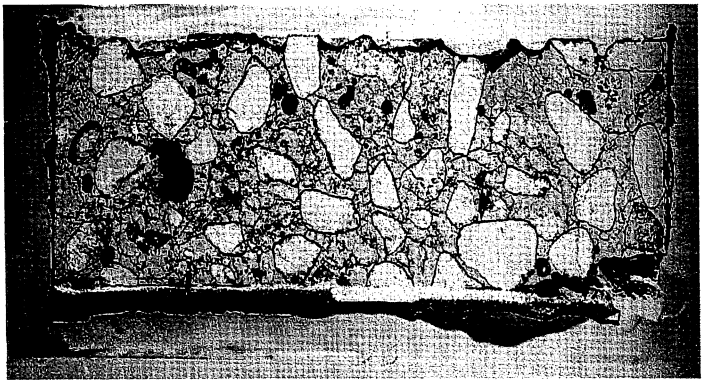

Figure 13. Many fine cracks in Mixture I after 112 freeze/thaw cycles (negative photo).

5 REPEATABILITY AND REPRODUCIBILITY OF UPV MEASUREMENTS

In this study, the standard procedure ISO 5725 (8) was employed for determining repeatability and reproducibility of UPV measurements. Owing to the page limitation, only Mandel's *k*-statistic diagram is shown in Fig. 14. It can be seen that, in general, the conic transducers give better repeatability and reproducibility than the standard transducers. It should be noticed that the analysis for the 150 kHz transducers was based on the data from only two laboratories.

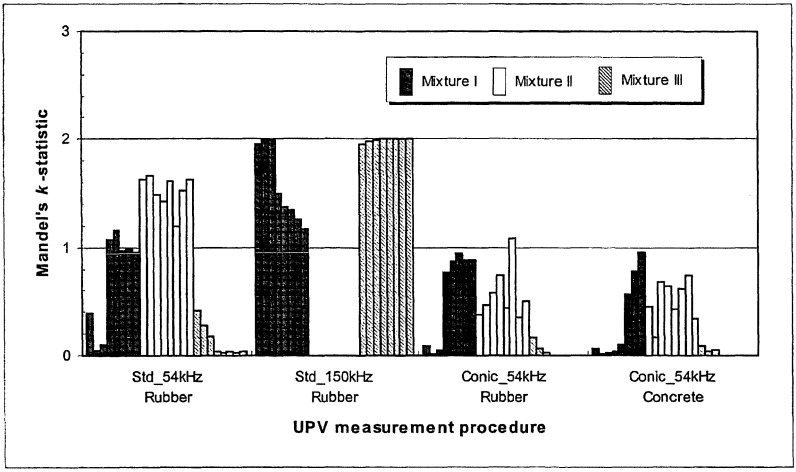

Figure 14. Mandel's k-statistic diagram according to ISO 5725.

6 CONCLUSIONS

UPV measurement can easily be employed in the slab test and can indeed detect the internal damage in concrete caused by freezing and thawing attack, especially for poor concrete.

All the four laboratories engaged in this project give the same judgment from their UPV measurement, that is, cracking has occurred in Mixture I (dense concrete) and Mixture III (poor concrete), but not in Mixture II (air-entrained concrete).

Conic transducers give better repeatability and reproducibility than standard cylindrical transducers. High frequency transducers seem more sensitive to detecting the internal damage, but further investigation is needed to confirm this.

For dense concrete, a little sudden decrease in UPV may imply a big drop in strength. If significant internal damage is suspected some auxiliary measurements may be necessary to ensure the judgment from the UPV measurement. This could be achieved by monitoring the water absorption or testing the final strength after terminating the freeze/thaw test.

7 REFERENCES

1. Swedish Standards Institution, "Concrete testing - Hardened concrete -Frost resistance", SIS, Stockholm, SS13 72 44, 3rd ed., 1995

2. Finish Standardization Association, "Concrete, Durability, Freezing dilation", SFS, Helsinki, SFS 5448, 1988
3. Fagerlund, G., Materials and Structures, Vol. 10, No. 51, 1977, pp. 217-229
4. RILEM TC 117-FDC, "Test methods for freeze/thaw resistance of concrete, Slab test and cube test", Materials and Structures, Vol. 28, No. 180, 1995, pp. 366-371
5. Malmström, K., "Scaling resistance of concrete structures - Studies in the field" (in Swedish), SP Report 1996-04, SP Swedish National Testing and Research Institute, Borås, 1996
6. Jacobsen, S., "Scaling and cracking in unsealed freeze/thaw testing of Portland cement and silica fume concretes", Doctoral thesis, NTH 1995:101, Div. of Structural Engineering, The Norwegian Institute of Technology, Trondheim, Norway, 1995
7. Tang L., Bager D., Jacobsen S. and Kukko H., "Evaluation of the Ultrasonic Method for Detecting Freeze/thaw Cracking in Concrete - NORDTEST Project no. 1321-97", SP Report 1997:37, SP Swedish National Testing and Research Institute, Borås, Sweden, 1997
8. ISO 5725-2:94, "Accuracy (trueness and precision) of measurement methods and results - Part 2: Basic method for the determination of repeatability and reproducibility for a standard measurement method", International Organisation for Standardisation, 1994

FROST INDUCED TRANSPORT OF SALTS IN CONCRETE

Marianne Tange Jepsen, M.Sc., Ph.D.-student
Concrete Centre, Danish Technological Institute
Gregersensvej, P.O. Box 141, DK-2630 Taastrup, Denmark
E-mail: marianne.t.jepsen@teknologisk.dk

1 INTRODUCTION

Concrete, which contains Portland cement in the binder phase, has been used as a construction material for more than 100 years. During this period of time, the concrete has undergone a development, so the concrete of today differs in many ways from the concrete of yesterday e.g. the concrete used at the turn of the century. Today, concrete is produced with lifetimes expected to last up to 100 years even for heavily exposed structures, but the durability cannot be proved sufficiently through experience, because experience with the actual material through such a large number of years is not available. It is necessary to base the estimation of a structure's service life on models, and then the frost resistance is an essential but very uncertain factor.

2 THE STARTING POINT OF A PH.D. PROJECT

Today's models for development of frost damage in concrete is based on the assumption that frost action initiates a pressure build up in the pore solution of the concrete. Roughly spoken, almost all the models are variations of three different mechanisms ([1], [2]):

- *Closed container mechanism.* Water expands, when it is transformed into ice (about 9%). If the volume expansion is hindered e.g. in a closed container, a static pore pressure will develop.
- *Hydraulic pressure.* During the transformation of water to ice, non-frozen water is expelled from the transformation zone to air filled voids and surfaces. This water flow causes a hydraulic pressure in the pores.
- *Microscopic ice lens growth.* At any given temperature, freezing initiates in the capillaries and then occurs in a minor scale in the gel voids. This means that the ice in the lager voids gets a lower Gibb's free energy than the water in the gel voids. Pore solution is drawn from the gel voids to the capillaries, where it is possible for the ice lens growth to continue until a new thermodynamic equilibrium is established.

The first two mechanisms mentioned deal with physical/mechanical processes, while only the microscopic ice lens growth originates from basic thermodynamic premises of ice formation.

The damaging mechanisms described above can take place in pure, free water - an idealised assumption often used. In reality, the pore solution contains a number of salts, both salts released during the cement hydration (e.g. Na_2O, K_2O and $Ca(OH)_2$) and salts supplied from the surroundings, for instance de-icing chemicals (e.g. NaCl and $CaCl_2$). The conditions are further complicated because the freezing process takes place in a material where not only free water but also several different water phases are present.

The basic idea of this Ph.D. project is to investigate from a thermodynamic point of view the interaction of the presence of salts and the ice formation. On one hand the concentration of salts has an effect on the ice formation, on the other hand the ice formation has an influence on the transport of salts in the concrete. The project consists of two parts. The first part is predominantly scientific, whereas the last part to a larger extent focuses on application.

3 SCIENTIFIC AIMS

The scientific aims of the project are to investigate:

- the dynamic and statistic characteristics of the ice formation in hardened cement paste
- the movements of salts and salt concentration profiles in cement bound materials placed in a saline environment and exposed to cyclic freeze/thaw load.
- the thermodynamic phase equilibriums, which appear when ice is formed in a saline pore solution in a porous system.

The investigations will be based on studies of literature, theoretical analyses, and laboratory testing. When the salt concentration of a liquid is altered, the freezing point of the liquid is altered too, and one of the hypotheses is that this under certain conditions may provoke a "sequential freezing" where non-frozen zones with a high local concentration of salts are trapped between frozen zones. If an unfrozen zone freezes later on (e.g. because the temperature is lowered) the conditions of freezing in the zone will be equal to those of a closed container.

In order to present the problems in question as clearly as possible, the scientific work will be carried out on cement paste, which is a much less complex system than concrete (i.e. no aggregates and no interfacial transition zones).

3.1 CTS – a new experimental technique

An experimental examination of the subject requires that the distribution of salts and moisture in the cement paste can be determined and the ice formation mapped, so these parameters can be compared. Methods to determine water contents (chemically bounded, adsorbed and free capillary water) and salt profiles are well known. But a new method is needed to follow the formation of ice in a specimen exposed to a frost attack. It is expected that such a method can be based on a principle of Continuous Temperature Scanning (CTS). When water is transformed into ice, it releases energy (heat of fusion) and in a super-cooled pore solution a local heating will occur. By continuous registration of the temperature profile in a test specimen exposed to frost load it is possible to trace the heat release or, which is the same, when and where ice is formed. The method is described in [3].

At present time, equipment for CTS measurements is being developed, see figure 1.

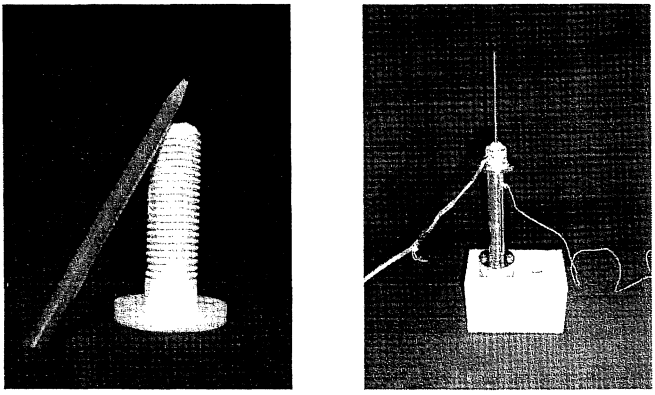

Figure 1. Test specimen and equipment for CTS measurements.

3.2 Computer simulation

A computer program is to be developed for numerical simulations of the freezing process in hardened cement paste exposed to frost load. It is basically a matter of translating relevant models from the theoretical analysis into algorithms. Thus this numerical tool will be based on simple models of diffusion of adsorbed water to the ice front, probability of the first ice formation, release of heat of fusion during transformation, and depression of freezing point caused by the presence of salt.

Results obtained by numerical simulations will be compared with results from the experimental investigation of cement paste in order to verify the computer program. The numerical simulations can by no means replace the experimental investigation, but the numerical simulations are particularly well qualified to estimate the sensitivity of the different processes to changing conditions and to the element of randomness due to the seeding.

4 AIMS OF APPLICATION

In the last part of the project the aim is to transfer experiences gained with cement paste to concrete, and therefore experimental work of course will be carried out on concrete samples. During this part of the project an investigation will be made into the influence of some selected parameters of the mix design on the frost resistance. The reason for this investigation is not only to make an intensive study of a certain mix parameter. This investigation is also intended to be a case study, which for example enables a comparison of measurements obtained by different test methods.

4.1 Comparison of test methods

The CTS equipment employed during the scientific part of the project is limited to measurements on hardened cement paste. The CTS measuring technique will be modified, so it can be applied to investigations of the freeze process in hardened concrete, which is exposed to frost action.

Besides the CTS measurements, air void analysis and traditional frost tests according to the existing standards will be carried out. The aim is to improve the relation between the durability of a concrete structure and results of laboratory testing. This can either be in the shape of a better theoretical background for the interpretations of the test results or the introduction of the CTS method, which offers further details in addition to test results of traditional methods.

4.2 Documentation of frost resistance

The conclusion of the utility-oriented part of the project will be a proposal of a procedure of practical use for testing, which focuses on the deterioration mechanisms that have been demonstrated during the project.

5 CONCLUDING REMARKS

New knowledge about the physical/chemical mechanisms in the concrete such as frost induced salt movements can be used when working out specifications of concrete. For instance today, there are rather rigid demands to the air content of concrete in structures exposed to frost [4]. A better understanding of the factors determining the frost resistance will make it possible to put up more sophisticated requirements and optimise the concrete mix design in order to get concrete types that are just exactly frost resistant. A specific case, where new knowledge can be implemented, is for the evaluation of the durability of the so-called green concretes, since the requirements of standards based on experience with conventional concrete might not be sufficient.

ACKNOWLEDGEMENT
The project is partly financed by the Danish Agency for Trade and Industry.

REFERENCES

1. Powers, T. C. (1955) *Basic considerations pertaining freezing-and-thawing tests*, Bulletin 58, Portland Cement Association.
2. Fagerlund, G. (1997) *Internal frost attack – state of the art*, proceedings of the RILEM Workshop of resistance of concrete to freezing and thawing with and without de-icing chemicals, E & FN Spon.
3. Jepsen, M. T. (1999) *Frost induced transport of salts in concrete*, proceedings of XVII Nordic Concrete Research Meeting, Reykjavik.
4. Danish Standard DS 481 (1999) *Concrete – Materials*, final edition dated 16.06.99.

SALT-FROST RESISTANCE OF CONCRETE IN HIGHWAY ENVIRONMENT

- A comparison with results from SS 13 72 44, the 'Slab Test'

Peter Utgenannt, Doctoral student
SP Swedish National Testing and Research Institute
Box 857
SE-501 15 Borås
e-mail: peter.utgenannt@sp.se

ABSTRACT

This paper presents results from an investigation of the salt-frost resistance of concrete in a highway environment. Over 100 concrete qualities, produced with different types of binders, varying water/binder ratios and air contents, have been exposed to an aggressive highway environment at a field test site located on highway RV 40, between Borås and Gothenburg, for three winter seasons. The results show that several qualities are severely damaged after only three winter seasons. Most of these qualities have a high water/binder ratio and low air content. A comparison between results from testing the salt-frost resistance in accordance with SS 13 72 44 (the slab test) and the results from the field test site shows that, in most cases, the slab test estimates the salt scaling resistance correctly. Two qualities containing slag and one containing silica fume as part of the binder show differences between laboratory and field results. The test method probably needs to be modified in order correctly to be able to estimate the salt-frost resistance for new qualities of concrete, especially when high contents of slag is used. More research is needed in this field.

INTRODUCTION

The salt-frost resistance of concrete is normally estimated in the laboratory by freeze/thaw test methods such as SS 13 72 44, the slab test. These test methods have been developed primarily on the basis of experience of concrete made with Ordinary Portland Cement and pure air entraining agents. When new types of concrete are produced - for example, with new binder types, filler material, new types of admixtures etc. - we do not know if the freeze/thaw test methods are relevant for testing the salt-frost resistance. More knowledge and experience of the salt-frost resistance of these new concrete qualities are needed.

One way to gain experience of the salt-frost resistance of concrete is to expose concrete specimens to a representative outdoor environment, such as an aggressive, saline highway environment. Such an investigation of the salt-frost resistance of different concrete qualities was started in 1996. In collaboration with the Swedish Road Administration, a field test site was built near Borås on highway RV 40, between Borås and Gothenburg. A large number of concrete qualities with different binder types/combinations, varying water/binder ratios and air contents were produced and placed at the field test site. After each winter season, measurements of the volume change and ultrasonic transmission time are carried out on each specimen in the laboratory.

The compressive strength and salt-frost resistance of all concrete qualities were tested in the laboratory, in accordance with normal laboratory standards, one month after casting. Results from the laboratory tests and the measurements on the specimens exposed at the field test site provide important knowledge of salt-frost resistance in terms of the correlation between results from the test methods used and the real outdoor environment.

This paper presents results after three winter seasons. The results presented here are valid only for the actual materials and material combinations tested. Other constituents and other combinations may lead to other results.

MATERIALS AND SPECIMENS

Nine different binder types/combinations were studied in this investigation: see Table 1. For chemical analyses, see [1].

Table 1. Binder types/combinations investigated

	Binder type/combination	Comments
1	**Degerhamn std. 'Civil engineering cement'**	Low alkali, sulphur resistant
2	**Slite std.**	
3	**Degerhamn std. + 5 % silica**	Silica in the form of slurry
4	**PK-cement**	Portland cement with limestone filler
5	**Finnish std.**	Finnish Portland cement with some slag
6	**Degerhamn std. + 30 % slag**	Ground blast furnace slag added in the mixer
7	**CEM III/B**	Dutch slag cement 70% slag
8	**Finnish rapid**	Finnish rapid hardening cement
9	**Finnish SRPC**	Finnish, sulphur resistant cement

15 concrete qualities were produced for all binder types/combinations, except binder types 8 and 9 where only 4 qualities were tested. Three different air contents (4.5%, 3% and 'natural' air), and five different water/binder(w/b) ratios (0.30, 0.35, 0.40, 0.50, 0.75), were used. 0-8 mm natural and 8-16 mm crushed aggregate were used for all concrete qualities. A naphthalene-based plasticizer, Melcrete, was used for qualities with w/b-ratio of 0.40 and lower. The air-entraining agent used, L16, is a tall-oil derivative.

All concrete batches were produced in the autumn of 1996 and placed at the field test site at ages of between two and four months. Two specimens (half 150 mm cubes) of each quality were placed in steel frames close to the traffic, see Figure 1. Figure 2 shows two severely damaged specimens.

Figure 1. Specimens in steel frame close to the traffic

Figure 2. Severely damaged specimens

TEST PROCEDURE

The volumes and the ultrasonic pulse velocity through each specimen were measured before the specimens were placed at the field test site. These measurements have been repeated after each winter season. The volume measurements are carried out by measuring the weight of the specimens under water and surface-dry above water. The ultrasonic pulse velocity - or more exactly, the ultrasonic pulse transmission time through the specimen - is measured on three locations on each specimen.

The salt-frost resistance and the compressive strength were measured on specimens from each concrete quality at the standardised age as specified in SS 13 72 44 and SS 13 72 10.

RESULTS

Figures 3 - 11 present the results from measurements of the volume change and the ultrasonic pulse transmission time for each concrete quality. Each figure shows the volume change and the transmission time for all qualities of each binder type/combination: 15 qualities for types/combinations 1-7 and 4 qualities for types 8 and 9. The volume changes are shown as the mean change for two specimens. The transmission times are presented as the mean value of results for two specimens, with three measurements on each specimen. Some qualities with significant changes in volume and/or transmission time are marked in the figures.

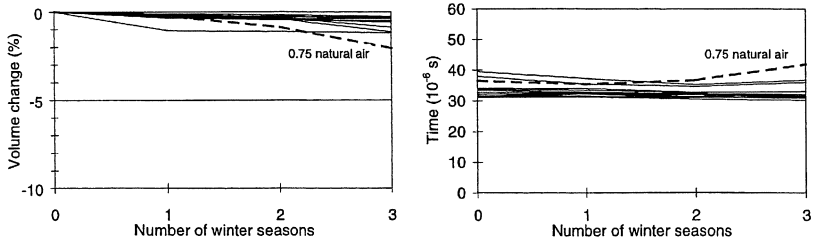

Figure 3. Concrete quality 1 "Degerhamn std". Volume change and transmission time.

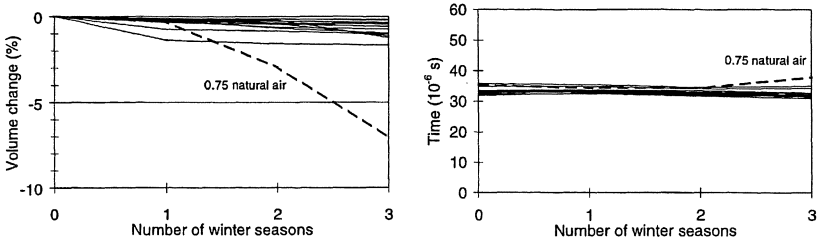

Figure 4. Concrete quality 2 "Slite std". Volume change and transmission time.

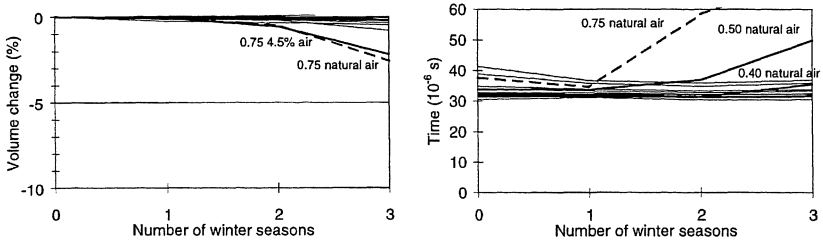

Figure 5. Concrete quality 3 "Degerhamn + 5% silica". Volume change and transmission time.

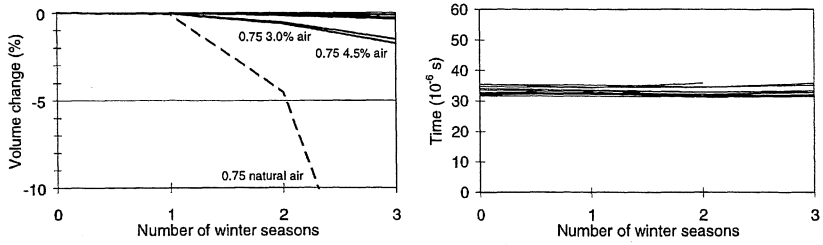

Figure 6. Concrete quality 4 "PK-cement". Volume change and transmission time.

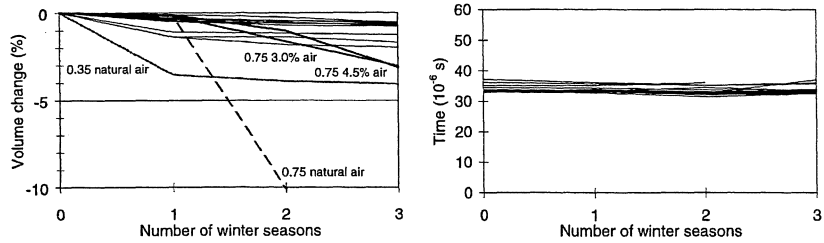

Figure 7. Concrete quality 5 "Finsk std.". Volume change and transmission time.

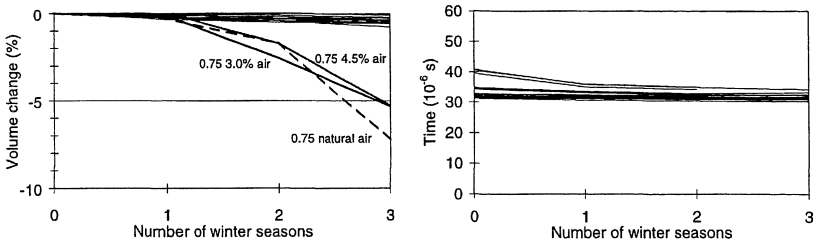

Figure 8. Concrete quality 6 "Degerhamn + 30% slag". Volume change and transmission time.

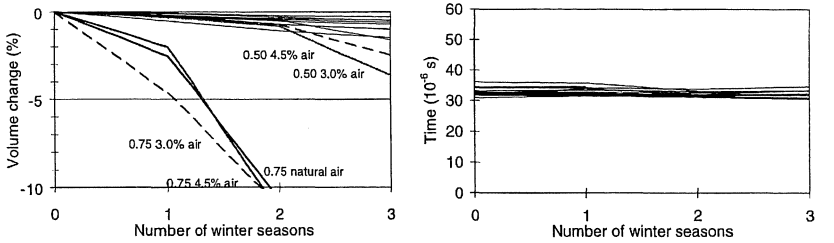

Figure 9. Concrete quality 7 "CEM III/B". Volume change and transmission time.

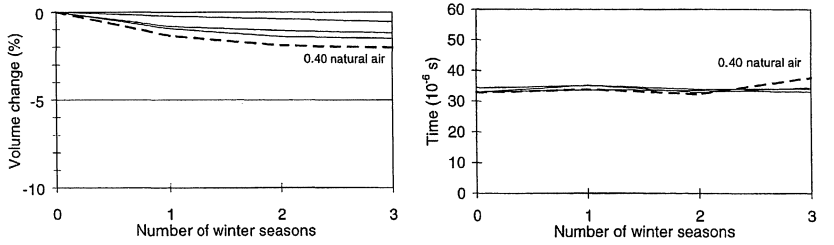

Figure 10. Concrete quality 8 "Finsk rapid". Volume change and transmission time.

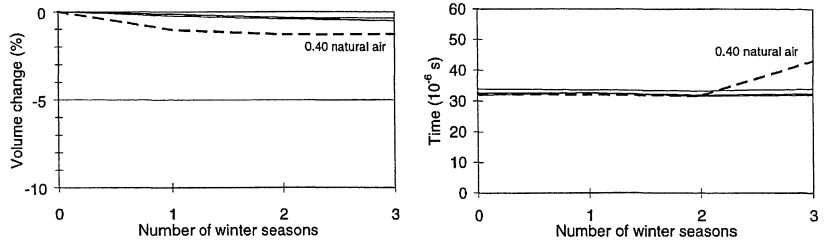

Figure 11. Concrete quality 9 "Finsk SRPC". Volume change and transmission time.

Table 2 shows a comparison between results obtained in the laboratory when testing the salt-frost resistanceaccording to to SS 13 72 44 with results from the field test site. Field and laboratory results are compared for those concrete qualities in figures 2-10 that showed the most damage, i.e. over about 1-2 % volume change after three years. The fourth column

indicates whether the results from the field agree with the results from the laboratory. A frequently used criteria for a salt-frost resistant concrete when tested by the slab test is a maximum scaling of 1 kg/m² after 56 freeze/thaw cycles and a rate of scaling that is not accelerating.

Table 2. Comparison between results from the field and from the laboratory.

Concrete quality	Volume change after three winter seasons (%)	SS 13 72 44 56 cycles kg/m²	Agreement
No.1 Degerhamn std.			
w/b-ratio 0.75, natural air	-2.07	D (4.3 at 28c)	Yes
No.2 Slite std.			
w/b-ratio 0.75, natural air	-7.05	D (4.8 at 14c)	Yes
No.3 Degerhamn std. + 5% silica			
w/b-ratio 0.75, natural air	-2.59	6.58	Yes
w/b-ratio 0.75, 4.5% air	-2.19	0.2	**No**
No.4 PK-cement			
w/b-ratio 0.75, natural air	-22.6	D (7.5 at 14c)	Yes
w/b-ratio 0.75, 3.0% air	-1.52	11.1	Yes
w/b-ratio 0.75, 4.5% air	-1.76	5.26	Yes
No.5 Finnish std.			
w/b-ratio 0.75, natural air	-24,8	D (4.9 at 14c)	Yes
w/b-ratio 0.75, 3.0% air	-3.04	3.40	Yes
w/b-ratio 0.75, 4.5% air	-3,10	1.25	Yes
w/b-ratio 0.35, natural air	-4.05	4.06	Yes
No.6 Degerhamn std. + 30% slag			
w/b-ratio 0.75, natural air	-7.23	4.37	Yes
w/b-ratio 0.75, 3.0% air	-5,33	0.60	**No**
w/b-ratio 0.75, 4.5% air	-5,27	0.54	**No**
No.7 CEM III/B			
w/b-ratio 0.75, natural air	-17.4	6.89	Yes
w/b-ratio 0.75, 3.0% air	-18.6	3.19	Yes
w/b-ratio 0.75, 4.5% air	-23,4	3.16	Yes
w/b-ratio 0.50, 3.0% air	-3,63	1.80	Yes
w/b-ratio 0.50, 4.5% air	-2,48	1.65	Yes
No.8 Finnish rapid			
w/b-ratio 0.40, natural air	-2.03	4.38	Yes
No.9 Finnish SRPC			
w/b-ratio 0.40, natural air	-1.28	6.91	Yes

D - Destroyed, end of test.

DISCUSSION

Some qualities exhibited considerable damage after three winter seasons. The majority of them have a high water/binder-ratio, and most have low air contents. It can be seen from Figures 3-11 that concrete qualities with some binder types exhibit more damage than others. Nos. 5 (Finnish std.), No. 6 (Degerhamn + 30% slag) and No. 7 (CEM III/B), for example, seem, according to the results in this investigation, to be less salt-frost resistant than most of the other binder types/combinations, at least for the damaged qualities.

Results from the ultrasonic pulse transmission time measurements show an increase in transmission time for some qualities. An increase in transmission time is probably an indication of interior frost damage. It is primarily concrete qualities with high water/binder-ratios and natural air contents that show an increase in transmission time. Most qualities that show increased transmission time also show a loss of volume. Only two qualities show a large increase in transmission time and no significant loss of volume: in fact, these qualities actually show some increase in volume after three winter seasons. These qualities are those with binder type No. 3 (Degerhamn + 5% silica) with natural air content and water/binder-ratio 0.40 and 0.50. Concrete quality No. 3 (Degerhamn + 5% silica) seems to be the one that is most susceptible to interior frost damage, at least for the damaged qualities. It has not been possible to measure the change of transmission time for specimens with very considerable damage (loss of volume). Some of these qualities would probably also show increased transmission times.

The comparison between results obtained in the field with the results obtained in the laboratory shows that the laboratory test (SS 13 72 44 [the slab test]) is, in most cases, able to identify concrete qualities with poor salt-frost resistance. That is, when testing a concrete which has a poor salt-frost resistance, the scaling exceeds 1 kg/m^2 after 56 freeze/thaw cycles. Three qualities, however, show considerable damage in the field but seem to be salt-frost resistant when tested in the laboratory: they are those with binder type/combination No. 3 (Degerhamn + 5 % silica) with w/b-ratio of 0.75 and 4.5% air, and No. 6 (Degerhamn + 30 % slag) with w/b-ratio of 0.75 and 3.0 % air as well as w/b-ratio of 0.75 and 4.5% air. It seems that the slab test fails to identify these qualities as susceptible to salt-frost damage.

For the Degerhamn + 5 % silica concrete, the reason for this can be that this particular quality might have some interior damage that may lead to surface scaling. The duration of the freeze/thaw test might be too short to detect this type of damage. A longer duration of the test or supplementary examination for interior damage, such as ultrasonic pulse velocity or length change measurements, might enable the freeze/thaw test to identify this quality as susceptible to frost damage.

For quality No. 6 (Degerhamn + 30 % slag), the discrepancy between results from the laboratory and from the field might be explained by the observed negative effect that carbonation has on the salt-frost resistance of concrete containing large amounts of slag in the binder [2]. One possible explanation for the discrepancy might be that concrete tested by the slab test, has been exposed to air for only seven days, - that is, for only seven days of carbonation - while the surface of a concrete in the field is being continuously carbonated. This results in a relatively limited scaling in the laboratory, but extensive damage in the field. To be able to correctly estimate the salt-frost resistance for these types of concrete it may be necessary to modify the slab test, e.g. by preconditioning the concrete specimens in different climates, one with normal air and one with increased CO_2 content. Figure 12 below presents results for one concrete quality (No. 6 Degerhamn + 30 % slag with w/b-ratio 0.75 and 4.5% air) that was tested by the slab test after being preconditioned for one week in three different environments: 1 % CO_2 by volume, a CO_2-free environment and normal air.

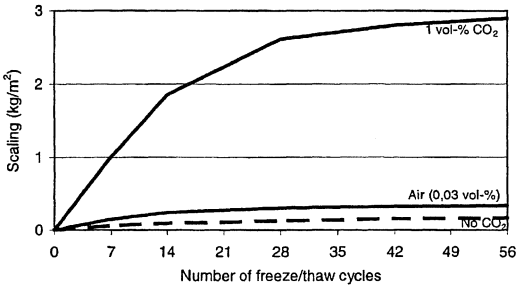

Figure 12. Scaling results from the slab test. Concrete with binder combination No. 6 Degerhamn + 30% slag with w/b-ratio 0.75 and 4.5% air, conditioned in different climates.

It can be seen from the figure that the concrete conditioned in an environment with elevated CO_2 content shows much higher scaling than specimens conditioned in normal air or air without CO_2. It can be seen from the appearance of the scaling curve for the concrete conditioned in elevated CO_2, that a layer, probably the carbonated skin, is scaled off during the first 28 freeze/thaw cycles. After that the rate of scaling slows and becomes comparable with the rate of scaling for the concrete specimens conditioned in normal air and air without CO_2.

For this type of concrete, preconditioning in an environment with 1 % CO_2 by volume for one week seems to give more relevant scaling results than conventional preconditioning in normal air when compared with the results from exposure in a aggressive highway environment.

Other preconditioning climates and durations might be more suitable for estimating the salt-frost resistance of other types of concrete qualities in the field. A proposal for how to modify the freeze/thaw standard in order to make it more 'general' and relevant for most concrete qualities is made in [3].

More experience about salt-frost resistance in the field and knowledge of the scaling mechanisms are needed in order to be able to create a freeze/thaw testing method capable of separate good concrete qualities from bad in terms of salt-frost resistance.

The results presented here are valid only for the actual concrete qualities tested. Other qualities with other type of admixtures, material proportions, binder types/combinations etc. would probably give other results.

CONCLUSIONS

The following conclusions can be drawn after three years' exposure of over 100 different concrete qualities at a field test site on RV 40 outside Borås (saline highway environment):

- Some qualities show considerable salt-frost damage. Most of these qualities have a high water/binder-ratio and a low air content.
- Some qualities show an increased ultrasonic pulse transmission time, which probably indicates interior frost damage. All of these qualities, except two with Degerhamn + 5 % silica (which show an increase in volume), also show a large loss of volume.

- Concrete qualities produced with binder types/combinations No. 5 (Finnish std.), No. 6 (Degerhamn std. + 30 % slag) and No. 7 (CEM III/B) show somewhat higher salt-frost damage than do other types/combinations.
- A comparison between results from the field investigation with scaling results from laboratory test method SS 13 72 44 (the slab test) shows that, for most concrete qualities, the slab test can correctly identify qualities with poor salt-frost resistance.
- Only three qualities suffer considerable damage in the field but are considered to be salt-frost resistant when tested in the laboratory with the slab test. Two of these qualities have a binder combination of Degerhamn std. 30 % slag. One possible explanation for this discrepancy might be the adverse effect of carbonation on the salt-frost resistance for qualities with a high slag content in the binder.
- To be able to test new types of concrete qualities, more knowledge is needed and the existing test methods probably need to be modified: perhaps by changing the preconditioning procedure to suit the concrete quality tested. Concrete containing large amounts of slag can, for example, be conditioned in climates with increased CO_2 content.

REFERENCES

1. Utgenannt, P. Delområde 2.3 - Bindemedlets inverkan på betongs frostbeständighet - Provkroppar tillverkade 1996 - Material- och tillverkningsdata samt resultat från beständighetsprovning i laboratorium, BTB-rapport nr 1 (1997)
(The effects of the binder on the frost resistance of concrete - Test pieces made in 1996 - Material and production data and results from life testing in the laboratory. BTB report no. 1 (1997)).
2. Utgenannt, P. Influence of carbonation on the scaling resistance of OPC concrete, Minneapolis Workshop on Frost Damage in Concrete, University of Minnesota, June 1999.
3. Petersson, P-E., Utgenannt, P. Parameters influencing the result when testing the scaling resistance of concrete, Minneapolis Workshop on Frost Damage in Concrete, University of Minnesota, June 1999.

PREDICTION OF SERVICE LIFE OF CONCRETE STRUCTURES WITH REGARD TO FROST ATTACK BY COMPUTER SIMULATION

Erkki Vesikari, Lic.Tech.
VTT Building Technology
PL 1805, 02044 VTT, Finland

1 INTRODUCTION

The importance of durability and service life has increased in today's structural design practice. This becomes evident e.g. from Eurocode 1 [1], where the durability and service life of structures are prominently emphasised and requirements for the design working life of structures are presented.

The European draft standard for concrete structures prEN206 [2] takes the Eurocode 1 requirements for service life as a stepping stone for further refined provisions of durability design. It presents a table of limiting values for water cement ratio, cement content, compressive strength and air-content categorised to several exposure classes as an equivalent for 50 years design working life (for normal building structures). These values are informative and shall be re-examined on national bases taking into account the local climatic features. However the limiting values shall be given corresponding to the design working life of at least 50 years.

There is no requirement for the air content for vertical structures in prEN206 (XF1). However, in Finland there has been an air content requirement of 4 % for facade concrete since the year 1976. In a vast microscopical research concerning facade concrete in Finland frost cracking was found in 57% of all cases of non-air-entrained concrete while no cracking was found in the cases of air-entrained concrete [3]. These observations support the prevailing practice of quality control for frost resistance in Finland. For horizontal structures, such as balcony slabs, prEN206 presents an air content requirement of 4% (XF3).

In this research the method for revision of the frost resistance requirements is computer simulation. By computer simulation the degradation of structures is emulated closely as it happens in natural conditions. This is important for degradation types like frost damage where the degradation is highly dependent on the occasional periods of rain, sunshine and other elements leading to very complex variation in the temperature and moisture content of the structure. While the field and laboratory tests fail to fulfil the needs of service life prediction with an accuracy and speed required for today's practice, computer simulation gives an interesting new possibility. It is both quick and relatively accurate and is applicable in any environmental conditions. However computer simulation requires a good theoretical background about materials, structures and calculation methods as well as calibration of calculations with field and laboratory test data.

2 PREDICTION OF SERVICE LIFE BY COMPUTER SIMULATION

2.1 Basic principles

Computer simulation refers to theoretical emulation of (1) climatic stresses (2) temperature and moisture variations in a cross-section of a concrete structure and (3) application of temperature and moisture sensitive degradation models so that the degradation in different parts of the structure can be predicted. The increment of time in the step-by-step calculation process is typically 1 hour. The total range of calculation covers typically 150 years [4, 5].

The structure is assumed to be exposed to normal climatic stresses (including variation in temperature and relative humidity of the air, solar radiation, wind and rain). Both daily and seasonal changes are taken into account in the weather models which are based on long term statistics of the local climate.

Thermal and moisture mechanical calculation methods are used in the determination of the temperature and moisture variations inside a structure. The structure may be either of slab type or of wall type. The dimensions and possible protective effect of the structure are taken into account. The surfaces of the structure may be exposed to all weathering stresses or protected from some of the stresses such as rain and radiation. The meteorological data comprise the boundary conditions in the mathematical problem, where inside temperatures and moisture contents are unknown. An interior climate may also be defined on one or both sides of the structure.

The degradation of a structure is monitored with the help of mathematical degradation models of concrete and reinforcement. The model of frost attack is based on the theory of critical degree of saturation, i.e. degradation is assumed to be increased if freezing occurs while the critical degree of saturation is exceeded. The rate of surface scaling is also evaluated especially in a case where the structure is exposed to deicing chlorides. The model of corrosion of reinforcement consists of an initiation period and a propagation period. The initiation of corrosion is assumed to occur when either the carbonation or the critical chloride content reaches the level of the reinforcement. After initiation the rate of corrosion depends on the temperature and moisture content of the concrete. The interaction of degradation factors is also considered.

2.2 Detailed description on the frost resistance calculations

Before any other calculations, the concrete is proportioned by the programme from initial data such as the nominal compressive strength, consistency of the fresh concrete, air content and the type of cement. As a result the contents of all mix ingredients are obtained. The changes in the porosity of concrete are followed during the hardening process. All the parameters of hardened concrete related to moisture and thermal transfer and degradation are given values on the basis of mix proportions and porosity. The formulae of these parameters were partly created specially for this work [6].

The cumulative volume distribution of the air pores was assumed to be of the following form:

$$a(r) = a_0 \cdot \left(\frac{r}{r_{max}} \right)^{n_r} \qquad (1)$$

where

a	is the cumulative volume distribution of the air pores as a function of the pore radius
a_0	air content of concrete ($r < r_{max}$)
r	pore radius
r_{max}	max pore radius (in this case 0.5 mm) and
n_r	exponent controlling the form of distribution.

The distribution is linear if the exponent n_r is 1. It means that there is the same amount of air in all size classes of pores. If n_r is smaller than 1 the relative volume of small pores is greater than that of big pores. If n_r is greater than 1 the relative amount of big pore is greater than that of small pores. A pore analysis carried out for a limited number of concrete samples revealed that the value of n_r may range from 1.3 to 0.7 having an average near 1 [6].

The moisture transfer in concrete is evaluated by a combined theory of three mechanisms: capillary suction, capillary water diffusion and water vapour diffusion. The theory of capillary

suction made it possible to evaluate also the filling of air pores with water. The following formulae of parameters for moisture movements and degradation were applied in the calculations.

$$k = 0.00016 \cdot P_{cap} \tag{2}$$

$$D_w = 1.25 \cdot 10^{-6} \cdot k \tag{3}$$

$$\delta_p = \delta_{p0} \cdot (1 + 10 \cdot \varphi^5) \text{ with } \delta_{p0} = 1.35 \cdot 10^{-5} \cdot D_w \tag{4}$$

$$\delta_l = 1 \cdot 10^{-11} \quad m^2 / s \tag{5}$$

$$L_{r,crit} = 0.4 \quad mm \tag{6}$$

where

k is	capillary index of concrete, kg/(m$^{2.\sqrt{}}$s)
P_{cap}	capillary porosity of concrete, kg/m^3
D_w	capillary water diffusivity, m^2/s
δ_p	diffusion coefficient of water vapour, kg/(m s Pa)
δ_l	diffusion coefficient of air in cement paste, m^2/s and
$L_{r,crit}$	critical spacing factor (corresponding to the critical moisture content), mm.

The degradation of concrete as a result of critical freezing events was assumed to take place according to the following formula [7]:

$$D = 1 - \frac{E_N}{E_0} = K_N \cdot (S - S_{crit}) \tag{7}$$

where

D is degradation of concrete i.e. relative diminishing of the dynamic E-modulus ($0 \leq D \leq 1$)

S	degree of water saturation
S_{crit}	critical degree of water saturation
K_N	coefficient of degradation and
N	number of critical freezing events.

Coefficient of degradation was determined from the formula:

$$K_N = A \cdot N^{\frac{1}{3}} \text{ with } A = 34.8 \cdot w/c - 7.6 \tag{8}$$

where w/c is the watercement ratio of concrete.

As the water content of concrete changes with time equation 7 was applied in the calculations in the following form:

$$D = \sum_i (K_i - K_{i-1}) \cdot \frac{(w_i - w_{crit})}{w_{tot}} \tag{9}$$

where

i	is the critical freezing event in sequence
K_i	coefficient of degradation at ith critical freezing event
w_i	the water content of concrete during the ith critical freezing event
w_{cr}	the critical water content of concrete and
w_{tot}	the maximum water content of concrete (corresponding to the total porosity).

The maximum allowable degradation of concrete, D_{max}, was 0.33.

3 CALCULATIONS

3.1 Facade element

3.1.1 Structural assumptions

Calculations of the facade element were performed using the structural assumptions and the climatic stresses presented in Figure 1. There were 11 nodal points, three of which were in the outer panel of the sandwich element (points 0 - 2). Four points were in the inner panel (points 7 - 10). Other nodal points were in the thermal insulation (glass wool) between the panels. There was no coating on the outer surface of the element but on the inner surface a paint was applied (not completely impermeable for water vapour).

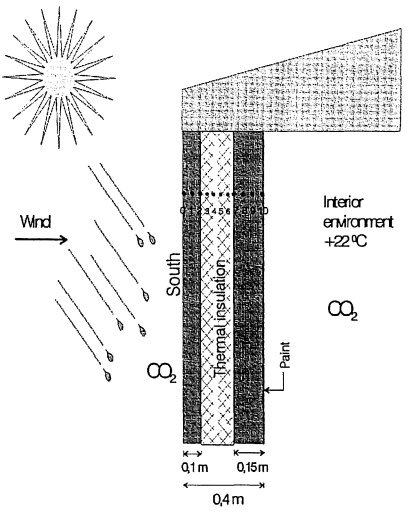

Fig 1. The climatic stresses and nodal points of the facade element.

The facade element was assumed to be placed on the southern wall of a building. The outer panel was burdened by variations in the temperature and the relative humidity of air, wind, solar radiation and driving rain. The building was assumed to be situated near Helsinki airport, i.e. the long term climatic statistics of Helsinki airport were used in the weather models. The purpose was to simulate the conditions of XF1 in prEN206.

On the other side of the facade element an interior climate was assumed. The room temperature was +22 °C or max. 3 °C above the air temperature outside. An extra moisture content of 4 g/m^3 was also assumed compared to the moisture content of the air outdoors.

The nominal compressive strength of concrete ranged from 35 to 50 MPa (referred later as K35 and K50). The cement was Rapid (CEM II 42,5 R) and the maximum grain size of the aggregate was 16 mm.

3.1.2 Cracking criteria

At this phase of the study the basic criteria was that no frost cracking in concrete was allowed. Consequently the air requirements should be imposed so that no critical freezing events are possible during the lifetime of the structure. The critical freezing events are defined as moments of time when the critical degree of saturation is exceeded simultaneously with temperature descending below 0 °C. The critical freezing events were counted in three years which period was considered to be long enough to make reliable conclusions.

The results of the calculations are presented in Figures 2 and 3. Figure 2 shows the number of critical freezing events as a function of air content. The parameter n_r shows the influence of the form of the air pore distribution. As can be seen critical freezing events and cracking may happen even by a very high air content if the air pore distribution is poor (n_r>1). On the other hand even a small content of air is sufficient to guarantee a crack free life for concrete if the distribution of air is good (n_r<0.8). The compressive strength of concrete has no practical meaning in the amount of critical freezing events.

In Figure 3 the amounts of critical freezing events are plotted as a function of Powers spacing factor. The spacing factor has been calculated from the assumed distribution of air pores having 10 μm as the minimum and 500 μm as the maximum radius of pores. From the figure one can readily observe that if the Powers spacing factor is smaller than 0.24 mm no critical freezing events take place. Even by 0.26 mm the number of critical freezing events is very limited.

The results show that the regulation of the frost resistance of concrete by the volume of air only is not possible. Instead the spacing factor concept seems to be an excellent way to guarantee a crack-free life for concrete. If the spacing factor is smaller than 0.24 mm no cracks can be produced in concrete facades irrespective of the air content, form of the air pore distribution or the compressive strength of concrete.

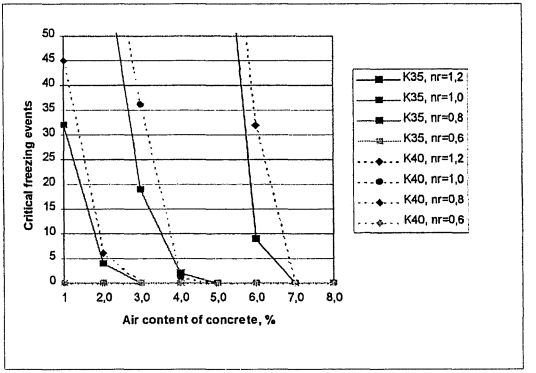

Fig 2. Critical freezing events as a function of air content of concrete, nominal strength of concrete and the exponent of air pore distribution.

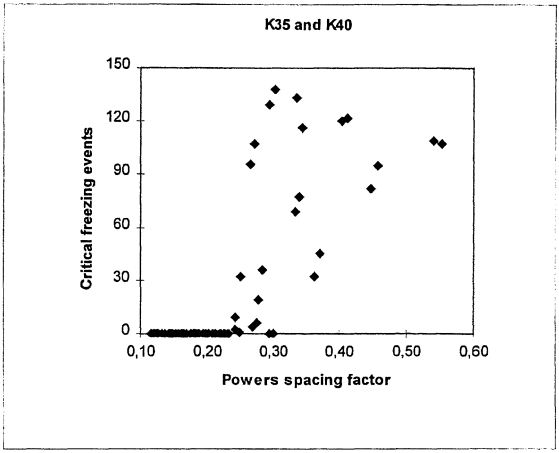

Fig 3. Critical freezing events as a function of Powers spacing factor. All results included.

3.1.3 Service life criteria

At this phase of the study the basic criteria for frost resistance was a service life of 50 years. So the aim was to find out the air pore characteristics which would be in conformity with the service life requirement. The service life was defined as the period of time within which the degradation is proceeded to its maximum allowable amount of 0.33.

The degradation of concrete at the outer surface of the outer panel was followed by computer simulation. An example of these calculations is shown in Figure 4.

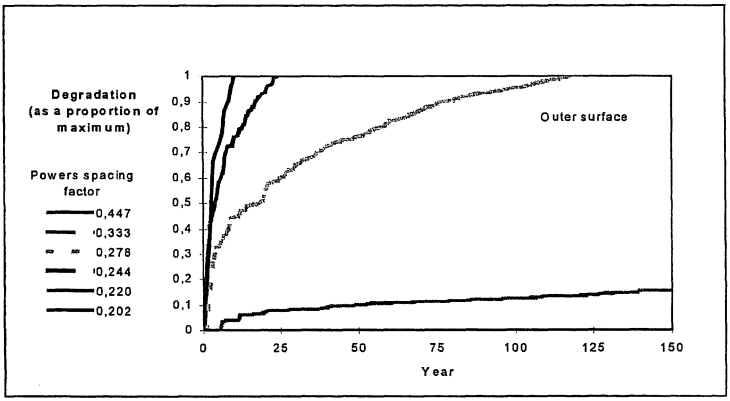

Fig 4. Degradation of concrete the outer surface of the outer panel as a function of time and Powers spacing factor (K35, n_r=1).

Based on the Equations 7 and 8 the following formula could be derived for the service life of concrete:

$$t_L = \frac{1}{n_{cf}} \cdot \left(\frac{D_{max}}{A \cdot (S - S_{cr})_{mean}} \right)^3 \qquad (10)$$

where

t_L is service life in years
n_{cf} number of critical freezing events per year
$(S\text{-}S_{crit})_{mean}$ average exceeding of the critical degree of saturation at each critical freezing event
D_{max} maximum allowable degradation and
A coefficient (see Formula 8).

Equation 10 helped analysing the results of simulation. The number of freezing events per year and the average exceeding of the critical degree of saturation at critical freezing events were determined in the course of calculation.
The final results of the calculation could be presented in the following form:

$$t_L = t_R \cdot f_1(L) \cdot f_2(w/c) \cdot f_3(n_r) \qquad (11)$$

where

t_L is service life, years
t_R reference service life, years
$f_1(L)$ function showing the effect of spacing factor (L) on service life
$f_2(w/c)$ function showing the effect of w/c on service life and
$f_3(n_r)$ function showing the effect of n_r on service life.

Only the mean service life was determined by the calculations. For the mean the reference service life is 145 years. To obtain the service lives corresponding to different safety levels P the distribution and the variance of service life had to be defined. The variance of service life is supposed to include all unintended variation of material parameters and structural dimensions as well as such environmental variations that are not considered by the weather models. In this study the form of service life distribution was assumed to be lognormal and the coefficient of variance was assumed to be 0.6. By these assumptions the safety factors (the relation of the mean service life and the service life corresponding to safety level P) could be determined [8]. In Table 1 these safety factors are presented together with the corresponding reference service lives $t_{R,P}$.

Table 1. Safety factors and reference service lives at different safety levels (Equation 11).

Safety level P	Safety factor γ_t	Reference service life $t_{R,P}$ (years)
95%	2.90	50
90%	2.37	61
80%	1.86	78
50%	1.17	124

The following formulae could be derived for the functions f_1, f_2 and f_3.

$$f_1(L) = \frac{1}{145} \cdot (27 + \frac{0.01}{(L - 0.24)^{3.4}}) \tag{12}$$

$$L > 0.24mm$$

$$f_2(w/c) = \left(\frac{9.8}{34.8 \cdot w/c - 7.6} \right)^3 \tag{13}$$

$$f_3(n_r) = 8.68 \cdot (1.49 - n_r)^{3.01} \tag{14}$$

$$0.6 < n_r < 1.2$$

The functions f_1, f_2 and f_3 are presented graphically in Figures 5, 6 and 7.

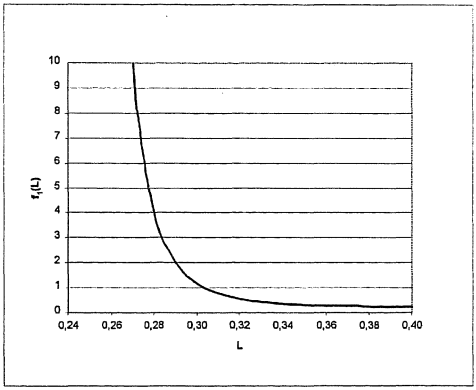

Fig 5. Function $f_1(L)$. Facade element.

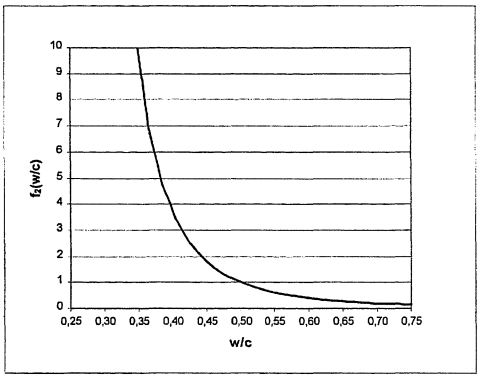

Fig 6. Function $f_2(w/c)$.

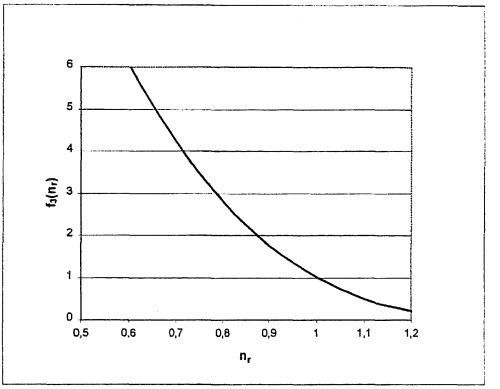

Fig 7. Function $f_3(n_r)$. Facade element.

The effects of spacing factor L and w/c on service life were as expected. By diminishing the spacing factor and reducing the water-to-cement ratio the service life can be multiplied. By reducing the spacing factor below 0.24 mm the service life of a structure is endless with regard to frost attack.

The effect of the exponent of air pore distribution was surprisingly great. Reducing n_r does not only have a positive effect on service life through the spacing factor L (which is reduced by diminishing n_r) but also through the number of critical freezing events and the average exceeding of S at critical freezing events (ref. Formula 10). The service life can be almost tripled by only reducing the value of n_r from 1 to 0.8. On the other hand the length of service life is dropped very sharply towards 0 if the value of n_r is greater than 1.

Equation 11 together with the equations 12 to 14 are applicable to service life design in practice. The formulae are in conformity with the standard ISO/DIS 15686 [9]. The service life requirement of 50 years at a 95% safety level is reached if the product of functions f_1, f_2 and f_3 is greater than 1. If n_r is not known the assumption $f_3 = 1$ is recommended ($n_r = 1$).

3.2 Balcony Slab

Another structure that was studied by the computer simulation was a balcony slab. The upper surface of the slab was fully exposed to rain and solar radiation but the lower surface was sheltered from them (Figure 8). There were no coatings on any surface of the slab. The purpose was to simulate the conditions of XF3 in prEN206. The mix design of concrete was the same as with the facade element.

3.2.1 Cracking criteria

Having 'no frost cracking' as the criteria for regulation of frost resistance the number of critical freezing events was counted during the first three years. The results of the calculation are presented in Figures 9 and 10.

The results showed similar trends as with the facade element. Neither the air content nor the compressive strength was found an important parameter for the restriction of frost cracking (Figure 10). The decisive factor was the Powers spacing factor (Figure 11). The critical limit of the spacing factor was 0.225 mm which is a little smaller than that found in the case of the facade element.

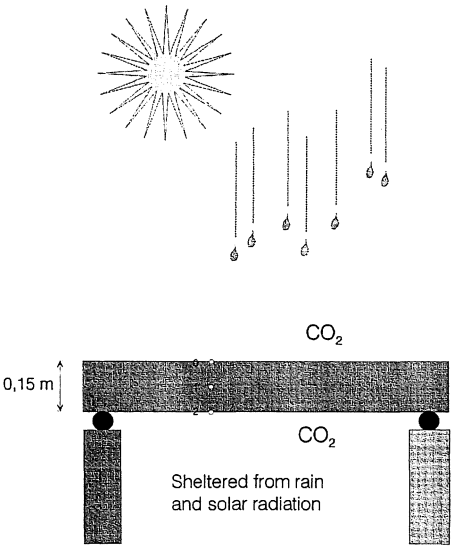

Fig 8. The climatic stresses and nodal points of the balcony slab.

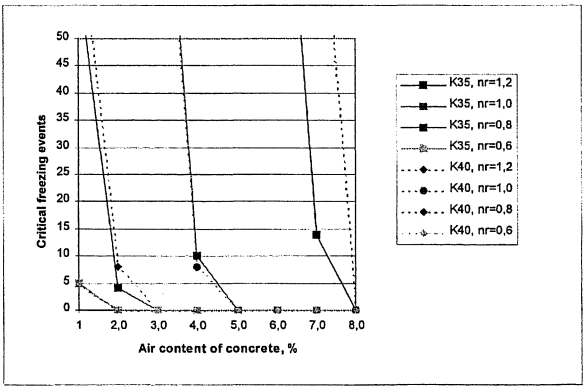

Fig 9. Critical freezing events in a balcony slab as a function of air content of concrete, nominal strength of concrete and the exponent of air pore distribution.

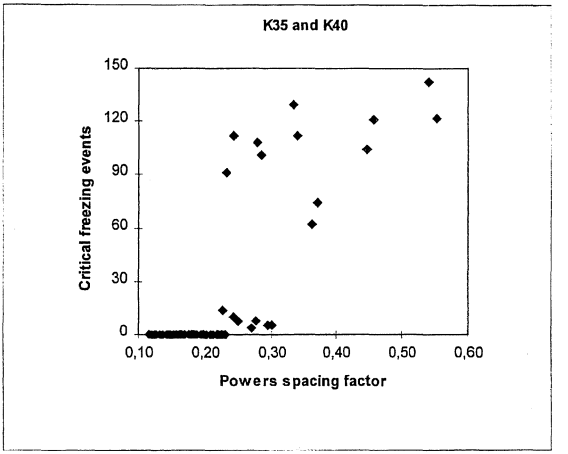

Fig 10. Critical freezing events in a balcony slab as a function of Powers spacing factor. All results included.

3.2.2 Service life criteria

Taking a '50 years service life' as the basic criteria, the degradation of concrete at the outer surface of the outer panel was monitored by computer simulation. An example of these calculations is shown in Figure 11.

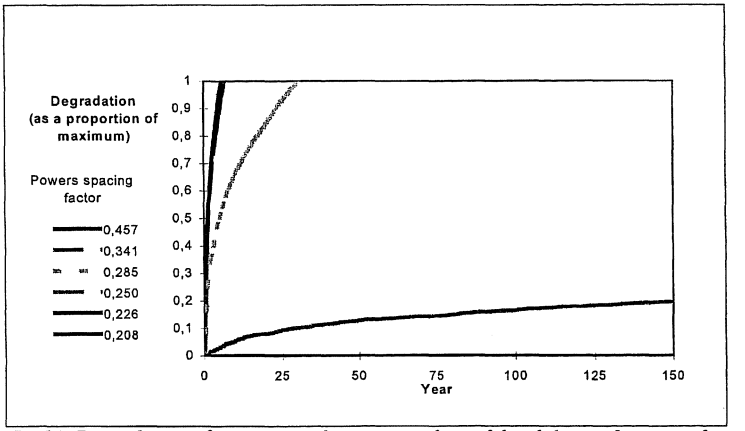

Fig 11. Degradation of concrete at the upper surface of the slab as a function of time and Powers spacing factor (K40, n_T=1).

The results of the service life were analysed in the same way as in the case of the facade element. Equation 11 is also applicable for the balcony slab. However, the functions f_1 and f_3 are determined from the following formulae:

$$f_1(L) = \frac{1}{145} \cdot (6 + \frac{0.001}{(L - 0.225)^{3.7}}) \qquad (15)$$

$$L > 0.225 \; mm$$

$$f_3(n_r) = 550 \cdot (1.35 - n_r)^{6.0} \qquad (16)$$

$$0.6 < n_r < 1.2$$

The function $f_1(L)$ and $f_3(n_r)$ are presented graphically in Figures 13 and 14.

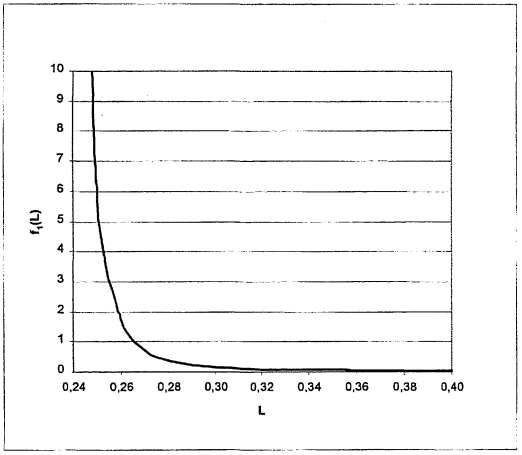

Fig 12. Function $f_1(L)$. Balcony slab.

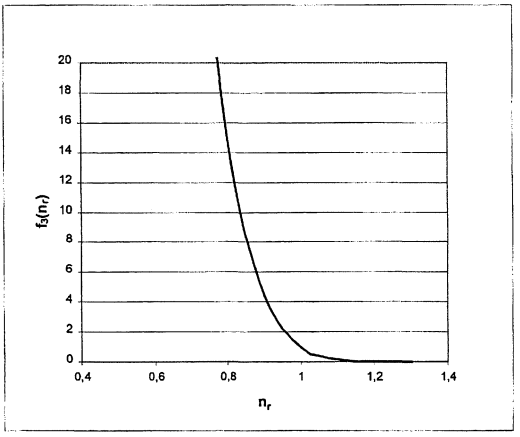

Fig 13. Function $f_3(n_r)$. Balcony slab.

The function f_2(w/c) is the same as in the case of facade element (Figure 6).

4 SUMMARY AND CONCLUSIONS

Computer simulation makes it possible to effectively study the influences of material properties, structural details and environmental conditions on the degradation and service life of concrete structures. As a result of a study on frost resistance requirements for facade elements and a balcony slabs the following conclusions could be made:

1. Air content is not an effective parameter for quality control of frost resistance. The 'quality' of air is more important than quantity.
2. The frost cracking of concrete can be effectively controlled by Powers spacing factor. An endless crack-free service life concrete can be guaranteed by keeping the Powers spacing factor smaller than the critical one. The critical spacing factor for facade elements is 0.24 mm and for balcony slabs 0.225 mm.
3. The service life of a facade element and a balcony slab with regard to frost attack can be evaluated as a function of Powers spacing factor L, water cement ratio w/c and the exponent of air pore distribution. The presented prediction method of service life is in conformity with ISO/DIS 15686 (factor method).

5 REFERENCES

1. Eurocode 1: Basis of Design and Actions on Structures. Part 1: Basis of Design. ENV 1991 - 1. CEN/TC250. 1993. 76 p.
2. prEN206 1997. European standard. Concrete - Performance, production and conformity. European Committee for Standardization CEN. Draft 1996. 59 p.
3. Pyy, H. 1996. The influence of air-entraining and other microstructure properties on the resistance of concrete - case study. Proceedings of a Nordic Research Seminar in Lund, April 16-17,1996. University of Lund. Lund Institute of Technology. Report TVB-3072. Pp. 38-48.
4. Vesikari, E. Betonirakenteiden käyttöiän arviointi tietokonesimuloinnilla (Prediction of service life of concrete structures by computer simulation). Helsinki University of Technology. Faculty of Civil and Environmental Engineering. Licentiate´s thesis. 131 p. In Finnish.
5. Vesikari, E. Computer simulation technique for prediction of service life in concrete structures. Proc. Int. Conf. Life Prediction and Ageing Management of Concrete Structures, July 1999. RILEM Expertcentrum. Bratislava. pp. 17-23.
6. Kuosa, H. & Vesikari, E. 1999. Moisture transfer in concrete and degradation by frost - experimental results and their analysis. Proc. Nordic Res. Sem. on Frost Resistance of Building Materials, Aug. 31 - Sept. 1 1999, Lund. Lund Institute of Technology, Division of Building materials. 18 p.
7. Fagerlund, G. 1996. Livslängdsberäkningar för betongkonstruktioner. Översikt med tillämpningsexempel. (Life assessment of concrete structures. Review and examples of application.) Lund, Lunds Tekniska Högskola, Byggnadsmaterial. TVBM-3070. 124p. (in Swedish)
8. Sarja, A. & Vesikari E. (Ed.) Durability Design of Concrete Structures. Report of RILEM Technical Committee 130 CSL. RILEM Report 14. E & FN Spon. London 1996. 165 p.
9. ISO/DIS 15686-1. Buildings - Service life planning - Part 1: General principles. ISO/TC59/SC14. 1998. 62 p.

LUND INSTITUTE OF TECHNOLOGY
Lund University